Effect of Nanoparticles on the Properties of Masonry Mortars and Assemblages at a Cold Temperature

By

Hooman Kazempour

A Thesis submitted to the Faculty of Graduate Studies of

The University of Manitoba

in partial fulfillment of the requirements of the degree of

Master of Science

Department of Civil Engineering

Faculty of Engineering

University of Manitoba

Winnipeg

ABSTRACT

Cold weather masonry construction is a major concern for contractors as they either have to implement heating practices for laying and curing masonry systems or postpone the construction to warmer periods. This can lead to loss of productivity rate and delays in construction schedules with associated extra costs. This thesis explores a novel approach for mitigating the adverse effects of cold weather on masonry construction in early fall periods through the application of nanoparticles in mortar joints. The effect of nano-alumina (NA) and nano-silica (NS) with dosages of 2, 4 and 6% by mass of cement on Type S masonry mortars mixed and cured at 5 ± 1°C was investigated. The water-to-binder ratio (w/b) was fixed at 0.4 and polycarboxylate based high range water-reducing admixture (HRWRA) was added to the mortar mixtures at a dosage range of 2 to 4% by mas of binder. Flowability, air content, heat of hydration and setting time of fresh mixtures and compressive strength of mortar cubes were determined at early and later ages (1, 3, 7 and 28 days). To capture the microstructural development and characterize the hydration products in the cementitious matrix, backscattered scanning electron microscopy (BSEM) with energy dispersive X-ray (EDX) and thermogravimetric analyses were carried out. In addition, four nano-modified mixtures were selected and used as mortar joints for construction of three and four course high masonry prisms assembled and cured at 5 ± 1°C. The prisms were tested for compressive strength, modulus of elasticity and bond strength. The bond strength was performed by the pull off and flexural bond methods. Test results indicated that the addition of nanoparticles affected the fresh and hardened properties of the mortar mixtures. They generally reduced the flowability, increased the air content and accelerated the hydration of cement. Larger specific surface area (SSA) of NA (170 m^2/g) compared to NS (80 m^2/g) required higher dosage

of HRWRA for obtaining the flowability of the mixtures. This led to longer setting times, compared to the control mixture at 5 ± 1°C. However, incorporation of NS in the mixtures shortened their setting time at 5 ± 1°C, compared to the control mixture. While NS accelerated the kinetics of hydration at early-age, thermal analyses of the mixtures mixed and cured at 5 ± 1°C revealed that the pozzolanic effect of NS was delayed by up to 25 days, compared to the mixtures mixed and cured at ambient lab temperature (22 ± 2°C). The mechanical properties tests on masonry prisms showed that the compressive strength of the mortar joints did not significantly affect the total compressive strength of the prism at 3 and 28 days. However, the modulus of elasticity of the prisms incorporating NS was improved at 3 days, compared to the control prisms. Generally, various test results show that NS can be successfully used to minimize the adverse effects of cold temperature on Type S mortar joints by speeding up the hydration of cement, shortening the setting time, and increasing the strength up to 72 h, which offers a promising approach for controlling the effects of cold weather on masonry construction, during early fall periods without the need for heating practices.

AKNOWLEDGEMENTS

My first and highest appreciation goes to my advisors without them foundation of this work would have not been shaped. I would like to express my appreciation to my principal advisor Dr. Mohamed T. Bassuoni, P.Eng, for his boundless guidance and responsibility during my graduate studies that enhanced my level of understanding of the topic. I would also like to thank him for the time and effort he dedicated to solve the research problems and revise the research work that improved my academic performance. I would also like to acknowledge my co-advisor Dr. Fariborz Hashemian, P.Eng, who always reinforced my research ideas and thoughts and helped me to implement my knowledge in practical applications.

I would like to acknowledge Manitoba Masonry Institute (MMI), Canadian Concrete Masonry Producers Association (CCMPA) and the University of Manitoba for providing financial support for this research program. I would also like to thank the support of Euro-Can Enterprises Ltd. Company, particularly Mr. Mark Laarveld for providing masonry resources for this research program.

Countless thanks to the McQuade heavy structures lab manager, Mr. Chad Klowak, P.Eng, and the technicians, Mr. Brendan Pachal and Grant Whiteside for providing valuable technical support for construction and testing the masonry specimens.

At last but absolutely not least, I would like to appreciate the emotional and financial support of my family and my dearest who backed me in every step of my life and my studies. Without your support I could never be in this position.

Table of Contents

List of Tables

List of Figures

List of Notations

A = percentage of air content

BSEM = Backscattered scanning electron microscopy

C_3A = Tricalcium aluminate

C_4AF = Tetracalcium aluminoferrite

CH = Calcium hydroxide, portlandite

C:HL:S = Cement-to-hydrated lime-to-sand ratio

CMU = Concrete masonry unit

C/S = Calcium-to-silicate ratio

C:S = Cement-to-sand ratio

C_2S = Dicalcium silicate

C_3S = Tricalcium silicate

C-S-H = Calcium silicate hydrate

CWAS = Cold weather admixture systems

D = density of the air-free mortar

Dc = density of cement,

Ds = density of sand, g/cm^3

Dw = density of water, g/cm^3

D_h = density of HRWRA, g/cm^3

D_n = density of nanoparticle, g/cm^3

DSC = Differential scanning calorimetry

EDX = Energy dispersive X-ray

E = Modulus of elasticity

f'_m = Compressive strength of masonry

f_b = Bond strength of masonry by pull-off method

f_r = Flexural bond strength of masonry by four point bending method

F_{cr} = Critical F value

GU = General use

HE = High-early strength

HRWRA = High range water-reducing admixture, superplasticizer

ITZ = Interfacial transition zone

L = Span length, mm

M = mass of mortar, g

NA = Nano-alumina

NS = Nano-silica

OPC = Ordinary portland cement

P = Maximum load measured by the testing equipment, N

S = Section modulus, mm^3

SCM = Supplementary cementing material

SEM = Scanning electron microscopy

SSA = Specific surface area

TGA = Thermogravimetric analysis

w/b = water-to-binder ratio

w/c = water-to-cement ratio

1 INTRODUCTION

1.1 Background

The inherent characteristics of masonry materials have always provided a feeling of high performance and safety of the masonry structure to the human being. There are numerous masonry heritage buildings that can still be seen all around the world. In fact, masonry is one of the oldest building materials used in construction with a history of thousands of years. Masonry is a composite building material consisting of load bearing elements (masonry units) and binders (joints). Generally, different materials have been used during the development of masonry construction. For example, stone and clay were used as masonry units, and bitumen, clay-straw mixtures, and lime were used as mortar joints to bind the masonry units long time ago. However, the invention of portland cement by Joseph Aspdin in the 18th century led to introduction of new materials with improved properties for masonry construction. The use of concrete masonry units (CMUs) and mortar mixtures containing portland cement increased in the 20th century in North America and numerous modern masonry buildings have been constructed since then. However, the development of masonry construction, because of its composite nature, is highly affected by several factors such as the availability of materials, environmental conditions and associated costs. Therefore, a uniquely adaptive masonry design is required to secure masonry construction performance and characteristics based on the prevailing factors.

1.2 Problem Definition

Masonry systems have been widely considered as reliable construction materials in terms of durability and strength for long time. However, their performance may be affected if exposed to cold temperature conditions. For example, the rate of strength development and setting time of the mortar joints are adversely affected by cold temperatures (Korhonen *et al*. 1997). Characteristics of the masonry mortar joints directly affect the masonry construction industry during cold seasons. In particular, in North America, cold weather masonry construction is a major concern for contractors as they either have to implement conventional mitigation practices (e.g. heating the job site) for laying and curing masonry systems or postpone the construction to warmer periods. This can lead to loss of productivity, delays in construction schedules, and inevitably extra cost.

Because of the vulnerability of mortar joints to delayed setting time and/or freezing at early-ages in cold temperature, North American standards stipulate that all masonry mortar constituents, concrete masonry units (CMUs) and masonry segments have to be heated and/or protected from cold temperature when the daily mean temperature is low. In the literature of cement-based materials, 5°C is generally known as the boundary temperature at which the rate of hydration activity of cementitious materials starts to cease (Bigelow 2005; Imoto *et al*. 2013). CSA A371-04 (CSA 2004a) outlines specific techniques for construction and curing of masonry sections when average daily temperature reaches and falls below 4°C. For example, in a temperature range between 0 to 4°C, sand or water should be heated to a temperature between a minimum of 20°C and a maximum of 70°C before mixing. In addition, constructed masonry segments shall be protected from precipitation for at least 48 h. In comparison, ACI 530.1-13/ASCE 6-13/TMS 603-13 (ACI/ASCE/TMS 2013) requires heating of the constituents to the

extent that a mortar mixture within a temperature range of 5 to 49°C is achieved. Although these heating practices are advantageous, they might be economically unfavorable. Equipment for generating heat and protecting materials needed for implementing the conventional mitigation methods usually incur additional cost for construction projects. In addition, these mitigation methods have some practical limitations. For example, special consideration is required for preparing mortar mixtures to comply with temperature limits specified by standards, which slows down the productivity rate of masonry construction.

1.3 Research Significance

Due to their ultrafine nature, nanoparticles (size scale of 1-100 billionth of a meter) can vigorously speed up the kinetics of cement hydration. Various studies (Givi *et al*. 2011; Jo *et al.* 2007; Oltulu and Şahin 2013; Senff *et al.* 2009; Senff *et al.* 2010; Sonebi *et al.* 2012) have shown that nanoparticles positively affect the properties of cementitious materials under normal mixing and curing temperatures (22 ± 2˚C) by refining and densifying the pore structure of hydrated cement paste. Their ultrafine nature provides more surface area to react with cementitious phases. Specifically, nano-alumina (NA) and nano-silica (NS) have been shown to impart beneficial effects on cement-based materials. They improve the compressive and flexural strengths of mortar mixtures and shorten the setting time by accelerating the hydration reactions and refining the pore structure at normal mixing and curing temperatures (22 ± 2˚C). Also, with addition of NS to cement-based materials, portlandite (CH) is converted to calcium silicate hydrate (C-S-H) via pozzolanic reaction. The secondary C-S-H formed by the pozzolanic activity improves the hardened and durability properties of cement-based materials. Yet, research on the effect of nanoparticles on the behaviour of cement-based materials under cold temperatures is still in its infancy, with no published data on temperature thresholds below 10˚C. Hence, the

main motive of this research is to investigate an innovative approach for speeding up masonry construction in early fall periods (temperature threshold of 5 ± 1˚C) by using nano-modified mortar joints.

1.4 Research Objectives

The primary objective of this research is to address cold weather masonry concerns by introducing innovative mixture designs for masonry mortars incorporating nanoparticles by:

- Investigating the effect of nano-alumina (NA) and nano-silica (NS) on the fresh, hardened and microstructural features of masonry mortar mixtures prepared and cured at 5 ± 1°C.
- Evaluating key mechanical properties of masonry assemblages fabricated using the newly developed nano-modified mortar joints prepared and cured at 5 ± 1°C.

1.5 Scope of Work

This study is mainly divided into two stages. At the primary stage, the effects of the addition of 2, 4 and 6% NA and NS by mass of cement on the flowability, air content, heat of hydration, setting time and compressive strength of the mortar mixtures were evaluated. In addition to the fresh and hardened properties, the effect of the nanoparticles (NS and NA) on the masonry mortar mixtures were investigated by thermal and microstructural analyses using DSC/TGA (differential scanning calorimetry/thermogravimetric analysis) and BSEM (back scattered electron microscopy) with EDX (energy dispersive X-ray) in order to study the evolution of microstructure and hydration products. In the ancillary stage and based on the results of the primary stage, selected nano-modified mortar mixtures were used as 10 mm mortar joints to construct concrete masonry prisms. The mechanical properties determined for the concrete

masonry prisms were the compressive strength, modulus of elasticity, and bond (direct and flexural) strength.

1.6 Thesis Organization

This thesis investigates the effect of the addition of 2, 4 and 6% NA and NS on the properties of masonry mortars and assemblages at a cold temperature of 5 ± 1˚C in five chapters as follows:

The first chapter of this thesis comprises a short history about masonry construction materials, cold weather masonry construction concerns and problem definition, research objectives, and scope of work.

The second chapter presents a comprehensive literature review about the cold weather masonry construction requirements by North American standards, practical mitigation methods and the effects of NA and NS on the fresh and hardened properties (e.g. flowability, setting time, compressive strength) of cementitious materials at normal and cold temperatures.

The third chapter of the thesis provides detailed information about the materials used in this research program. It also contains the mixture design of the mortar mixtures, the mixing and curing condition of the specimens and the test methods that were followed for each particular test on mortar mixtures and masonry assemblages.

In the fourth chapter of this dissertation, results of the fresh, hardened and microstructural tests on the mortar mixtures are presented, analyzed and discussed. This chapter also includes the results and discussion of the mechanical behavior of masonry prisms bonded by nano-modified mortar joints.

The fifth chapter includes summary and conclusions of the research program as well as recommendations for future work.

2 LITERATURE REVIEW

2.1 Key Issues of Cold Weather Masonry Construction

Masonry construction materials have been considered as sustainable and durable building materials since long time. However, masonry systems have shown to be vulnerable to cold climates during construction and service. Masonry systems are mainly composed of mortar joints, grout and masonry units. The mortar joints are applied to bind the masonry units (i.e. concrete masonry units (CMUs), bricks, tiles) of a typical masonry structure. Masonry mortar is a blend of masonry sand, cementitious binder and water. Almost 10-18% by mass of conventional mortar or grout is composed of water (Essroc 2012a) which is a key component of mortars and grouts. Water is not only needed for the hydration of cement but also for obtaining the desired flowability. Hydration is a chemical reaction between cement and water which results in hardening of the cementitious matrix. However, hydration activity of cement is highly dependent on the environmental conditions during mixing and curing. In particular, hydration of cement particles is adversely affected by cold temperatures (Bigelow 2005) . When the ambient temperature drops, the rate of the hydration activity decelerates which leads to delayed setting time and extremely low early-age compressive strength. This behavior of the hydration of cement imparts delays on masonry construction and extra costs. Additionally, the microstructure of cement-based materials will be impaired if the water content freezes before or shortly after initial setting time (Korhonen 1990). The expansion of ice creates micro-cracks and fissures which affect the strength of the matrix and may lead to durability problems (Korhonen 2002). In the literature of cementitious materials, 5°C is the critical temperature below which the hydration

of cement is significantly slowed or ceased (Bigelow 2005; Hatzinikolas *et al.* 1984; Imoto *et al.* 2013). Therefore, in this thesis, based on the cold weather construction and curing requirements of North American masonry standards ((CSA A371-04 (CSA 2004a) and ACI 530.1-13/ASCE 6-13/TMS 603-13 (ACI/ASCE/TMS 2013)) and the technical literature, the term 'cold' refers to a temperature in the range of $5.0 \pm 1^{o}C$.

The other concerns of cold weather masonry construction can be related to the masonry units. Masonry units can be classified into two main categories based on their porosity and capillary coefficient. For the case of highly porous masonry units, water is rapidly transferred into the units due to capillary suction during construction. Therefore, at very low temperatures, the masonry bond between the masonry unit and the mortar joint will be altered if the absorbed water in the masonry unit or on the interface of unit and mortar joint freezes before adequate strength is gained (Hatzinikolas *et al.* 1984) . The expansion of water at the freezing point creates micro-cracks in the unit and the joint that lead to a reduction in the bond strength (Cultrone *et al*. 2007). Masonry units with lower capillary coefficients may raise another concern due to freezing of water. The CMU which has low capillary characteristics does not efficiently absorb the water existing in conventional mortar or grout mixture (Drysdale and Hamid 2005). Under very cold weather conditions the unabsorbed water freezes over at the masonry joint, which leads to a significant decrease in bond strength or debonding of the masonry system. Therefore, special care should be taken to prevent the concerns related to cold weather masonry construction.

2.1.1 **Cold Weather Masonry Construction Practices**

In this section cold weather masonry construction mitigation methods recommended by masonry practitioners as well as North American code requirements are discussed. These methods include

heating of the masonry mortar constituents and masonry units and the application of chemical admixtures.

2.1.1.1 Heating the Materials

The primary and most common way to accelerate the hydration of cement and prevent mortar joints from freezing is heating the mixing water or sand (Fig 2.1). Water has good ability to transfer the energy (heat) to the other constituents of the masonry mortar mixtures. Heating of water is usually done by use of a heating rod or heating a water drum over a propane stove, as shown in Fig. 2.1(a). It is recommended to keep the water temperature below 60^{o}C as higher temperatures will increase the risk of flash setting of mortar (Bigelow 2005; TCC 2011). Adding sand to the heated water before cement is also recommended to avoid flash setting. This method is generally in agreement with the cold weather construction requirements of Canadian standards. For example, CSA A371-04 (CSA 2004a) states that when the air temperature is below 4ºC, mixing water shall be heated to a minimum of 20ºC and a maximum of 70ºC for masonry construction. According to CSA A371-04 (CSA 2004a), the optimum temperature range of a mortar mixture is between 15.6^{o}C to 26.7^{o}C. Overheating of the mixture more than 48.9^{o}C may lead to lower compressive strength and reduced bond strength. In addition, CSA A371-04 (CSA 2004a) recommends maintaining the temperature of masonry mortar below 50^{o}C to avoid flash setting. It has also been mentioned that overheating of mortar can lead to color changes. However, In order to comply with the temperature requirements mortar should be mixed in small amounts during winter and therefore, continuous supply of mortar is need to prevent delays (International Masonry Institute 2010) .

Warming the units before installation or keeping them in an insulated place is another alternate way to prevent cold weather masonry construction issues. However, it is recommended

to always wrap and keep the masonry units and mortar constituents on a pallet with enough height from ground to be protect them from snow built-ups and precipitation (Bigelow 2005).

Fig. 2.1. Conventional methods for heating the constituents of masonry mortar: (a) heating water using a heating rod, and (b) heating sand using an electric heater.

2.1.1.2 Other Mitigation Methods

The other approach recommended by masonry practitioners is to use slightly less amount of water in the mortar mixture. The lower water content of the mortar leads to higher compressive strength and shortened setting time. However, unlike concrete, the amount of water content of masonry mortar is highly dependent on the experience of the mason. Reducing the hydrated lime content, using masonry cements and increasing the sand content of the mortar mixture were also recommended in the literature (Brick Industry Association 2006). However it has been found that changing the materials or adding admixtures may change the color of finished work (Throop 2005), which might raise some cosmetic concerns. Using Type 30 (HE: high-early strength) portland cement has been found to beneficial for minimizing cold weather masonry construction concerns (Bigelow 2005). Type HE cement accelerates the hardening rate at early-ages due to its

higher tricalcium silicate (C_3S) content and fineness, compared to Type GU (general use) cement.

2.1.1.3 North American Standards for Cold Weather Masonry Construction

CSA A371-04 (CSA 2004a) requires a minimum and maximum grout temperature of 20 and 50ºC for grouted cold weather masonry construction, regardless of the temperature ranges given for mortar mixtures. According to clause 6.7.2.1 of CSA A371-04 (CSA 2004a), minimum requirements should be met when the average daily temperature reaches and falls below 4ºC. These minimum requirements are given in Table 2.1. For example, in a temperature range of 0 to 4ºC, sand or water should be heated to have a temperature range of 20 to 70ºC. However, when the air temperature is between -4.0 to 0ºC both sand and water should be heated to meet the temperature range requirement of 20 to 70ºC. As the temperature gets lower other necessities such as a source of heat and a minimum temperature of the masonry unit are also required.

Cold weather masonry construction requirements are also outlined in ACI 530.1-13/ASCE 6-13/TMS 603-13 (ACI/ASCE/TMS 2013) . The requirements of ACI 530.1-13/ASCE 6-13/TMS 603-13 (ACI/ASCE/TMS 2013) are given in Table 2.2. Similar to CSA A371-04 (CSA 2004a), requirements are given within a temperature range of about 4.0 ºC. However, some differences are observed. For example, in CSA A371-04 (CSA 2004a) the minimum temperature requirements were based on the temperature of mortar constituents. However, ACI 530.1-13/ASCE 6-13/TMS 603-13 (ACI/ASCE/TMS 2013) restricts the temperature range of the mortar mixture. In addition, the maximum allowed mortar temperature to avoid flash setting by CSA A371-04 (CSA 2004a) is 50ºC, while ACI 530.1-13/ASCE 6-13/TMS 603-13 (ACI/ASCE/TMS 2013) allows temperatures up to 60ºC. In addition to the requirements listed in

Table 2.2, according to ACI 530.1-13/ASCE 6-13/TMS 603-13 (ACI/ASCE/TMS 2013) masonry units which are frozen or have temperature below -6.7 ºC should not be laid.

Table 2-1- Cold weather masonry construction requirements according to CSA A371-04 (CSA 2004a)

Air temperature, ºC	**General requirements during construction**
0 to 4	Sand or mixing water shall be heated to a minimum of 20 ºC and a maximum of 70 ºC.
–4 to 0	Sand and mixing water shall be heated to a minimum of 20 ºC and a maximum of 70 ºC.
–7 to –4	1- Sand and mixing water shall be heated to a minimum of 20 ºC and a maximum of 70 ºC. 2- Source heat shall be provided on both sides of the walls under construction. 3- Windbreaks shall be employed when the wind speed exceeds 25 km/h.
–7 and below	1- Sand and mixing water shall be heated to a minimum of 20 ºC and a maximum of 70 ºC. 2- Enclosures and supplementary heat shall be provided to maintain an air temperature above 0 ºC. 3- The temperature of the unit when laid shall be not less than 7 ºC.

Table 2-2-Cold weather masonry construction requirements according to ACI 530.1-13/ASCE 6-13/TMS 603-13 (ACI/ASCE/TMS 2013)

Ambient air temperature, ºC	**Construction Requirements**
4.4 to 0	Water or sand has to be heated to give a mortar mixture temperature between 4.4ºC to 48.9ºC.
0 to -3.9	All requirements in previous section plus maintain the mixture temperature before laying the masonry. Grout water and aggregates should be heated to give temperature between 21.1ºC to 48.9ºC. Temperature should be kept to a minimum of 21.1 ºC before placement.
-3.9 to -6.7	All requirements in previous temperature range plus, Windbreak should be used if wind velocity is more than 24 km/h. All masonry under construction / and for grouting should be heated to 4.4ºC.
-6.7 and below	Masonry must be protected in an enclosure having temperature above 0 ºC.

2.1.2 **Cold Weather Masonry Systems Protection Practices**

Protecting constructed masonry wall segments from freezing is a key practice in cold climates. The commonly used techniques for warming and protecting constructed masonry segments are using electric and insulating blankets, tarps and heated enclosures as shown in Fig. 2.2(a). One of the concerns for using industrial heaters is that they usually do not provide uniform heat along the constructed segment. Therefore, the degree of hydration of mortar joints will vary along a

segment due to temperature gradients, which may lead to deformation of the constructed masonry segment (Essroc 2012b). For this reason, electric fans are often used in the field to evenly distribute the heat, as shown in Fig. 2.2(b). One of the other conventional heating methods is the use of fossil fuels. However, under certain conditions carbon dioxide emitted by fossil fuels may cause carbonation of the cementitious material which leads to durability concerns (Neal 2002). In addition, it is indicated that providing heated enclosures can incur additional cost up to 100% of the initial value of the project (Korhonen 2002).

2.1.2.1 North American Standards for Cold Weather Masonry Protection Requirements

Depending on the weather conditions and the mean daily temperature North American standards require different types of protections for masonry segments. For example, when the mean daily temperature is between 0 and 4.0^{o}C, CSA A371-04 (CSA 2004a) requires the contractors to protect the masonry section from precipitation for at least 48 h.

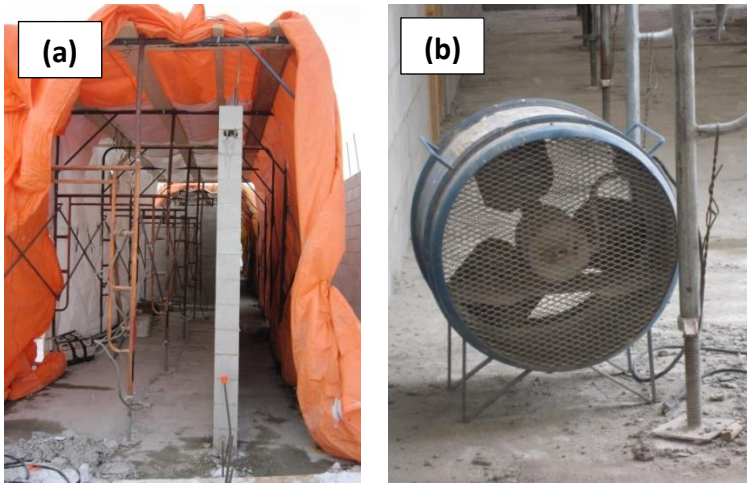

Fig. 2.2. Cold weather masonry protection practices: (a) protecting a masonry wall using tarps, and (b) utilizing electric fans for heat distribution.

According to CSA A371-04 (CSA 2004a) to protect the masonry segment after construction in cold weather, the practices listed in Table 2.3 should be followed. According to these requirements, it can be concluded that for all temperature ranges below 4^{o}C masonry should be protected for at least 48 h. Therefore, scaffolds are usually erected and used as the main structure for protecting the masonry in cold weather construction as shown Fig 2.2(a).

Table 2-3- Cold weather masonry protection requirements according to CSA A371-04 (CSA 2004a)

Mean daily temperature, °C	**Protection Requirements**
0 to 4	Masonry shall be protected from rain or snow for 48 h.
–4 to 0	Masonry shall be completely covered for 48 h.
–7 to – 4	Masonry shall be completely covered with insulating blankets for 48 h.
–7 and below	The masonry temperature shall be maintained above 0 ºC for 48 h. by enclosure and supplementary heat.

Table 2.4 lists the cold weather masonry protection requirements according to ACI 530.1-13/ASCE 6-13/TMS 603-13 (ACI/ASCE/TMS 2013). It can be noted that unlike the CSA A371-04 (CSA 2004a), ACI 530.1-13/ASCE 6-13/TMS 603-13 (ACI/ASCE/TMS 2013) requires a minimum a protection for only 24 h.

Table 2-4- Cold weather masonry protection requirements according to ACI 530.1-13/ASCE 6-13/TMS 603-13 (ACI/ASCE/TMS 2013)

Mean daily temperature, °C	**Protection Requirements**
4.4 to -3.9	Cover newly constructed masonry with a weather-resistant material for at least 24 h after construction.
-3.9 to -6.7	Cover newly constructed segments with insulating blankets for at least 24 h after construction. Protect grouted masonry for 48 h unless Type III cement is used in grout.
-6.7 and below	Maintain the masonry temperature above 0 by means of insulating blankets, infrared lamps, etc. for at least 24 h. Extend the protection time to 48 h for grouted masonry unless the cement used is Type III.

2.2 Application of Chemical Admixtures in Cold Weather Construction

Use of chemical admixtures is typically more cost effective than the thermal protection of the cement-based mixtures (Dolgikh and Rapoport 2005). Considerable amount of money which is dedicated to labor cost, heat, electricity and materials can be saved by using chemical admixtures (Korhonen 2002).

2.2.1 **Accelerators**

Accelerators are chemical admixtures in the form of powder or liquid which are added to the cementitious materials to accelerate the kinetics of hydration of cement and shorten the setting time. In cold weather, use of accelerators can help speeding up the masonry construction and

eliminate or minimize the protection requirements. However, accelerators neither heat the mortar mixture up nor depress the freezing point. Therefore, accelerators may not eliminate the need of insulations (Throop 2005). Accelerators are divided into two major groups: 1- soluble inorganic salts and 2- soluble organic salts. The most effective soluble inorganic salts used for accelerating the hydration of cement are calcium based salts such as calcium chloride and calcium nitrate. Calcium chloride is considered as the most effective accelerator for cementitious mixtures, as at a low dosage of about 2% it can double the compressive strength at one day (Mindess *et al.* 2003). However, the addition of this admixture to cementitious materials promotes the corrosion issues with metallic inserts (Korhonen 1990). Organic accelerators used in cementitious materials are: calcium formate, calcium acetate and triethanolamine. However, studies have shown that organic accelerators may provide flash setting or retardation if the proper dosage is not used (Mindess *et al.* 2003). The use of accelerators in cementitious materials is not covered further beyond this point as according to clause 5.5.4 of CSA A179-04 (CSA 2004a), using any kind of accelerators for shortening the setting time in masonry mortars is prohibited.

2.2.2 **Antifreeze Admixtures**

Under very cold conditions, cementitious materials may freeze before setting. In this situation the use of accelerators may be not sufficient for minimizing the effects of cold weather on masonry construction, as accelerators do not prevent the mortar mixture from freezing (Korhonen 2002). Therefore, admixtures that depress the freezing point of water have been developed. Antifreeze admixtures are normally alcohol based (e.g., polyethylene glycol) and their use allow the cementitious matrix to set at low temperatures. However, it has been reported in the literature that antifreeze admixtures significantly affect bond strength of the masonry mortar and masonry units (Brick Industry Association 2006). This might be the reason for

prohibition of the use of any type of antifreeze admixtures in masonry mortar by CSA A179-04 (CSA 2004a).

2.2.3 **Water-Reducing Admixtures**

Water-reducing admixtures are generally added to the cementitious materials in order to reduce the water demand for the desired workability. They basically free the bound water molecules in the agglomerated paste by repelling and dispersing the cement particles (Mindess *et al*. 2003). Providing the cement content of a cementitious material is constant, the introduction of water-reducing admixtures reduces the w/c (water-to-cement) ratio of the matrix. The lower w/c ratio improves the compressive strength of the mixture at all the ages. It also reduces the porosity and enhances the long-term durability of the cementitious matrix (Mindess *et al.* 2003). Water-reducing admixtures are generally classified into three groups of low-range water-reducing admixtures, mid-range water-reducing admixtures and high-range water-reducing admixtures (HRWRA) based on their performance to reduce the water demand. The low-range water reducing admixtures reduce the water demand by about 5% and are classified as Type A according to ASTM C494 (ASTM 2013a). High-range water reducing admixtures or superplasticizers (classified as Type F) reduce the water demand of the cementitious mixture by up to 30%. The increased compressive strength at early ages (1 and 3 days) may be helpful to discount the effect of cold weather on the strength development rate. Therefore, some researchers have studied the effect of a combination of water-reducers and accelerators for cold weather construction as discussed in the following section. However, the high dosages of water-reducing agents has shown to impart delaying effect on the hydration reaction of cement (Mindess *et al.* 2003).

2.2.4 **Cold Weather Admixture Systems**

Cold weather admixture systems (CWAS) are chemical compounds added to the cement-based materials during cold weather construction. These admixtures are incorporated to depress the freezing point and accelerate the hydration rate of cement paste at the same time (ACI 2010). ASTM C1622-10 (ASTM 2010a), defines cold weather admixture systems as the admixture added to concrete when the temperature is below -5°C. Cold weather admixture systems are usually composed of accelerators and antifreeze compounds. However, high dosages of accelerators (chlorides, nitrates and nitrites) have also been found to impart beneficial effect on depressing the freezing point of water (Mindess *et al.* 2003). Hence, calcium-based (calcium nitrate, calcium nitrite, calcium chloride) accelerators are sometimes used as CWAS. For example, studies have shown that high dosage (6% by mass of cement) of calcium nitrate can depress the freezing point and accelerate the hydration of cement. Karagol *et al.*(2013) studied the effect of calcium nitrate addition at a dosage of 6% by mass of cement to concrete mixtures at a temperature range of -5 to -20^{o}C. The compressive strength results indicated that the mixtures containing calcium nitrate had higher compressive strength after 7 days of curing at cold temperature. For example, the compressive strength of the mixtures containing calcium nitrate was about 453% higher than that of the control mixture at -5^{o}C. However, the effect of calcium nitrate diminished as the temperature was dropped. For example, the improvement of the compressive strength was reduced to about 230% when the curing temperature was -20^{o}C compared to the control mixture.

In a study by Korhonen and Orchino (2001), the effect of different combination of chemical admixtures was assessed on the setting time and the compressive strength of mortar mixtures at -5^{o}C. The results indicated that with a combination of two different types of commercial accelerators and water reducing agents, the freezing temperature of the mortar

mixture was reduced to about -5^{o}C, while the control sample froze at about -2^{o}C. However, the water reducing agent imparted a delaying effect on the mixture so that the initial and final setting times were about 2 h longer than that of the control mixture. Therefore, using a combination of chemical admixtures may depress the freezing point of water but may not accelerate the hydration and eliminate the need for heat and protection (Arslan *et al*. 2011). Barna and Korhonen (2012) also studied the effect of combination of different chemical admixtures on concrete and concluded that by combining the admixtures (accelerators, water reducing agents, etc.), freezing point of concrete can be reduced to -5^{o}C. However, the effectiveness of CWAS is a function of ambient condition in a sense that different ambient temperatures lead to different setting time and compressive strength values (Karagöl *et al.* 2013).

Yet, use of neither accelerators nor antifreeze admixtures to produce CWAS is currently allowed in masonry construction according to clause 5.5.4 of CSA A179-04 (CSA 2004b). In addition, more investigations on the effect of cold weather chemical admixtures on cement-based materials are still needed. For example, insufficient data are available regarding the durability performance of the mixtures incorporating CWAS. An innovative approach to address cold weather masonry construction issues might be to investigate the effect of novel supplementary cementing materials (SCMs) (e.g. nanoparticles) on masonry mortar properties at cold temperature (5 ± 1°C). Hence, in the following sections, the effects of nanoparticles on properties of cement-based materials at are reviewed.

2.3 Application of Nanoparticles in Cement-Based Materials

2.3.1 **Nanoparticles**

The technology of the production of nanoparticles (particle size in the range of 1 to 100 nm) was originally introduced by Nobel laureate, Richard P. Feyman in 1959. His invention let scientists

to use the nano-sized particles in different disciplines such as physics, biology, chemistry and engineering. Nanoparticles can be produced by two main mechanisms, as shown in Fig. 2.3. The first mechanism is called “top-down” method. In this method the larger particles are ground down to nanoscale without any alteration to their molecular composition. The second method implements the opposite approach. In this approach, the molecules of the materials are engineered and aggregated together to form a nanoscale particle. This method is referred as “bottom-up” approach. Most of the nanoparticles used in cementitious materials are produced by the “top-down” method(Sanchez and Sobolev 2010).

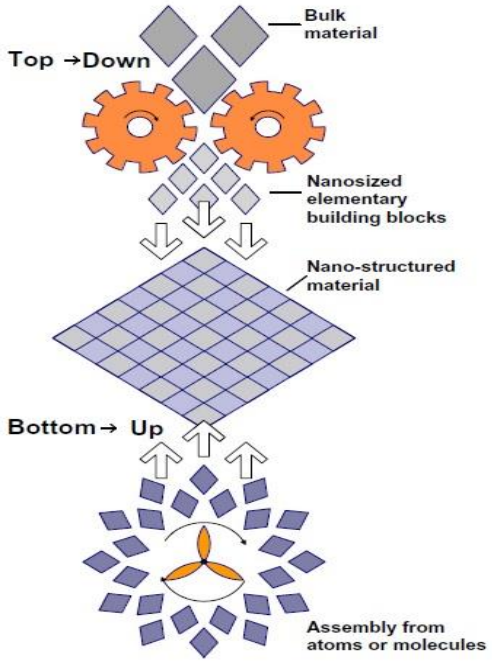

Fig. 2.3. Schematic of nanotechnology production methods, reproduced from Sanchez and Sobolev (2010), with permission from Elsevier.

Nanoparticles are added to cementitious materials with the purpose of enhancing the mechanical and durability properties. The high surface-to-volume ratio of nanoparticles (specific

surface area, SSA) provides nucleation sites for chemical reactions. Their ultrafine nature provides more surface area to react with cementitious phases (Fig. 2.4); for instance, a nanoparticle with a size of 4 nm has more than 50% of its atoms at the surface (Senff *et al.* 2009). Nanoparticles also work as fillers to densify the microstructure of a cementitious material and reduce the porosity (Ji 2005; Kawashima *et al*. 2013). In addition, nanoparticles are sometimes introduced into the cementitious matrix to add new properties to the mixture. For example, they have been added to cement-based materials to provide self-healing, self-cleaning and low electrical resistivity properties.

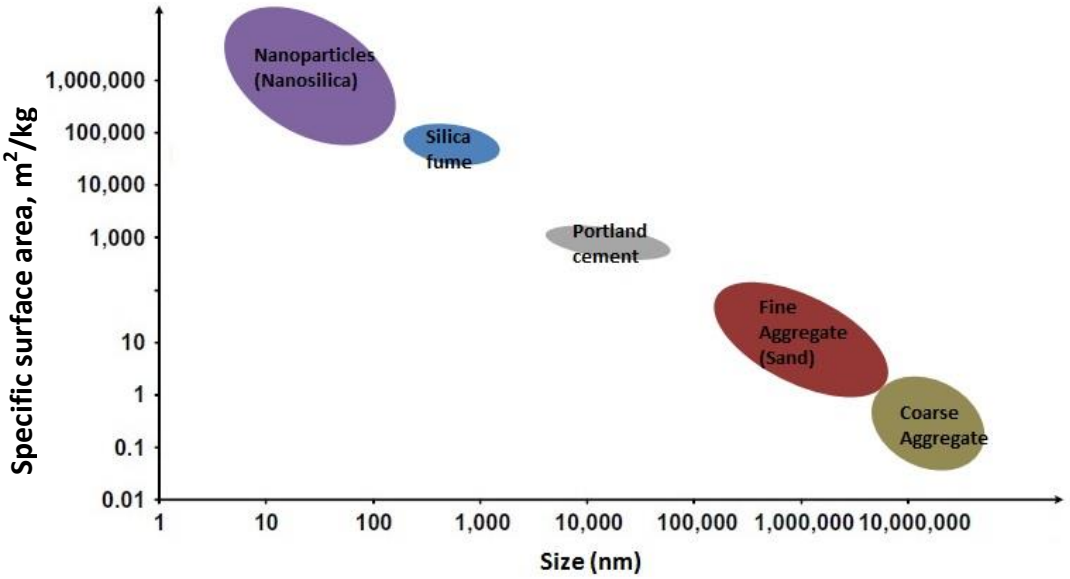

Fig. 2.4. Comparison of the size and SSA of nanoparticles and other concrete constituents, reproduced from Sanchez and Sobolev (2010).

2.3.2 **Chemistry and Hydration of Cement**

Upon the creation of portland cement by Joseph Aspdin in 1824, by calcinating ground limestone and clay, the use of cement rapidly increased all around the world due to its superior properties

compared to hydraulic lime and clayey materials. Portland cement is mainly composed of four raw materials: Lime (CaO), Silica (SiO_2), Alumina (Al_2O_3) and Iron oxide (Fe_2O_3) (Mindess *et al. 2003)*. To produce portland cement, raw materials are primarily ground, blended and preheated. Then the mixture of the raw materials is sent to a rotary kiln at 1500°C to produce cement clinker. The clinker is then ground with other additives (e.g. gypsum) and impurities to a fine powder. After cooling and crystallization of cement particles the major constituents of a portland cement particle are formed, as listed in Table 2.5. Tricalcium silicate (C_3S) is mainly responsible for early hydration strength (70% hydrates by 28 days) while, dicalcium silicate (C_2S) does not contribute to the early strength development of a cementitious matrix as it mostly reacts after 28 days. C_3A does not significantly contribute to the strength; however, it evolves large amount of heat at the early stage of the hydration process (Hewlett and Massazza 2003; Neville 1996).

Upon the introduction of water to cement particles, C_3S and C_2S start to form the hydration products according to the following equations:

$$2C_3S + 6H \rightarrow C_3S_2H_{3+} 3CH \quad \text{(Eq. 2.1)}$$

$$2C_2S + 4H \rightarrow C_3S_2H_{3+} CH \quad \text{(Eq. 2.2)}$$

In a hydrated cement particle, calcium silicate hydrate ($C_3S_2H_3$) has a fibrous crystalline structure and is responsible for the strength of the matrix. The exact chemical combination of calcium silicate hydrate is still not fully understood; therefore in the literature calcium silicate hydrate is usually denoted as C-S-H (Mindess *et al.* 2003). Calcium hydroxide (CH) is another hydration product of hydration of C_3S and C_2S which does not significantly improve the mechanical properties of a cementitious matrix. CH which is also termed portlandite may react

Table 2-5- Portland cement main constituents

Compound name	Chemical Formula	Chemical Notation	Approximate Mass Percentage
Tricalcium Silicate (Alite)	Ca_3SiO_5	C_3S	40-70%
Dicalcium Silicate (Belite)	Ca_2SiO_4	C_2S	20-40%
Tricalcium Aluminate	$Ca_3Al_2O_6$	C_3A	10%
Tetracalcium Aluminoferrite	$Ca_4Al_2Fe_2O_6$	C_4AF	8%

with other substances (sulfates, etc.) to form deleterious products which affect the durability of the cementitious material (Neville 2004; Skalny *et al.* 2002). The hydration of C_3A produces huge amount of heat and causes rapid setting of the cementitious matrix. To decrease the amount of the released heat and delay the setting time, calcium sulfate dehydrate (gypsum) is usually interground with clinker. Therefore, upon addition of water, C_3A reacts with gypsum and water to form another hydration product called ettringite ($C_6AS_3H_{32}$) as follows (Hewlett and Massazza 2003; Mindess *et al.* 2003):

$$C_3A+3CSH_2+26H \rightarrow C_6AS_3H_{32} \qquad \text{(Eq. 2.3)}$$

A typical heat evolution curve for the hydration of calcium silicates (C_3S and C_2S) of portland cement is composed of five stages as shown in Fig. 2.5. At the first stage, large amount of heat is released from the sample due to the mechanical interaction between the particles during mixing. Calcium and hydroxyl ions are released and pH rises to about 12. At the second stage called dormant or induction period, the amount of released heat drops for about 4 h. The

hydrolysis continues until a critical value of ions concentration is reached. At this point crystals of CH start to precipitate in the solution and C-S-H layers start to form on the calcium silicate phases. This period is important for determination of transport time of a mixture as it determines the initial setting time. At the third stage the rate of hydration reactions rise and the amount of evolved heat increases due to formation of hydration products. C-S-H forms a thick barrier on the surface of the calcium silicates for ingress of water. This stage denotes the final setting time of the cementitious mixture. During the fourth stage hydration reactions slow down as the C-S-H barrier gets thicker and the diffusion of water gets harder. This stage usually denotes the early strength of a mixture under normal temperature conditions. At the last stage, reactions continue to slow to a steady state as the diffusion of water decelerates. This stage denotes the later strength values (Hewlett and Massazza 2003; Mindess *et al.* 2003; Neville 1996) .

The main goal of this thesis is to assess the effect of two types of nanoparticles (nano-alumina [NA] and nano-silica [NS]) on the hydration of masonry mortar mixtures at a cold temperature of 5 ± 1°C. Hence, in the following sections, a review of the technical literature on NA and NS particles is presented.

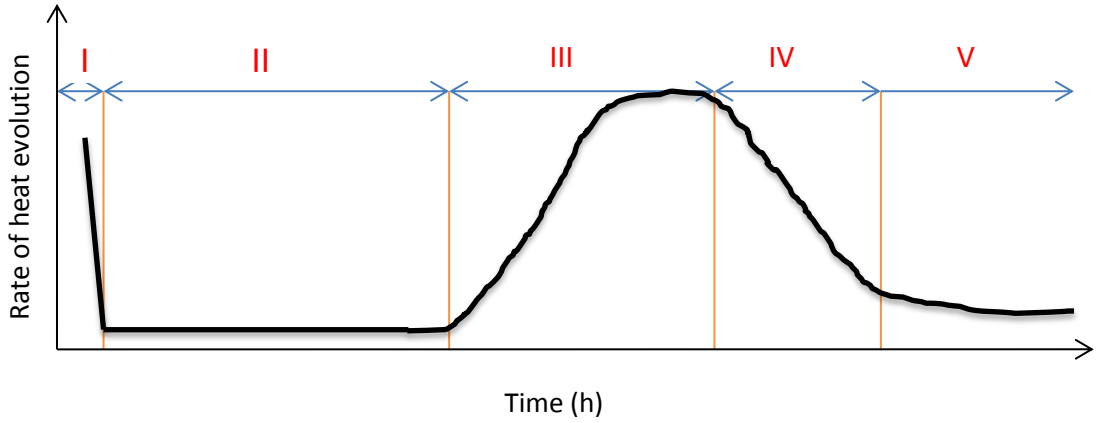

Fig. 2.5. Typical heat evolution rate curve of cement during hydration reproduced from Mindess *et al*. (2003).

2.3.3 **Nano-alumina (NA)**

Nanoscale particle of Al_2O_3, nano-alumina (NA), is one the nanoparticles that has shown to impart beneficial properties to cementitious materials. It has been reported that NA particles improve the compressive and flexural strengths of mortar mixtures and shortens the setting time by accelerating the hydration reactions and refining the pore structure under normal mixing and curing temperatures (22 ± 2˚C) (Campillo *et al.* 2007; Nazari *et al.* 2010a; Oltulu and Şahin 2011). It has also been shown by Li *et al.* (2006) that NA reduced the porosity of cement mortar at the interfacial transition zone (ITZ) and increased the modulus of elasticity.

Oltulu and Sahin (2011) studied the effect of NA, NS and nano-Fe_2O_3 on the compressive strength of cement mortars containing silica fume at normal mixing and curing temperature. NA was used at dosages of 0.5, 1.25 and 2.5% by mass of the cementitious binder and the compressive strength of the mortar samples was determined at 3, 7, 28, 56 and 180 days. In this study, it was concluded that NA generally improved the mechanical performance of the mortar mixtures containing silica fume. The authors observed an improvement in the compressive strength of all mixtures, except the mixture containing 2.5% NA at 3 and 7 days, as shown in Fig. 2.6. The improvement of the compressive strength was in the range of 10 to 20%, compared to the control specimen. In another study by Oltulu and Sahin (2013) the effect of 0.5, 1.25 and 2.5% NA was assessed on the compressive strength of mortar mixtures containing fly ash at 3, 7, 28, 56 and 180 days. The water-to-binder (w/b) ratio was maintained at 0.4 and the mixing and curing temperature was about 22 ± 2˚C. They concluded that the dosage of 0.5% NA did not significantly affect the compressive strength values at all ages. On the other hand the addition of 1.25% NA to the mortar mixtures seemed to slightly increase the compressive strength at all ages, while the dosage of 2.5% NA did not improve the compressive strength. It was concluded

that the effect of NA was less pronounced on the mixtures containing fly ash compared to the mixtures containing silica fume.

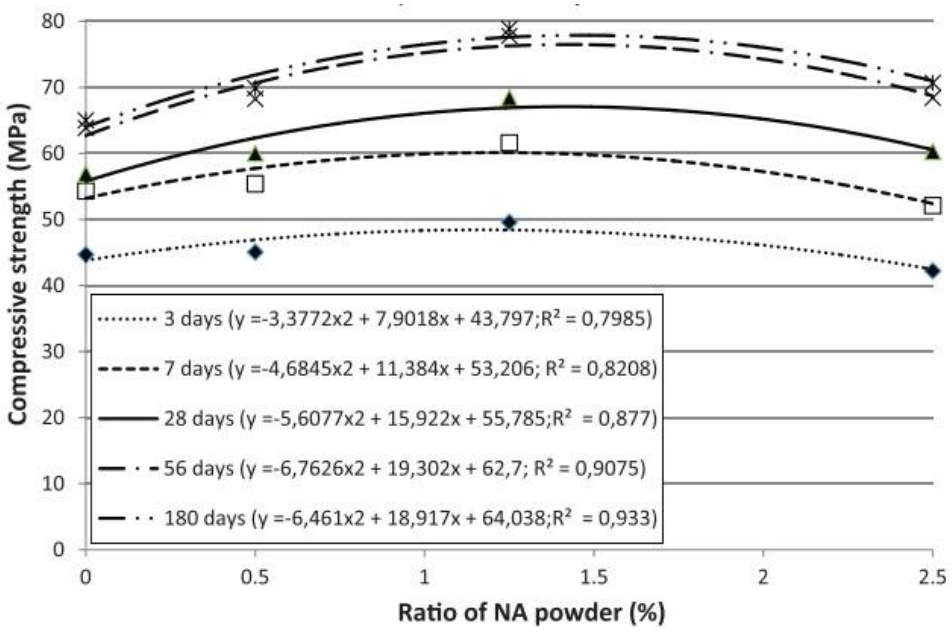

Fig. 2.6. Effect of NA on the compressive strength of mortar mixtures, reproduced from Oltulu and Şahin (2011), with permission from Elsevier.

In a study by Nazari *et al*. (2010b), NA was introduced to concrete mixtures prepared from ordinary portland cement at replacement dosages of up to 2% and w/b of 0.4. In this work the effect of the dosage of NA was investigated on the flexural strength and the setting time of concrete. It has been observed that with the introduction of NA, the flexural strength was increased and the initial and final setting times were shortened. The effect of NA on shortening the setting time was more pronounced as the dosage of NA increased. For example, when 2% of the mass of cement was replaced by NA, the initial and final setting times were about 42% shorter, as compared to the control mixture without NA. In another study by Nazari *et al.*

(2010a) with the same mixture design and curing conditions, the effect of NA on the slump and compressive strength of concrete samples was investigated. They observed that NA reduced the slump of concrete. The highest drop in the slump value was achieved when 2% (highest dosage of NA) was added to the mixtures which was about 75% of the control mixture's slump. The compressive strength of the mixtures increased as the dosage of NA increased up to 1.5%, at 7, 28 and 90 days. However, at a dosage of 2%, a comparable compressive strength to the control mixture was observed at all the ages.

The initial mechanical properties of belite cements with addition of NA were assessed by Campillo *et al*. (2007). In their study, mortar samples were prepared with a w/b ratio of 0.8 and mixed and cured under a normal temperature range of 22 ± 2˚C. The NA was added at dosages of up to 9% by mass of cement. The maximum increase in the compressive strength was achieved when the highest dosage of NA (9%) was added to the mixtures. This improvement was about 84 and 113% at 7 and 28 days respectively, compared to the control mortar. These findings are in conformance with the study conducted by Vikulin *et al.* (2011) on concrete mixture prepared in a sense that NA increased compressive strength of the concrete mixtures.

Li *et al.* (2006) investigated the compressive strength and modulus of elasticity of mortars containing different dosages of NA (3, 5 and 7% by mass of cement). The w/b ratio was 0.4 and the mixing and curing took place at a normal temperature (22 ± 2˚C). The addition of 7% NA to the mortar mixtures seemed to increase the compressive strength by 30% at 7 days, while other dosages of NA seemed to not significantly affect the compressive strength. However, in this study, the improvement of the modulus of elasticity was more pronounced. It was observed that when 5% NA was added to the mixtures, the highest modulus of elasticity was obtained. This improvement was about 54, 141 and 143% at 3, 7 and 28 days, respectively.

In a study by Arefi and Sarajan (2012), the addition of NA to mortar mixture prepared from GU cement at dosages of 1, 3 and 5% by mass of cement seemed to affect the compressive, flexural and tensile strengths at 7 and 28 days. The compressive strength of the mortar samples increased as the dosage of NA increased to 3%. This improvement was about 80 and 200% at 7 and 28 days. However, higher dosages of (5%) seemed to mask the effect of NA on the mechanical properties of the mortar mixtures. The compressive strength of the mixture containing 5% NA was comparable to the control mortar mixture at both ages. A similar trend was observed for tensile and flexural strengths. For example, when 3% NA was added to the mixtures, the highest compressive strength was achieved. However higher dosages of NA led to strength values comparable to the control mixtures. It was concluded that that the filler effect of NA increased the mechanical properties of mortar mixtures.

Although limited data are published regarding the effect of NA on the properties of cementitious materials, results from current literature indicate that NA particles may improve the compressive strength, flexural strength and shorten the setting time of cement-based materials. NA seems to accelerate the hydration reactions at early ages and refine the pore structure under normal mixing and curing temperatures (22 ± 2˚C). Yet, no data was published on the effect of NA on cementitious systems mixed and cured at colder temperatures.

2.3.4 **Nano-silica (NS)**

The nano-sized particle of SiO_2 (NS) has shown to improve the fresh, hardened and durability properties of cementitious materials. The ultrafine nature of NS provides more surface area working as nucleation sites for hydration reactions. With addition of NS to cement-based materials, portlandite (CH) is converted to calcium silicate hydrate (C-S-H) via pozzolanic reaction as shown below (Senff *et al.* 2009, 2012).

$$Ca(OH)_2 + H_4SiO_4 \rightarrow Ca^{2+} + H_2SiO_4^{2-} + 2\ H_2O \rightarrow CaH_2SiO_4 \cdot 2\ H_2O \qquad \text{(Eq. 2.4)}$$

$$\text{Denoted as:} \quad CH + SH \rightarrow C\text{-}S\text{-}H \qquad \text{(Eq. 2.5)}$$

The secondary C-S-H formed by the pozzolanic activity improves the hardened and durability properties of cement-based materials.

Senff *et al*. (2009) studied the fresh properties of cement pastes and mortars incorporating NS. Under normal lab temperatures (22 ± 1˚C), GU cement was replaced by NS at dosages of 1, 1.5, 2 and 2.5%. The w/b was fixed at 0.35 and a superplasticizer was added at a dosage of 2% by mass of the binder to maintain the flowability. Their study revealed that, although superplasticizer was added to the mixtures, the flowability was reduced with addition of NS. The higher dosages of NS led to lower flow table values of the mortar mixtures. The flow value of the mixtures was reduced by about 33% at 2.5% NS, compared to the control mixture. They also indicated that increasing the dosage of NS by 1.5% (from 1 to 2.5%) decreased the flow value by about 20%. In addition to the flowability, the setting time of the mixtures incorporating NS was shortened, where it was indicated that the mortar mixture with 2.5% NS was not flowable after 75 min. As depicted in Fig. 2.7, at a dosage 2.5% NS, it was shown that the initial and final setting times were shortened by about 60%, compared to the mixtures without NS. The hydration temperature of the cement pastes measured by use of thermocouples showed that mixtures containing NS required less time to reach to the peak temperature. For example, for the mixtures containing 2.5% NS the peak was reached about 10 h earlier than the mixture without NS. This showed that NS accelerated the kinetics of hydration which led to shortened setting times. NS seemed to decreases the apparent density of the mortar mixtures. This led to increased air content of the mixtures. For example, the air content was increased by 79% for the mixtures containing 2.5% NS as compared to the control mixtures.

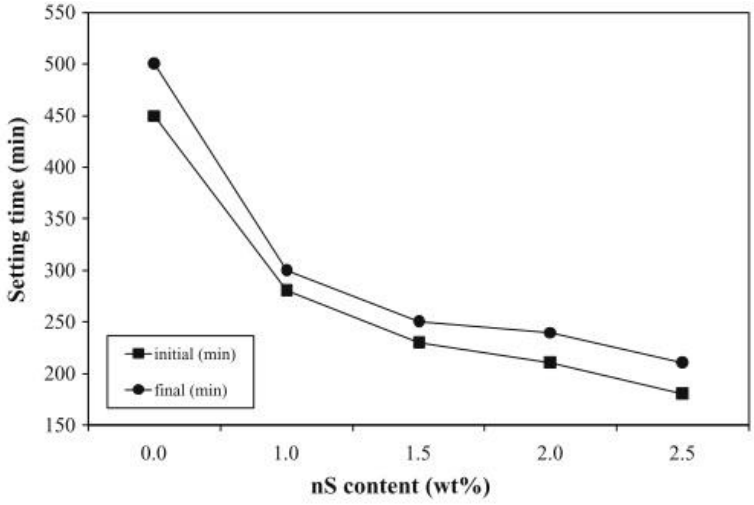

Fig. 2.7. Setting time of mortar mixtures incorporating NS, reproduced from Senff *et al*. (2009), with permission from Elsevier.

Another study was conducted by Senff *et al.* (2010) on the effect of NS and micro-silica (particle size of 0.1 to 100 μm) on the properties of cement pastes and mortars. In this study, they assessed the microstructural and hardened properties of the mixtures containing 3.5% NS by mass of cement, prepared and cured at 21˚C. The compressive strength results at 7, 28 and 90 days yielded an improvement of about 14, 20 and 11% for the mixtures incorporating 3.5% NS as compared to the mixtures without NS. They concluded that the high SSA of the NS increased the compressive strength at early ages (7 days). However, at later ages the improvement of NS was mostly related to the pozzolanic effect and consumption of CH as was shown by XRD (X-ray diffraction) analysis. Although superior mechanical properties were observed in the mixtures containing NS, the SEM micrographs from their samples showed that the NS was not properly dispersed. This suggested that with proper dispersion of NS, better performance can be expected.

The effect of NS was evaluated in another investigation by Senff *et al.* (2012) on mortar mixtures prepared with ordinary cement and w/b of 0.5 under normal temperature conditions (22

± 1˚C). In their experiment NS was added at a dosage range of 0 to 1.3% by mass of cement. Similar to their previous studies, they concluded that the addition of NS decreased the flowability of the mixtures. The hydration temperature curve of the mixtures containing NS showed that the temperature peak was higher and reached about 2 h earlier than that of the mixture without NS, when 1.3% NS was added to the mixtures. The measurement of the compressive strength at 28 days showed that the compressive strength was increased by only 3.7 MPa for the mixtures containing 1.3% NS compared to the control mixtures.

The microstructural and mechanical properties of concrete samples containing NS were studied by Said *et al.* (2012) under mixing and curing temperature of 23 ± 2˚C. In this study the effect of NS on the concrete mixtures containing Type II portland cement and Type II portland cement with fly ash (replacement level of 30%) was assessed. The w/b ratio was maintained at 0.4 and HRWRA was added to achieve the desired slump. The results from the heat evolution rate of the mixtures containing NS revealed that the hydration peak temperature of the mixtures containing NS occurred earlier than that of the control mixtures, regardless of the incoporattion of fly ash. For the mixtures without fly ash, the peak temperature of the mixture containing 3% NS was reached after 10 h, which is about 4 h earlier than the control sample (Fig. 2.8). However, 6% NS seemed to be less effective than the 3%NS as its peak occurred about 2 h before the control mixture. Although the addition of NS accelerated the kinetics of hydration of the mixtures with fly ash, the effect of higher dosages of NS (6%) seemed to be less significant, compared to the mixtures containing 3% NS. For these mixtures the hydration peaks were almost overlapped after about 10 h. The earlier temperature peak revealed the acceleration effect of NS on the kinetics of hydration by providing nucleation sites for hydration of cement. The compressive strength of the samples was measured at 3, 7 and 28, 90 and 365 days. Results

showed an improvement in the compressive strength of the concrete mixtures containing NS and Type II portland cement at all ages. For example, at 3 and 7 days the compressive strength of the sample containing 6% NS was 39 and 58 MPa. These values showed about 18% improvement of the compressive strength compared to the control mixtures. It was concluded that the higher compressive strength of the mixture incorporating NS can be related to its physical and pozzolanic effects on the cementitious binder. This was supported by microstructural observations as refined and densified ITZ was detected for the mixtures containing NS *(Said et al.* 2012).

The compressive strength of concrete and mortar samples containing NS prepared from (OPC) ordinary portland cement was measured at 3, 7 and 28 days by Vera-Agullo *et al.* (2009).They found that the compressive strength of the mixtures containing NS was superior to the control mixtures at 3, 7, 28 and 56 days. This improvement was about 26, 12 and 4% compared to the control specimen at 3, 7 and 28 days, respectively.

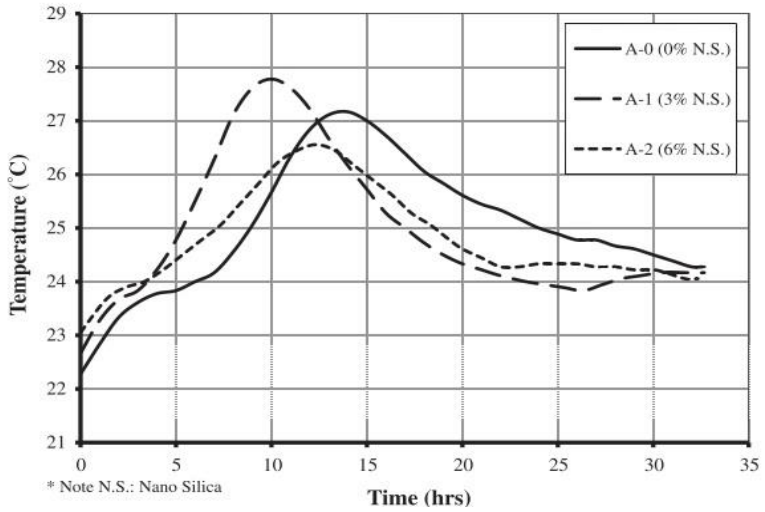

Fig. 2.8. Temperature of concrete incorporating 3 and 6% NS, reproduced from Said *et al.* (2012), with permission from Elsevier.

Jo *et al.* (2007a) studied the effect of different water to cementitious materials ratios (w/cm) of 0.23, 0.25, 0.32, 0.35 and 0.48 on the mortar mixtures incorporating different dosage of NS. The NS dosages in their study were 3, 6, 9 and 12% by mass of cement. In this research they compared the results obtained from NS and silica fume and concluded that for all mixtures NS resulted in better performance in terms of compressive strength at 7 and 28 days. The heat evolution curves revealed that the dormant period of the mixtures containing NS was shortened by about 2 h, compared to the mixtures without NS. The hydration temperature curve also indicated that the hydration peak of the samples containing NS was higher than the plain sample. The SEM micrographs showed a reduction of the CH content at the age of 7 days for the mixtures containing NS. The incorporation of NS led to superior microstructural and hardened features at all w/c. In another study by Jo *et al*.(2007b) the effect of 3, 6, 10 and 12% by mass of cement NS on the compressive strength (at 3 and 28 days) and the microstructure of mortar samples was investigated. In this work the w/c ratio was selected at 0.5 and a superplasticizer was added for obtaining the desired flowability. It was observed that the mortar mixtures containing up to 12% NS had higher compressive strength values at 3 and 28 days. The compressive strength for these mixtures was 280 and 270% higher than the control sample. As shown in Fig. 2.9. Again, the micrographs of mortar mixture containing NS showed a densified and compacted microstructure as compared to the mixture without NS.

The beneficial effect of NS was also investigated in sludge/fly ash mortars by Lin *et al.* (2008). The w/b was 0.7 and the dosage of the NS was selected at 1, 2, and 3% under normal temperature of 22 ± 2˚C. They observed that the addition of NS at all dosages improved the delaying effect of sludge and fly ash on the mortar by its filler and pozzolanic effect. The

introduction of NS accelerated the hydration of the mortar samples and improved the compressive strength at 28 days.

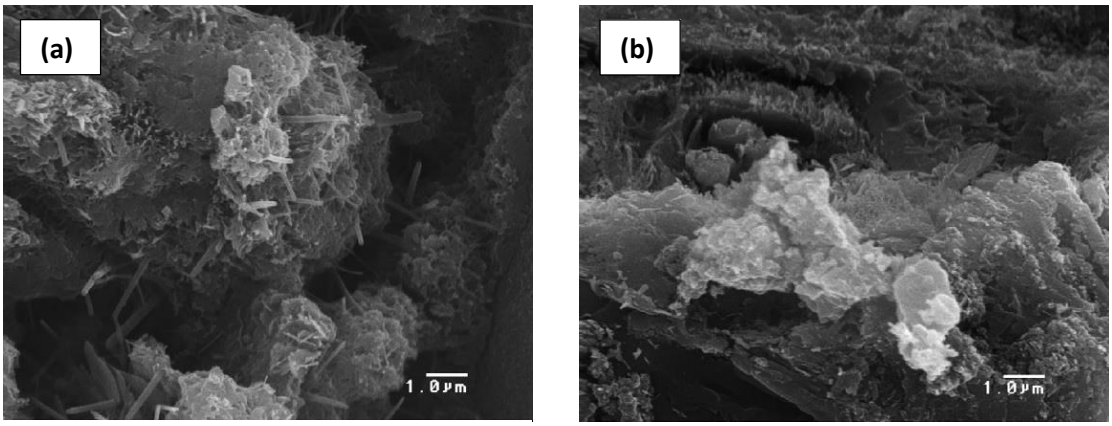

Fig. 2.9. Microstructure of mortar mixtures: (a) without NS, and (b) with NS, reprinted from Jo *et al*. (2007), with permission from Elsevier.

The results from other studies (Bjornstrom *et al.* 2004; Guefrech *et al*. 2011; Oltulu and Şahin 2013; Shih *et al.* 2006) about the effect of NS on the fresh, hardened and durability properties of cement-based materials are in agreement with the aforementioned trends. Generally, all these studies have shown that the addition of NS accelerates the kinetics of hydration, shortens the dormant period and the setting time and improves the compressive strength of any cementitious material. This is mainly related to their filler effect and ultrafine size which accelerates the hydration C_3S (Bjornstrom *et al.* 2004). It has also been shown by thermal and microstructural analyses that the mixtures containing NS have lower amount of CH and a densified and refined microstructure. The lower amount of CH is related to the pozzolanic reaction of NS by which CH is converted to C-S-H. As a result, higher compressive strength values were obtained at later ages and porosity was less for the mixtures containing NS. This ensures better hardened properties and durability performances.

2.4 Closure

In this chapter, the key issues and the practical mitigation methods of cold weather masonry construction were discussed. However, these mitigation methods impart concerns for the masonry industry. For example, extra cost should be allocated for implementing the heating and protection practices. Also, special consideration is required for preparing mortar mixtures to comply with temperature limits required by standards, which slows down the productivity rate of masonry construction. In addition to the conventional mitigation methods, the application of different types of chemical admixtures in cold weather masonry construction was explained. Although they may be beneficial for minimizing the cold weather masonry construction issues, use of any kind of chemical admixtures is currently prohibited in masonry construction according to clause 5.5.4 of CSA A179-04 (CSA 2004b).

Various studies (Damasceni *et al.* 2002; Givi *et al.* 2011; Jo *et al.* 2007; Oltulu and Şahin 2011, 2013; Senff *et al.* 2009; Sonebi *et al.* 2012) have shown that NA and NS positively affect the properties of cementitious materials under normal mixing and curing temperatures (22 ± 2˚C). They improve the compressive and flexural strengths of mortar mixtures and shorten the setting time by accelerating the hydration reactions and refining the pore structure. However, there is only one published study about the effect of nanoparticles on the properties of cementitious materials at lower temperatures (10˚C) by Camiletti *et al*. (2012), which justifies the need for research in this area. Hence, the main motivation of this research which investigates the effect of NA and NS on the hydration of masonry mortar joints in early fall periods (temperature threshold of 5 ± 1 ˚C) is an attempt to address some of the issues for cold weather masonry construction.

3 EXPERIMENTAL PROGRAM

In this chapter, all the materials, mixture design and experimental methods used in the current research program are described.

3.1 Materials

The two types of cement used in this study to prepare Type S masonry mortars were masonry cement Type S meeting CSA A3002-08 (CSA 2008a), and GU cement meeting CSA A3001-08 (CSA 2008b). Hydrated lime was added to the mixtures prepared from the GU cement according to CSA A179-04 (CSA 2004b). The chemical composition and physical properties of the cements and hydrated lime are listed in Table 3.1. Local masonry sand with a maximum particle size of 5 mm, specific gravity of 2.65, and absorption of 2% was used to prepare the mortar mixtures. Sieve analysis test was performed on the sand to confirm its suitability for masonry mortar according to Table 1 in CSA A179-04 (CSA 2004b). Colloidal nanoparticles used in this study were nano-SiO_2 (NS) and nano-Al_2O_3 (NA). The colloidal NS had solid amorphous silica (SiO_2) content of 50% by mass, mean particle size of 35 nm, pH of 9.5, specific surface area of 80 m^2/g, and specific gravity of 1.4. The colloidal NA had a solid content of 20%, mean particle size of 50 nm, pH of 4.0, specific surface area of 170 m^2/g, and specific gravity of 1.19. To maintain the flowability of mortars within a desirable range, high-range polycarboxylate polymer-based water-reducing agent (HRWRA) meeting ASTM C494-13 (ASTM 2013a) was added to the mortar mixtures. Standard concrete masonry units (390×190×190 mm) with specified compressive strength of 30 MPa were used for fabrication of masonry prisms and the pull-off tests.

Table 3-1- Chemical and physical properties of cements and hydrated lime

	GU Cement	Type S Masonry Cement	Hydrated Lime
Chemical Composition			
SiO_2 (%)	19.5	17.5	--
Al_2O_3 (%)	4.5	4.6	--
Fe_2O_3 (%)	3.0	2.0	--
CaO (%)	61.1	58.9	--
MgO (%)	4.4	2.1	--
SO_3 (%)	3.0	2.6	--
Na_2O (%)	0.6	--	--
$Ca(OH)_2$ (%)	--	10	92-100
$CaCO_3$	--	37.5	--
LOI*	1.0	9.9	--
Physical Properties			
Fineness (m^2/Kg)	391	425	--
Specific Gravity	3.15	2.99	2.30

*Loss on ignition at 550°C

3.2 Methodology

Fourteen mixtures were designed according to CSA A179-04 (CSA 2004b) requirements for laboratory experiments. The mixtures were classified into two main groups: masonry (M) and portland (P) cements. Group M had a masonry cement-to-sand (C:S) volumetric ratio of 1:3, while group P was designed with a general use cement-to-hydrated lime-to-sand (C:HL:S) volumetric ratio of 1:1/2:4. Each group comprised seven mixtures (one control mixture, three mixtures containing NA and three mixtures comprising NS). The coding of mixtures designated the binder used and type and dosage of nanoparticles. For example, PHLC stands for a control

mixture containing GU portland cement and hydrated lime, whereas MS4 stands for a mixture prepared with masonry cement and 4% NS. The water-to-binder ratio (w/b) was maintained at 0.4 for all the mixtures. The target flow (110 ± 5%) for this study was attained by adding 2, 2.5 and 4.0% HRWRA by mass of binder to the control mixtures, mixtures containing NS and mixtures incorporating NA, respectively. NA and NS were added to the mixtures at dosages of 2, 4 and 6% by mass of cement. The mixture design proportions to prepare about 20 kg of mortar are shown in Table 3.2.

Table 3-2- Proportions of mortar mixtures (20 kg batch)

	Materials (g)	**MC**	**MA2**	**MA4**	**MA6**	**MS2**	**MS4**	**MS6**
Group M	Cement	3925	3925	3925	3925	3925	3925	3925
	NS	----	----	----	----	157	314	471
	NA	----	393	785	1178	----	----	----
	Sand	14219	14219	14219	14219	14219	14219	14219
	Water*	1570	1287	1005	722	1523	1476	1429
	HRWRA	79	180	184	187	100	102	104
	Materials (g)	**PHLC**	**PHLA2**	**PHLA4**	**PHLA6**	**PLHS2**	**PLHS4**	**PLHS6**
Group P	Cement	3870	3870	3870	3870	3870	3870	3870
	Hydrated lime	823	823	823	823	823	823	823
	NS	----	----	----	----	155	310	464
	NA	----	387	774	1161	----	----	----
	Sand	13165	13165	13165	13165	13165	13165	13165
	Water*	1877	1599	1320	1041	1831	1784	1738
	HRWRA	94	191	194	197	95	97	99

* The amount of water was adjusted by water content of NS and NA.

In this study, all materials were put at least one day before mixing/fabrication in a walk-in environmental chamber set at a temperature of 5 ± 1°C to simulate field conditions in late September and October in Canada. In addition, all mixing, casting and curing procedures were

conducted in this chamber, which was maintained at the same temperature (5 ± 1°C). The mortar mixtures were prepared in a 5-L planar-action high-shear mixer in four steps. At the first step, approximately one-third of the gauging water was mixed with sand for 30 s. Then, masonry cement or GU cement and hydrated lime were added and mixed for another minute. At the third step, NA or NS and HRWRA were added to the remaining water and mixed at high speed for about 20 s until a consistent solution was obtained. Finally, the solution was added to the mixture and blended for about 2 min. Mortar mixtures were cast into cube moulds (50×50×50 mm) for compressive strength test, differential scanning calorimetry (DSC) analysis and microstructural observations at various ages, as shown in Fig. 3.1. After 24 h, specimens were demoulded and cured in lime saturated water with lime concentration of 2 g/l. Four mixtures (MC, MS4, PHLC and PHLS4) were selected and used as mortar joints for fabrication of masonry prisms. The prisms were constructed at 5 ± 1°C by a certified mason inside the walk-in environmental chamber (Fig. 3.2). Subsequently, the prisms were covered by polyethylene sheets for 7 days and kept in the chamber until the age of testing.

Fig. 3.1. Partially demoulded masonry mortar cubes.

Fig. 3.2. Construction of the masonry prisms in the walk-in environmental chamber.

3.3 Test Methods on Masonry Mortar

Flowability of the fresh mortars was determined in conformance with the test method described in CSA A3004-C1-08 (CSA 2008c) by using a standard flow table (Fig. 3.3). For this test, the cone mold was put at the middle of the flow table and filled with mortar mixture to a thickness of about 25 mm which was tamped 20 times. Then, the cone was fully filled with the mortar mixture and tamped for 20 more times. Subsequently, mold was quickly removed and mortar was dropped 25 times in 15 s by rotating the flow table handle. Finally, the increase in the diameter was measured along the designated lines at 45° on the flow table. The measurements were averaged for calculation of flow value.

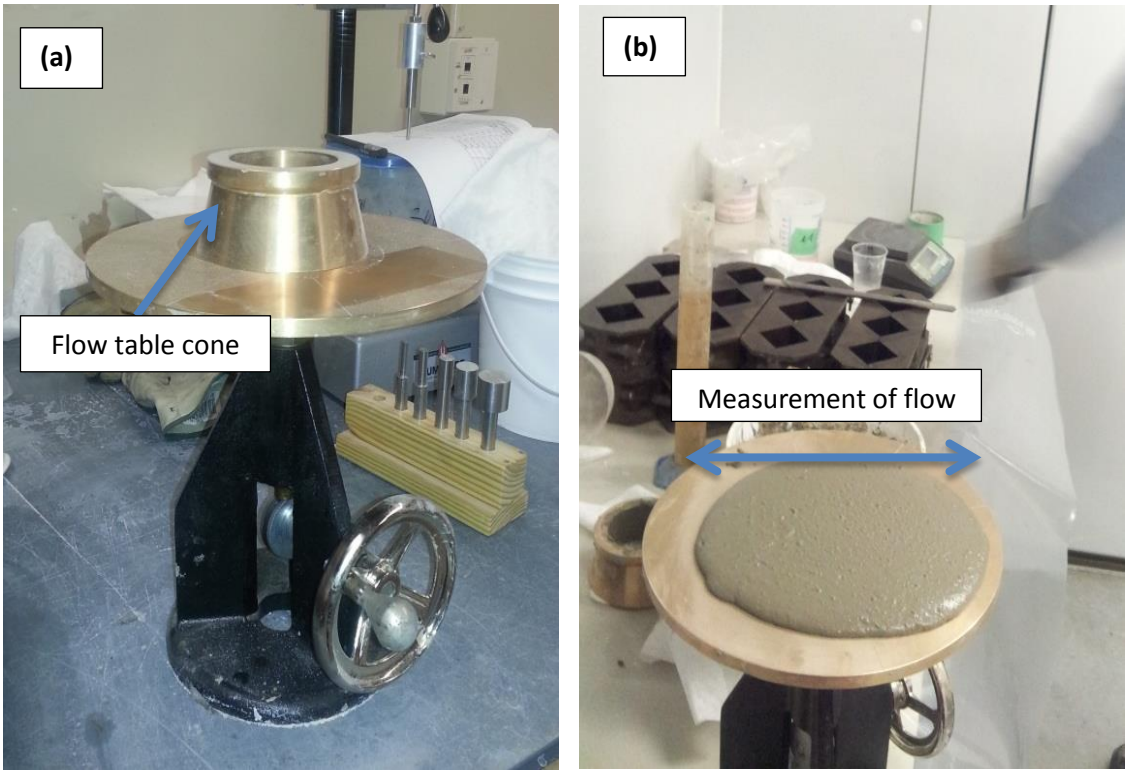

Fig. 3.3. Flow test: (a) flow table, and (b) flow of a masonry mortar mixture.

The air content of fresh mortar mixtures was determined according to CSA A3004-C4-08 (CSA 2008d), test method based on fresh mortar with a volume of 400 cm^3. For calculation of the air content, mass and density of the nanoparticles as well as the HRWRA were taken into consideration according to the following equation:

(Eq. 3.1)

$$D = \frac{cement\ mass + sand\ mass + water\ mass + HRWRA\ mass + nanoparticle\ mass}{\frac{cement\ mass}{Dc} + \frac{sand\ mass}{Ds} + \frac{water\ mass}{Dw} + \frac{HRWRA}{Dh} + \frac{nanoparticle\ mass}{Dn}}$$

Where:

D = density of the air-free mortar

Dc = density of cement,

Ds = density of sand, 2.65 g/cm^3

Dw = density of water, g/cm^3

D_h = density of HRWRA, g/cm^3

D_n = density of nanoparticle, g/cm^3

The air content was then calculated according to the following equation:

$$A = 100 - \frac{M}{4D} \quad \text{(Eq. 3.2)}$$

Where:

A = percentage of air content

M = mass of mortar, g

To study the evolution of the hydration process, hydration temperature of cement pastes, with the same mixture design of the paste component of the mortar mixtures, was determined by an isothermal calorimeter set at 5°C for approximately 7 days after mixing in conformance with ASTM C1679-14 (ASTM 2014), as shown in Fig. 3.4. The cement pastes were mixed in the environmental chamber and discharged into the test ampules. The mass of the samples was selected according to the reference samples in the isothermal calorimetry cells, which was about 5 g. Finally, ampules were capped and put in the test cells and the heat flow relative to the reference samples was recorded during the experiment by isothermal calorimeter.

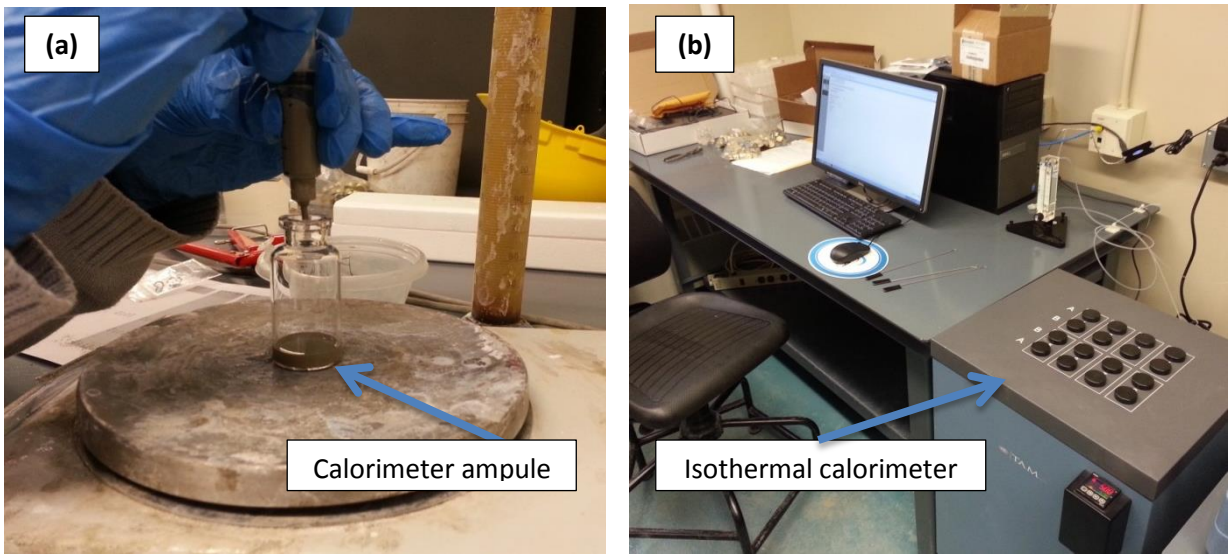

Fig. 3.4. Heat of hydration: (a) sample preparation, and (b) isothermal calorimeter.

The setting time test was conducted according to ASTM C403-08 (ASTM 2008) using ACME penetrometer (Fig. 3.5). Samples of mortar were placed in test containers and tested at different time intervals for the initial and final setting times of 3.5, and 27.6 MPa, respectively. The test was started by penetrating the largest needle, which gives the lowest penetration resistance value, and was progressed towards the smaller needles. At least eight penetration readings were recorded for each mixture to assure the accuracy of the setting time curves. For each reading the load was measured by the equipment and then divided by the area of the appropriate needle for calculation of the penetration resistance.

The compressive strength of mortar cube triplicates was determined at 1, 3, 7 and 28 days according to the method described in CSA A3004-C2-08 (CSA 2008e) using the MTS system shown in Fig. 3.6. For this test, mortar cubes were cast in cube molds in two layers and tamped 32 times. Two steel plates with dimension of 50 × 50 × 4 mm were put on the side surfaces of the cubes, the sides which were in contact with mold, and load was applied at a rate of 1000 N/s.

Subsequently, the failure was observed by a drop in the applied load and cracking of the mortar cubes.

Fig. 3.5. Setting time testing equipment (ACME penetrometer).

The microstructural analyses of the mortar samples were performed on carbon-coated thin sections (Fig. 3.7) having an age between 7 to 10 days by backscattered scanning electron microscopy (BSEM) and energy dispersive X-ray (EDX) (Fig. 3.8). These sections were prepared from vacuum-dried mortar slices which were cut using a diamond saw to a thickness of about 1 cm. The mortar slices were then impregnated in a low viscosity epoxy and glued on glass slides. At the final stage, samples were ground and polished to an average thickness of 30-50 µm.

Fig. 3.6. Compressive strength testing equipment of mortar cubes (Instron 300-DX).

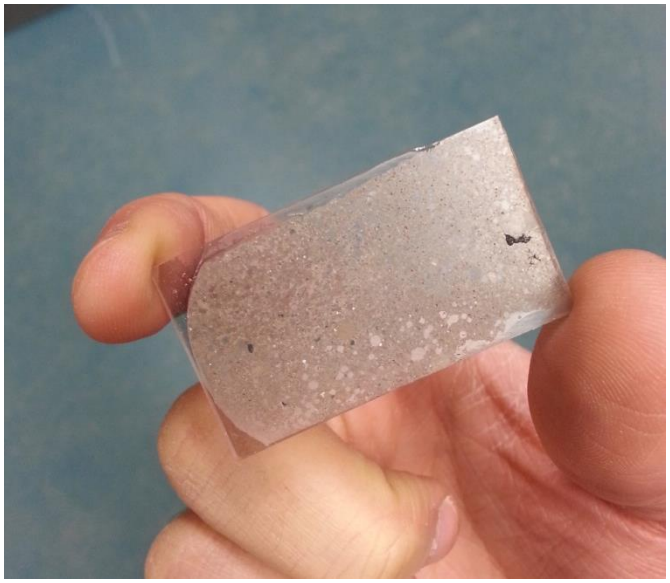

Fig. 3.7. An exemplar thin section prepared from the mortar samples.

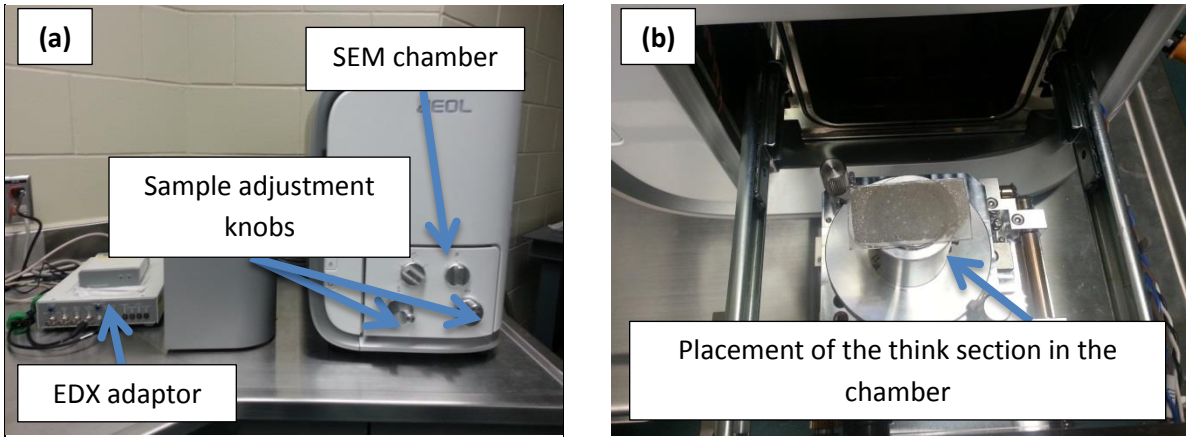

Fig. 3.8. (a) scanning electron microscopy (SEM) and energy dispersive X-ray (EDX) and, (b) placement of the sample.

To characterize the hydration products, differential scanning calorimetry (DSC) (Fig. 3.9) and thermogravimetric analysis (TGA) at a heating rate of 5°C/min was conducted on powder samples collected from the mixtures at different ages (3, 28 and 75 days). These samples were prepared by crushing and grinding the hardened mortar to a fine powder passing sieve #200 (75µm).

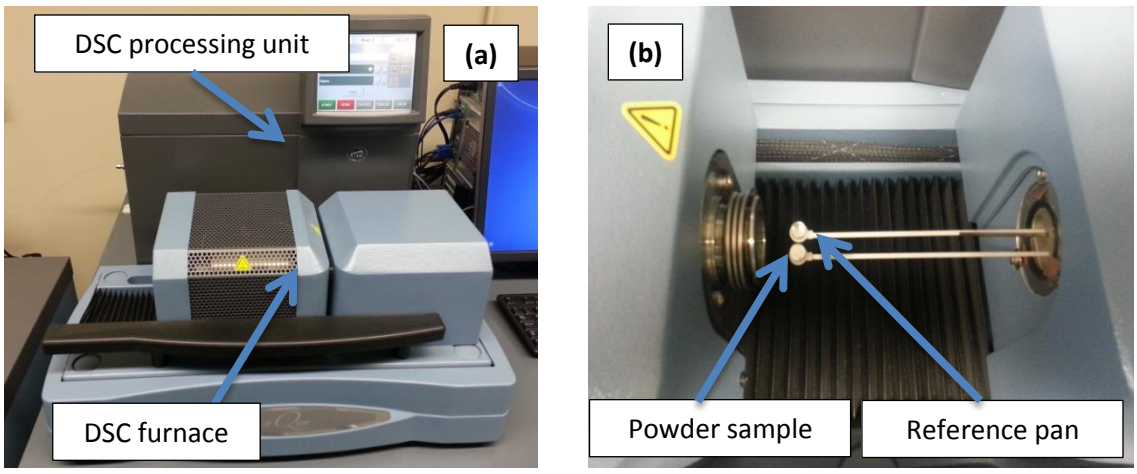

Fig. 3.9. (a) differential scanning calorimetry (DSC), and (b) placement of the sample.

3.4 Test Methods on Masonry Assemblies

The compressive strength and modulus of elasticity of the masonry prisms were determined according to ASTM C1314-12 (ASTM 2012a) and annex D of CSA S304.1-04 (CSA 2004c) on three course high masonry prisms, at the age of 3 and 28 days. As shown in Fig. 3.10, the masonry prisms were capped by use of plaster and loaded until failure. According to annex D of CSA S304.1-04 (CSA 2004c) load can be initially applied at any convenient rate up to the half of the ultimate load. The remaining load should be applied at rate that leads to failure between 1 to 2 min. In this study, the loading rate was adjusted and selected at about 85 N/s so that the failure of the specimens occurred in less than 4 min. Two pi gauges were put and centered on each side of the masonry prisms to measure strains, as shown in Fig. 3.10. The strains readings by the four pi gauges were recorded using data acquisition system (DAQ) and averaged for each prism to calculate the chord modulus of elasticity between 5 to 33% of the compressive strength.

The direct bond strength test (Fig. 3.11) was done by a direct tension (pull-off) method according to CSA A23.2-6B-14, Procedure B (CSA 2014). To prepare the specimens for this test, approximately 10 mm of mortar were laid on the side surface of CMUs to simulate the thickness of a mortar joint in a masonry assembly. Consequently, copper rings with a dimension of 50×10 mm were cut, lubricated and embedded in the fresh mortar, to prepare mortar discs and eliminate the effect of side friction. The mortar layer was then wrapped with plastic bags and two masonry units were placed on the assembly to simulate the condition of a 10 mm mortar joint in a masonry prism. The specimens were kept in the walk-in environmental chamber at 5±1˚C until the day of testing. The mortar discs were pulled off by the equipment and the load and mode of failure was recorded. Subsequently, the load was divided by the area and converted to bond strength.

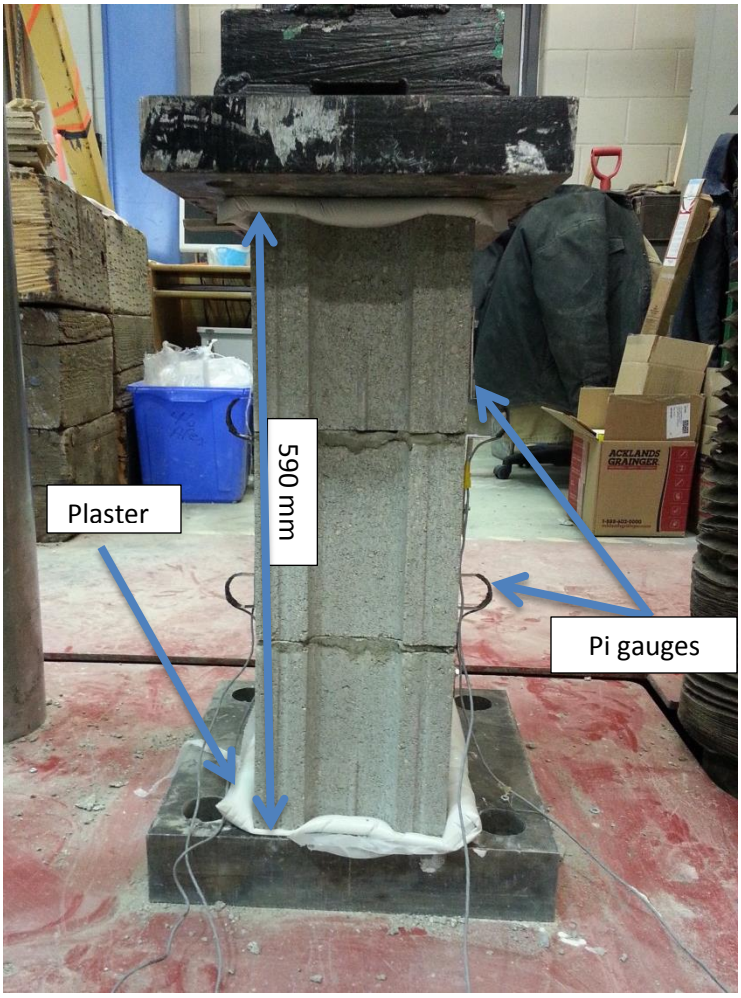

Fig. 3.10. Masonry prism compression test configuration.

In addition to the pull-off test method, the flexural bond strength of four course high masonry prisms were tested according to ASTM E72-13 (ASTM 2013b) and ASTM E518-10 (ASTM 2010b) at 3 days. ASTM E518-10 (ASTM 2010b) describes a procedure by which the constructed masonry prism is subjected to four point bending in a horizontal configuration. However, due to the fact that the hydration of cement is markedly delayed and the strength development rate is affected by the low temperature (5 ± 1°C); the mortar joints are highly

vulnerable at early ages. This promoted the chance of failure of the joint under the dead weight of the prism in the horizontal configuration at 3 days.

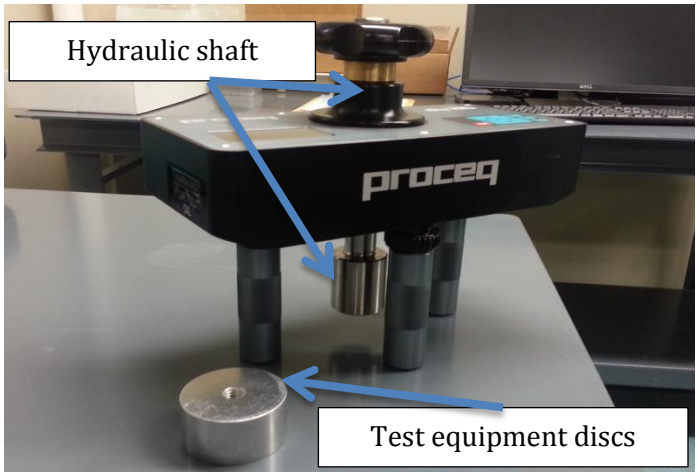

Fig. 3.11. Direct bond strength (pull-off) test equipment.

Therefore, in order to address this concern, the test setup was modified according to ASTM E72-13 (ASTM 2013b). As shown in Fig. 3.12, in this configuration, which is originally used to test the deflection of masonry panels, the prisms are subjected to four point bending in a vertical configuration. The specimens were supported by means of roller supports at a distance of 600 mm and load was applied at a rate of about 200 N/s by an actuator so that the failure occurred between 1 to 3 min. The failure was subsequently observed by a drop in the applied load and cracking in the mid joint. Similar to the compressive strength test, the masonry prisms for the flexural bond test were constructed by a certified mason in the environmental chamber, and covered by polyethylene sheets until the day of testing. A summary of the test methods followed in this study is given in Table 3-3.

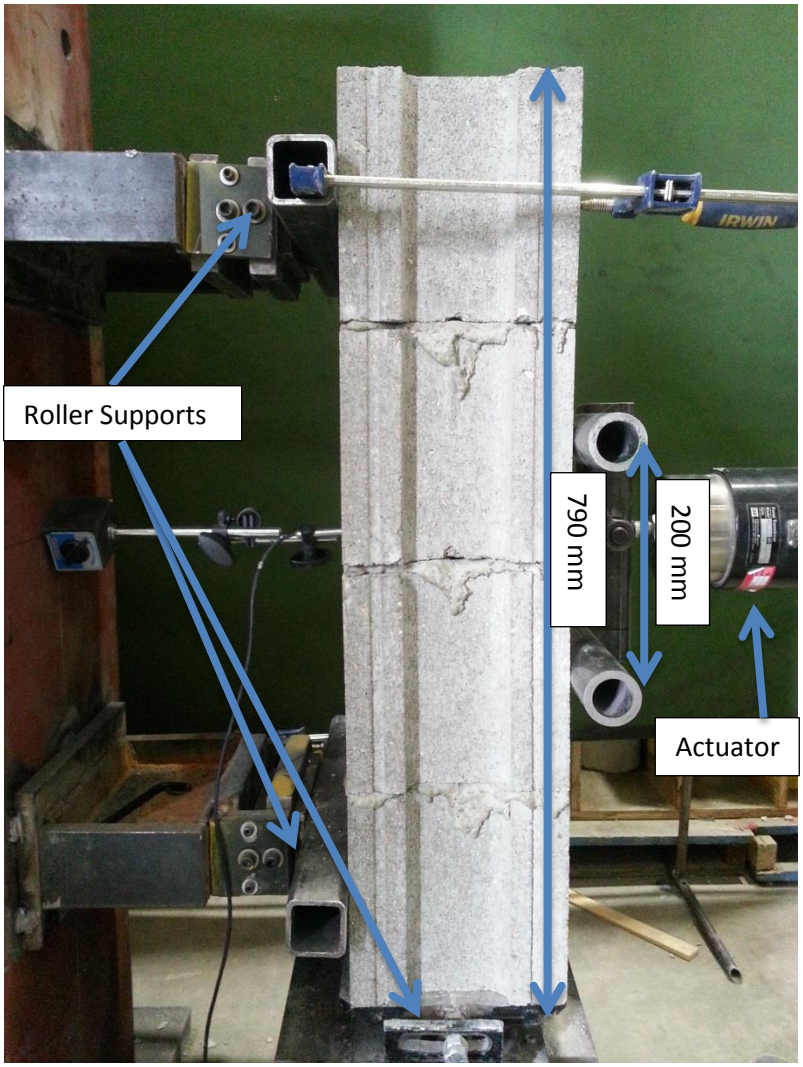

Fig. 3.12. Flexural bond test set-up configuration.

Table 3-3-Test methods summary table

Test method	Application	Phase of work
CSA A3004-C1	Determination of flow	
CSA A3004-C4	Determination of air content	
ASTM C1679	Measuring hydration kinetics of hydraulic cementitious mixtures using isothermal calorimetry	I
ASTM C403	Measuring time of setting of concrete mixtures by penetration resistance	
CSA A3004-C2	Determination of compressive strength of cubes	
ASTM C1314 and Annex D, CSA S304.1	Determination of compressive strength of masonry prisms	II
CSA A23.2-6B	Determination of bond strength of mortar and CMU	
ASTM E72-13	Determination of flexural bond strength	

4 RESULTS AND DISCUSSION

4.1 Fresh Properties

4.1.1 **Flow Test Results**

To obtain the desired flowability (110 ± 5%), trial batches indicated that moderate dosages of 2.0 and 2.5% of HRWRA by mass of binder were needed for the mixtures containing NS in groups P and M, respectively. However, a larger dosage (4.0%) of HRWRA was required for the mixtures containing NA in both groups. This can be ascribed to the very high specific surface area (SSA) of NA (170 m^2/g) compared to NS (80 m^2/g). It is worth mentioning that the dosage of HRWRA was kept constant for each mixture within each group, as shown in Table 3.2.

The incorporation of nanoparticles affected the flowability of the mortar mixtures as depicted in Figs. 4.1 and 4.2. Flow values indicated that increasing the dosage of the nanoparticles decreased the flowability of the mortar mixtures. For example, as shown in Figs. 4.1a and 4.1b as the dosage of NA increased from 2% to 4%, the flow value was reduced by 7% and 10% for the MA and PHLA mixtures, respectively. Despite the higher dosage of HRWRA (4.0%), when 6% NA was incorporated in the mortar, the target flow of 110 ± 5% could not be achieved in group M. As shown in Fig. 4.1a, the flow value of MA6 (87%) was 26% and 18% lower than MA2 and the minimum requirements, respectively. Comparatively, the addition of 6% NA to group P mixtures slightly affected its flowability (mixture PHLA6). This can be related to the fact that PHLA mixtures had higher water content as they have larger amount of binder, compared to MA mixtures. For example, PHLA6 had about 1.5% more water content

compared to MA6 (Table 3.2). In addition, the higher fineness of masonry cement provided better interaction with NA, which led to a drop in the flow value.

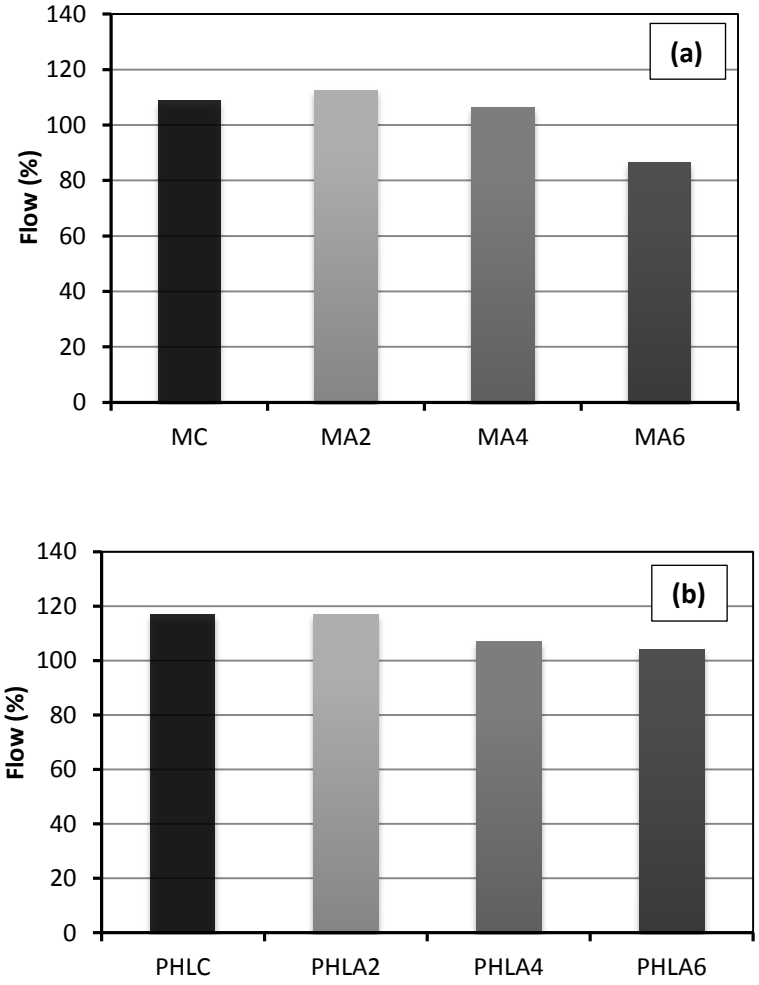

Fig. 4.1. Flow table results for mixtures containing NA: (a) Group M, and (b) Group P.

Similarly, the addition of higher dosages of NS led to reducing the flow values compared to the control mixtures (Fig. 4.2). However, this reduction was within a narrower range compared to the mixtures containing NA. For example, when the dosage of NS was increased

from 2 to 6%, the flow value was reduced by 10% in both groups (Figs. 4.2a and 4.2b), while the increase of NA from 2 to 6% led to 26% loss in the flow value (Fig. 4.1a). The difference in behaviour between the two types of nanoparticles can be ascribed to the very high SSA of NA (170 m^2/g) compared to NS (80 m^2/g). Within each group, higher dosage of nanoparticles decreased the flowability of mortar at a constant w/b due to increasing the cohesiveness of the mixtures. The ultrafine nature of nanoparticles improved the interaction between grains, and thus van der Waals based particle-particle attractions may become increasingly important *(Sonebi et al.* 2012).

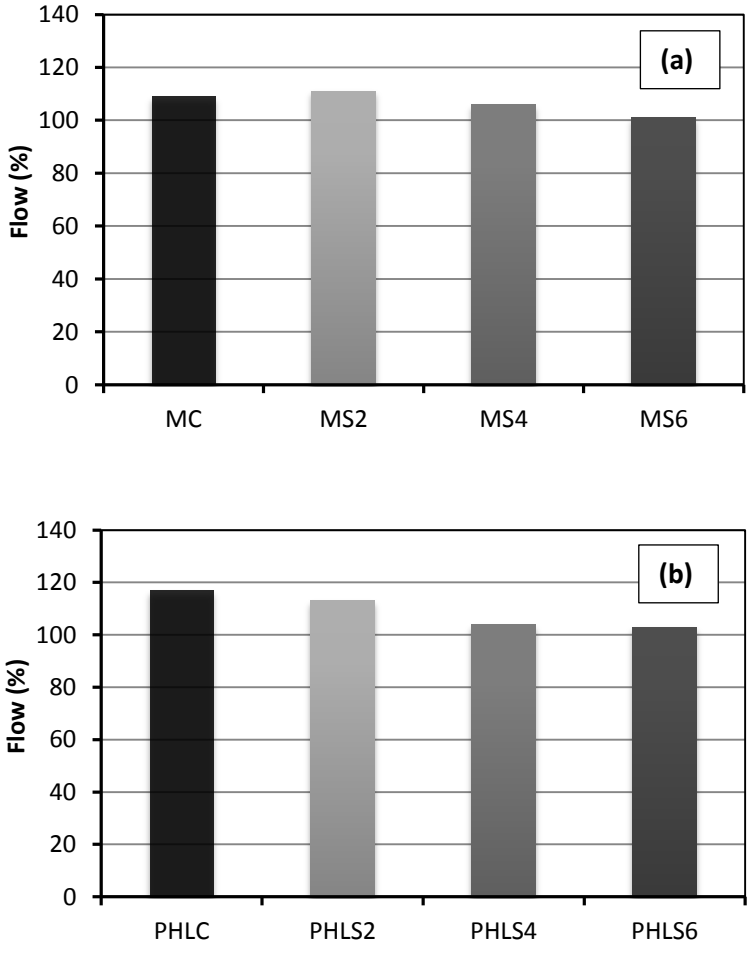

Fig. 4.2. Flow table results for mixtures containing NS: (a) Group M, and (b) Group P.

4.1.2 **Air Content**

The incorporation of nanoparticles (both NA and NS) in mortar mixtures increased their fresh air content as presented in Table 4.1. In general, the increase in the dosage of nanoparticles increased the air content of the fresh mortar mixtures. For both groups, the increase in the air content of the NA and NS mixtures in a range of about 40% of the air content of control mixtures. In group M, mixtures incorporating 6% nanoparticles (MA6 and MS6) had the highest air content of 21%, while in group P, the highest air content (14%) was achieved when 6% NS was added to the mortar mixtures (PHLS6). The lower density of fresh mortar mixtures incorporating nanoparticles was an indication of the higher air content which is in agreement with other studies [e.g. (Senff *et al.* 2009)]. It is likely that the dispersing agent in the colloidal NA and NS caused air entrainment of the cementitious matrix, which increased with the dosage of nanoparticles (Table 4.1). The difference between the air content of group P mixtures might be explained by the fact that group P mixtures generally contained less amount of cement (3870 g) in their binder compared to group M mixtures (3925 g). The difference in the amount of cement resulted in a reduction in the quantity of added nanoparticle, which led to a reduction of air entrainment in the binder. In addition, air entraining admixtures are usually added in form of powders to masonry cement during manufacturing (Mindess *et al.* 2003). The added air entrainment admixture to the masonry cement increased their fresh air content of group M control mixture (15%) compared to the control mixture of group P (10%) .

Table 4-1- Density and air content of fresh mortar mixtures

Group	Mixture	Density (g/cm^3)	Air Content (%)
M	MC	1.98	15
	MA2	1.90	18
	MA4	1.86	20
	MA6	1.83	21
	MS2	1.95	16
	MS4	1.89	19
	MS6	1.84	21
P	PHLC	2.02	10
	PHLA2	2.04	11
	PHLA4	2.03	12
	PHLA6	2.01	13
	PHLS2	2.03	11
	PHLS4	1.99	12
	PHLS6	1.96	14

4.1.3 **Heat of Hydration**

Using an isothermal calorimeter set at a temperature of 5°C, the heat of hydration of the cement pastes was measured over 7 days (168 h), as shown by heat flow curves in Figs. 4.3a and 4.4a and cumulative heat evolved in Figs. 4.3b and 4.4b. For all mixtures, the rate of heat evolution increased after about 12 to 18 h within the acceleration and hardening periods until a main hydration peak was reached. The increase in heat flow was followed by a drop during the deceleration period (after 30 to 70 h) until a relatively constant value was observed after about 7

days. This generally indicated that the hydration development rate of the cement pastes at 5°C was delayed, as compared to the heat flow curve of a typical paste at normal temperature. The hydration peak for a typical mixture at normal temperature (22 ± 2°C) occurs in a range of 4 to 8 h depending on the mixture design (Mindess *et al.* 2003). However, in this study the earliest hydration peak (Fig. 4.3a) was reached after about 30 h. This shows a delay of up to 26 h of the hydration of the mixtures mixed ad cured at a low temperature (5°C), compared to mixtures at normal temperature (22 ± 2°C). The results indicated that the range of heat flow peak of group M samples (0.69 to 1.05×10^{-3} W/g) was generally higher that than of group P mixtures (0.43 to 0.58×10^{-3} W/g). In addition, the total heat released by the group M samples was in a range of 95 to 195 J/g while group P mixtures had a cumulative heat of 145 to 160 J/g.

For group P, on the other hand, the higher dosage of HRWRA extended the dormant period by about 14 h when 2% NA was added, as shown in Fig. 4.4a. This showed the retardation effect of HRWRA on the hydration kinetics of the binder. However, this effect was diminished as the dosage of NA increased. For example, with addition of 6% NA (PHLA6) to the mixtures (Fig. 4.4a) the peaking time was shortened by about 3 h, compared to the control mixture (PHLC). The higher dosage (4% by mass of binder) of HRWRA also affected the total heat released by the samples during hydration. As shown in Fig. 4.4b, the total heat evolved by PHLA6 (149 J/g) had a reduction of about 12% as compared to that of PHLC (167 J/g). In general, the reduction of peaking time and dormant period at higher dosages of NA reveals the accelerating effect of ultrafine NA (average particle size of 50 nm and SSA of 170 m^2/g) particles on the cementitious paste. However, the variable behavior of group M relative to group P mixtures can be ascribed to the difference in the type of binder used in each group. The masonry cement used in group M was manufactured by intergrinding fillers (hydrated lime and

calcium carbonate) with cement clinker, resulting in more uniformity and fineness, and thus better interaction with nanoparticles than blended GU cement with hydrated lime, which was used in group P. This led to faster hydration activity of masonry cements, until the peaking time (end of acceleration period). However, since the clinker content in PHL binders are more than

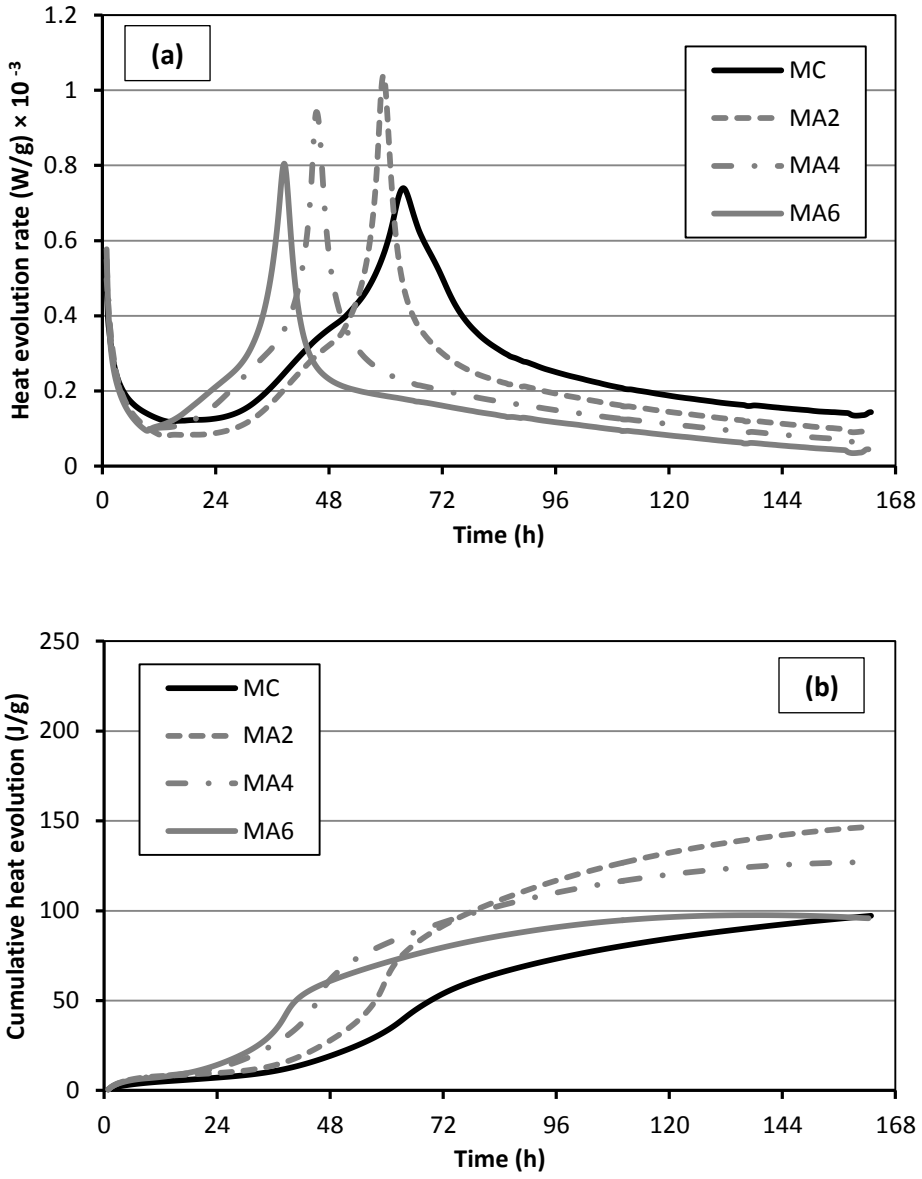

Fig. 4.3. Isothermal calorimetery results for mixtures incorporating NA in Group M: (a) rate of heat evolution, and (b) cumulative heat evolved.

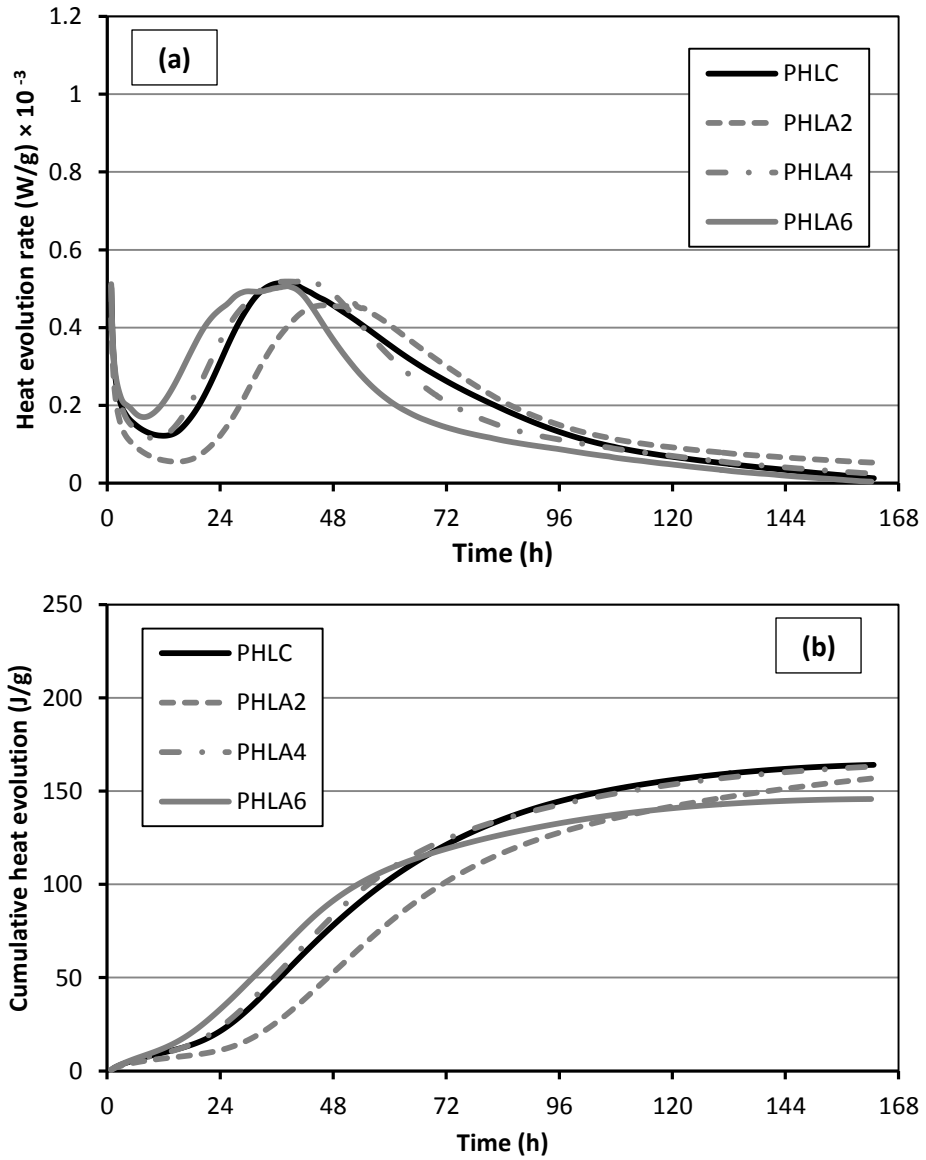

Fig. 4.4. Isothermal calorimetery results for mixtures incorporating NA in Group P: (a) rate of heat evolution, and (b) cumulative heat evolved.

masonry cement, the total hydration activity (cumulative heat realised) was higher. This aspect also affected the setting time and hardened properties as will be shown later in the text.

Addition of NS to the pastes also affected the rate of heat of hydration at 5°C. Samples incorporating NS generally exhibited shorter dormant periods as compared the control samples.

This trend was more pronounced for group M samples. As shown in Figs. 4.5a and 4.5b, increasing the dosage of NS from 0 to 6% shortened the dormant period by 20 h and increased the total released heat by up to 100% compared to the control mixture (MC) (95 J/g); consequently, the required time for final setting of the mixtures containing NS was reduced, as will be discussed in following section. For example, at dosages of 4 and 6% NS the main hydration peak was reached about 15 and 17 h, respectively earlier than that of the control sample (MC), which was reached after 70 h. This signified the effect of NS on speeding up the kinetics of hydration despite of mixing at a cold temperature. Although the same trend was noted for group P, the accelerating effect of NS seemed to be less effective in these mixtures (Fig. 4.6). This may be ascribed to the difference of the binders used in group M and P mixtures as explained earlier in the text. As shown in Fig. 4.6a, the hydration peak occurred 8 and 11 h before that of the control mixture (36 h) when 4% and 6% NS was added to the pastes, respectively. The reduction of the dormant period may be ascribed to the abundance of NS (average particle size of 35 nm and SSA of 80 m^2/g) particles in the matrix, which provided nucleation sites and catalyzed hydration reactions even at 5°C. It should be noted that the occurrence of hydration peaks at earlier time intervals is an indication for the progression of hydration activity, but it does not necessarily correspond to higher strength values as will be discussed later in the text.

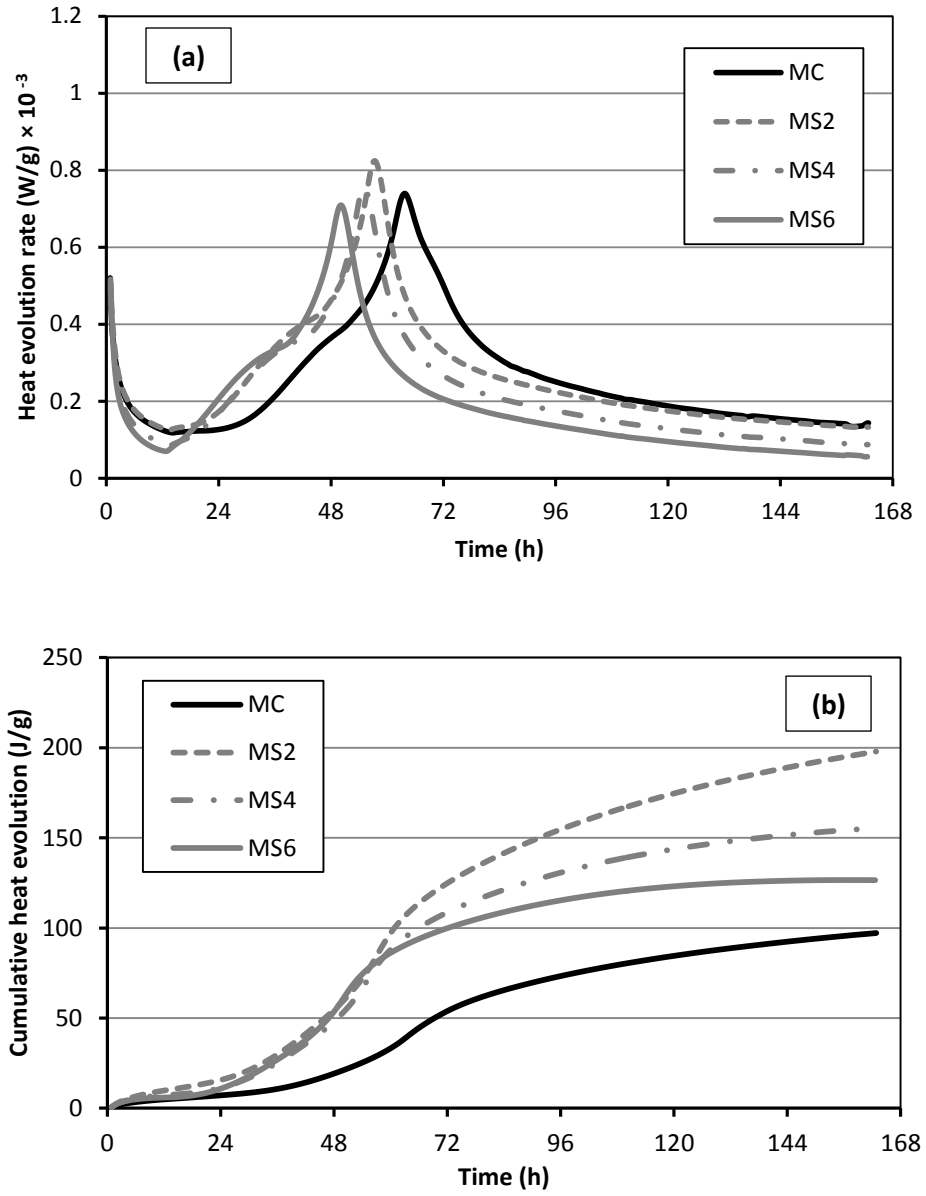

Fig. 4.5. Isothermal calorimetery results for mixtures incorporating NS in Group M: (a) rate of heat evolution, and (b) cumulative heat evolved.

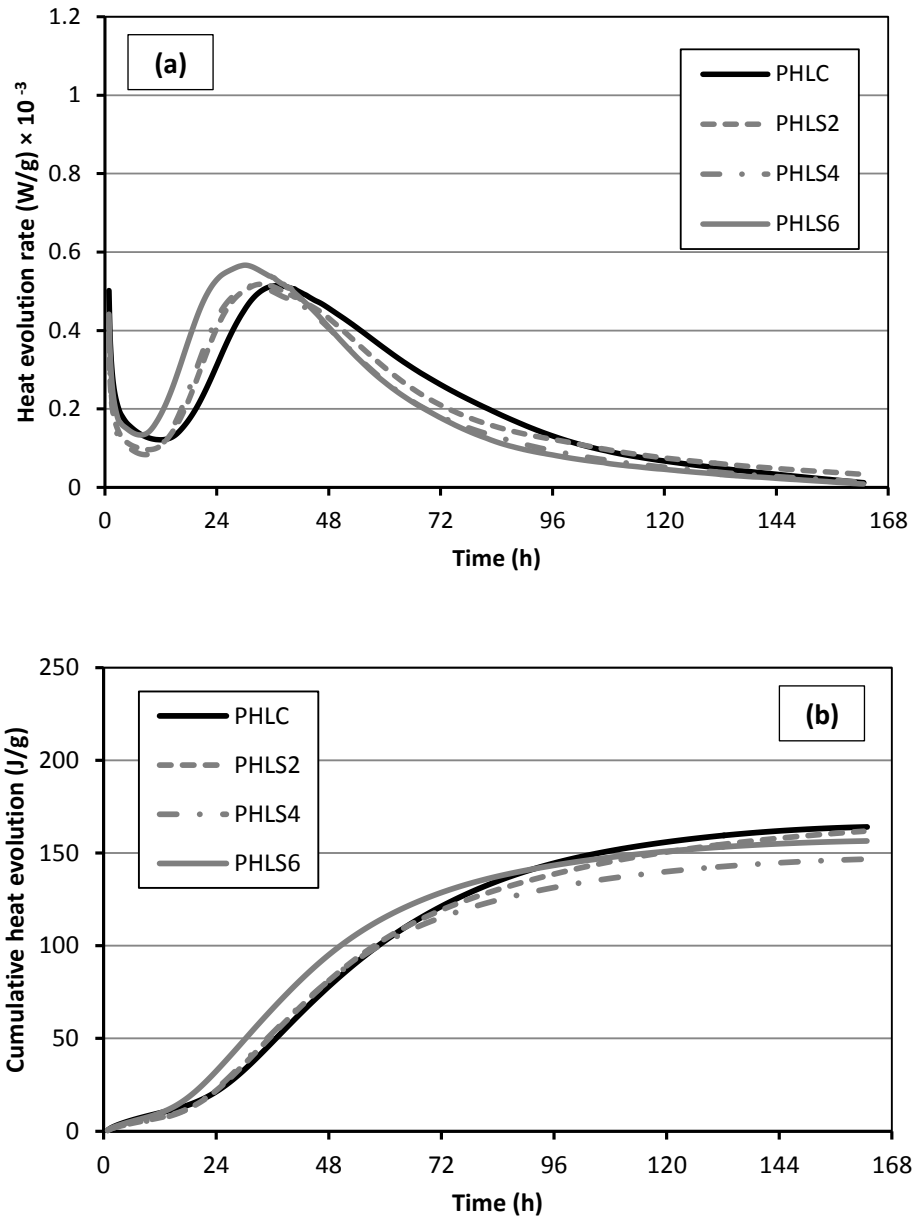

Fig. 4.6. Isothermal calorimetery results for mixtures incorporating NS in Group P: (a) rate of heat evolution, and (b) cumulative heat evolved.

4.1.4 **Setting Time**

Samples of mortar mixtures were tested for setting time at different time intervals, according to ASTM C403-08 (ASTM 2008), which stipulates penetration resistance values of 3.5 MPa and 27.6 MPa for the initial and final setting times, respectively. The setting time results generally

indicated that the setting time of group P mixtures were shorter than the corresponding group M mixtures. This trend is in agreement with the heat of hydration curves where the average hydration peak of group P mixtures was reached about 20 h before group M mixtures, due to the difference in clinker (cementitious) content as discussed earlier. As shown in Figs. 4.7a and 4.7b, the incorporation of NA affected the initial and final setting times of the mortar mixtures in both groups. This was statistically supported by analysis of variance (ANOVA) at a significance level of $\alpha = 0.05$. ANOVA for the initial setting time of group M mixtures showed that the increase in the dosage of NA from 0 to 6% had F value of 3415.52 which is larger than the F_{cr} value of 4.06. Similarly, ANOVA for group P mixtures showed the significant effect of the increase of the dosage of NA on the final setting time with F and F_{cr} values of 52.62 and 5.14, respectively.

The average setting times test results are listed in Table 4.2. Generally, average setting time results for mixtures containing NA (except MA6) indicated a delay in both initial and final setting times compared to the control mixtures (Figs. 4.7a and 4.7b). For example, the delay in the initial setting time for MA2 and PHLA2 was 336 min (39%) and 168 min (30%), respectively relative to that of MC and PHLC (Table 4.2). In addition, the final setting time for MA2 and PHLA2 occurred after 1830 min and 1200 min, which indicated a delay of 402 (28%) and 234 (24%) min, respectively, relative to MC and PHLC. However, the results showed a notable reduction in the setting time as the dosage of NA increased. For example, the final setting time was shortened by 84 min when the dosage of NA increased from 2 to 4% in group P. This effect was more pronounced for group M mixtures, where the incorporation of 6% NA had

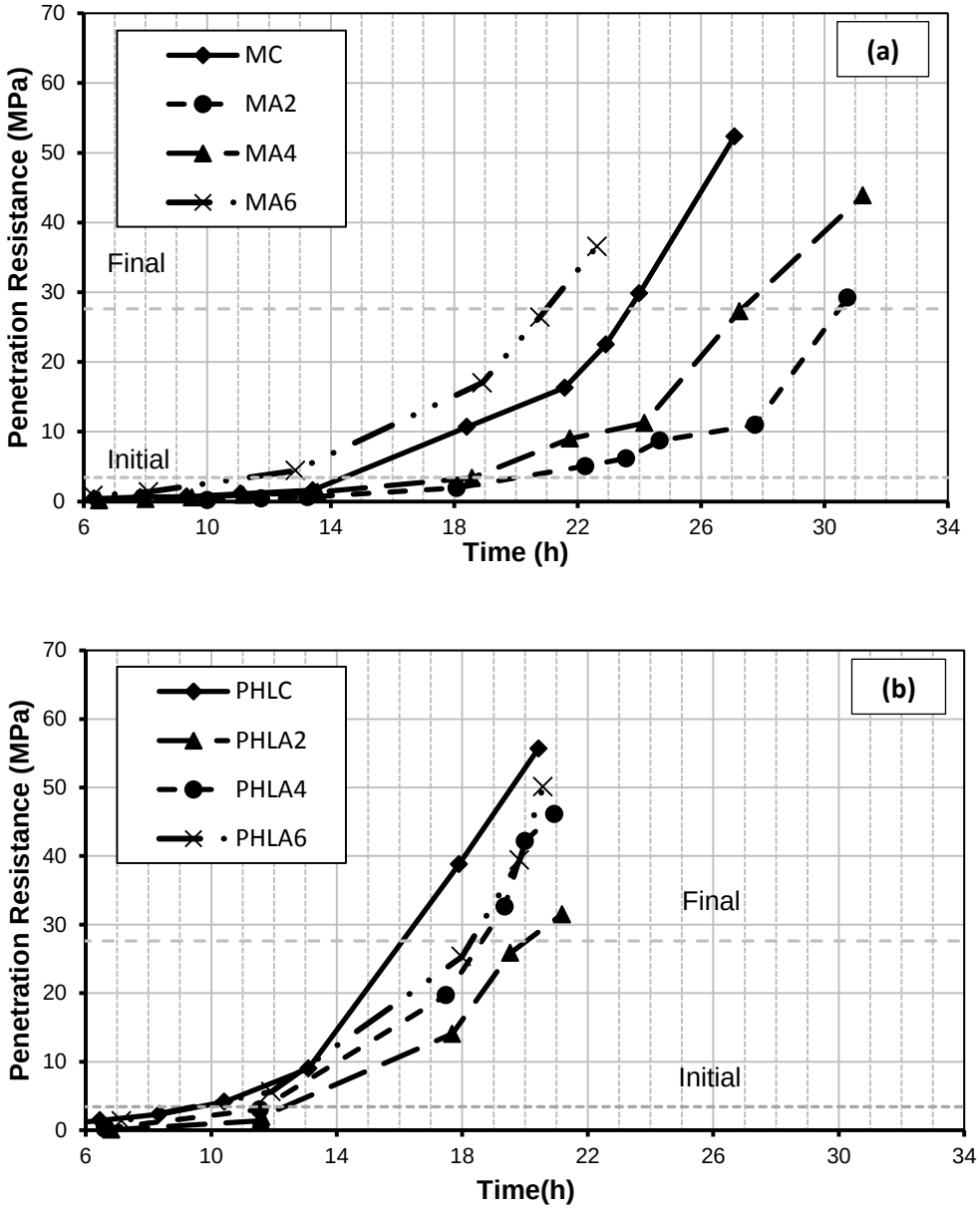

Fig. 4.7. Setting time results for mixtures containing NA: (a) group M, and (b) group P.

a comparable reduction of 198 (23%) and 168 (12%) min in the initial and the final setting times, respectively compared to MC. The latter effect is generally in agreement with the heat of hydration results in the sense that higher dosages (6%) of NA sped up the kinetics of hydration

as indicated by shortening the dormant period and reducing the peaking time. The hardening trend is also in agreement with the flowability test results where higher dosages of NA reduced the flow values in the range of 10 to 26%, compared to the mixtures containing 2% NA, respectively. The loss of flow caused a reduction in plastic sedimentation which led to shorter setting time readings.

The longer setting times associated with almost all the mixtures incorporating NA, as measured by the penetration resistance, may be attributed to the dominant effect of the higher dosage (4%) of HRWRA on retarding the rate of hardening towards the threshold resistance values (3.5 MPa and 27.6 MPa), compared to the mixtures without NA. The higher dosage of HRWRA increased the rates of sedimentation and bleeding, which were also observed in the heat of hydration samples (pastes). However, as explained earlier, the heat of hydration results were less affected by this retardation effect, as the heat flow is collected from the bottom of the test veils by the isothermal calorimeter. Sedimentation and bleeding in these mixtures produced a soft surface, for penetration of the needles, which led to longer setting time readings.

The addition of lower dosages of NS led to a delay in the initial setting time of group M, as shown in Fig. 4.8a. For example, the initial setting time for MS2 and MS4 was 960 min and 900 min, respectively compared to 870 for the control mixture MC. The delay in the initial setting time of the mixtures may be ascribed to the adverse effects of a moderate dosage of HRWRA (2.5%) and cold temperature on the mixtures. However, increasing the NS dosage to 6% (MS6) led to a notable shortening of 18% (156 min) of the initial setting time suggesting that the effect of HRWRA on the early hardening process was offset. On the contrary, contribution of NS generally shortened the final setting time of the mixtures of group M. For example, when 4

Table 4-2- Average setting time results

Group	Mixture	Setting Time (min)		Setting time compared to control (min)	
		Initial	**Final**	**Initial**	**Final**
M	MC	870	1428	0	0
	MA2	1206	1830	336	402
	MA4	1110	1632	240	204
	MA6	672	1260	-198	-168
	MS2	960	1338	90	-90
	MS4	900	1290	30	-138
	MS6	714	1254	-156	-174
P	PHLC	570	966	0	0
	PHLA2	738	1200	168	234
	PHLA4	690	1116	120	150
	PHLA6	588	1092	18	126
	PHLS2	540	996	-30	30
	PHLS4	542	980	-28	14
	PHLS6	540	951	-30	-15

and 6% NS was added to the mixtures, the final setting time was reduced by 138 min (10%) and 174 min (12%) relative to MC. The setting time results indicate that the effect of HRWRA on delaying the initial hardening rate of mixtures with 2 or 4% NS diminished with time and all the MS mixtures had higher rates of hardening beyond 18 h in group M. In group P, addition of NS slightly affected the setting time results as shown in Table 4.2. The initial setting time of the mixtures containing 2, 4 and 6% NS was about 30 min (5%) shorter than that of the control

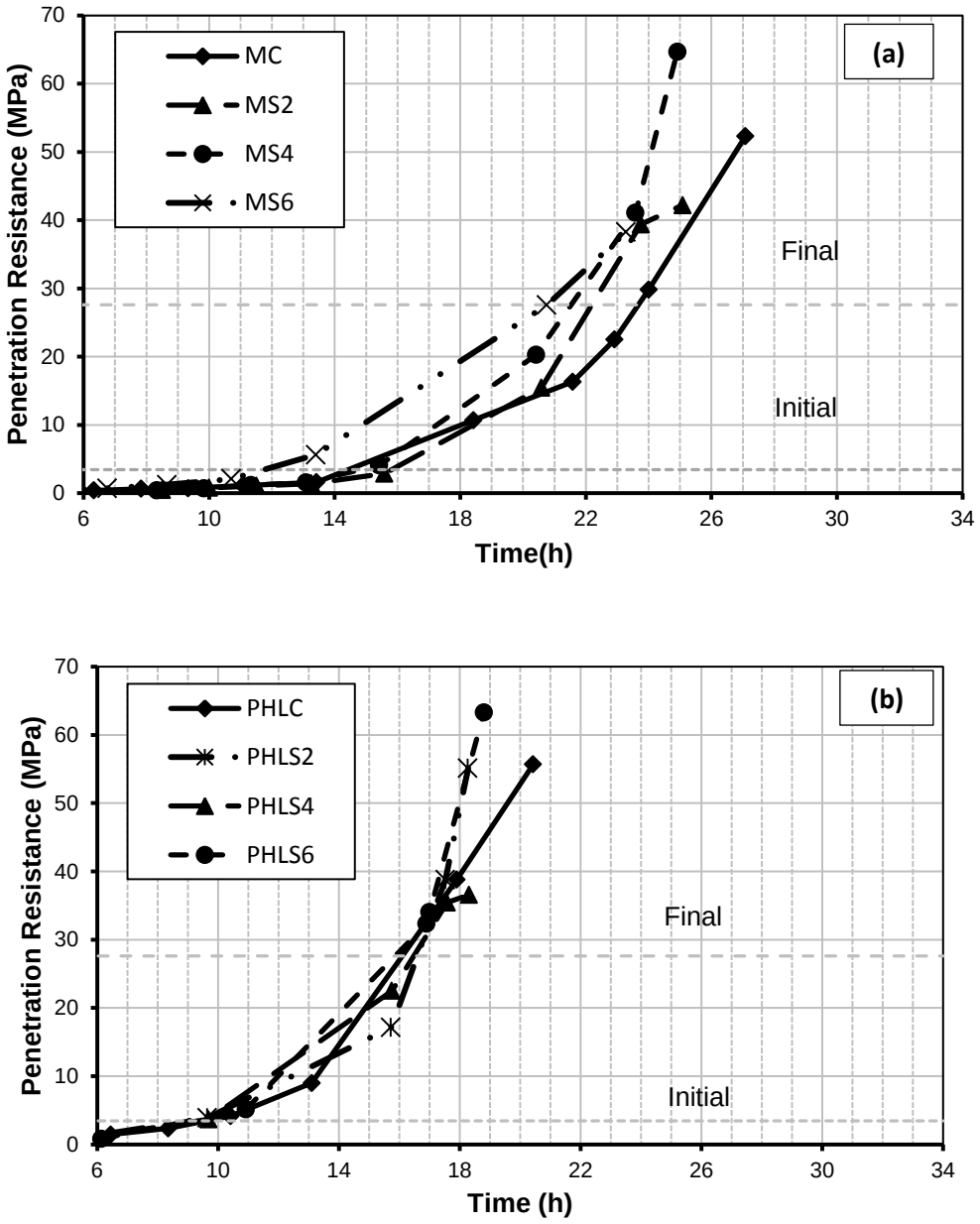

Fig. 4.8. Setting time test for the mixtures containing NS: (a) group M, and (b) group P.

specimen (PHLC). This revealed that the increase in the dosage of NS did not affect the initial setting time (Fig. 4.8b). ANOVA statistically confirmed the insignificant effect of the dosage of NS on the initial setting time with F and F_{cr} values of 0.84 and 5.14, respectively. One the other hand, the contribution of NS in this group was more noticeable when 6% NS was added where

the final setting time was shortened by 45 and 15 min compared to PHLS2 and PHLC, respectively. The slight improvement of the kinetics of hydration in this group can be mainly related to the fact blended and coarser cement exhibited slower reactivity with nanoparticles compared to masonry cement. In general, the trends of reduction in setting times of the mixtures containing NS are in agreement with the heat of hydration results since the hydration peaks relatively occurred earlier than the control mixtures.

4.2 Hardened Properties

4.2.1 **Compressive Strength**

The type of binder and dosage of nanoparticles affected the compressive strength of the mixtures, depending on the age of testing (Figs. 4.9 and 4.10). Generally, group P mixtures had higher compressive strength compared to group M mixtures. This conforms to the air content results since group P mixtures had lower air content (up to 8%) as compared to group M mixtures. Also, the higher clinker content in the PHL binders led to this increase in strength, as depicted by the higher total heat related and shorter setting times of these binders.

To capture the effect of NA on the early-age strength of mortar specimens, the compressive strength results at 1 and 3 days are listed in Table 4.3. The results indicate that MA2 had a marked reduction in compressive strength (up to 32%) at 1 day. However, as the dosage of NA increased, higher compressive strength values were obtained. For example, as shown in Table 4.3, the compressive strength of mixture containing 4 and 6% NA (MA4 and MA6) increased by 52 and 159% relative to MA2. This respectively indicated a comparable and about 76% increase in the compressive strength at 1 day compared to MC. The compressive strength of PHLA2 and PHLA4 mixtures, in group P, also were increased at 1 day, compared to the control

mixture (PHLC). This improvement was in the range of 21 to 47%, respectively. However, addition of 6% NA (PHLA6) led to a notable reduction in the compressive strength at 1 day, relative to 4% NA. This behaviour may be attributed to the dominant effect of higher air content (14%) created by the dispersing agent of the nanoparticles on the strength of the matrix at early-age.

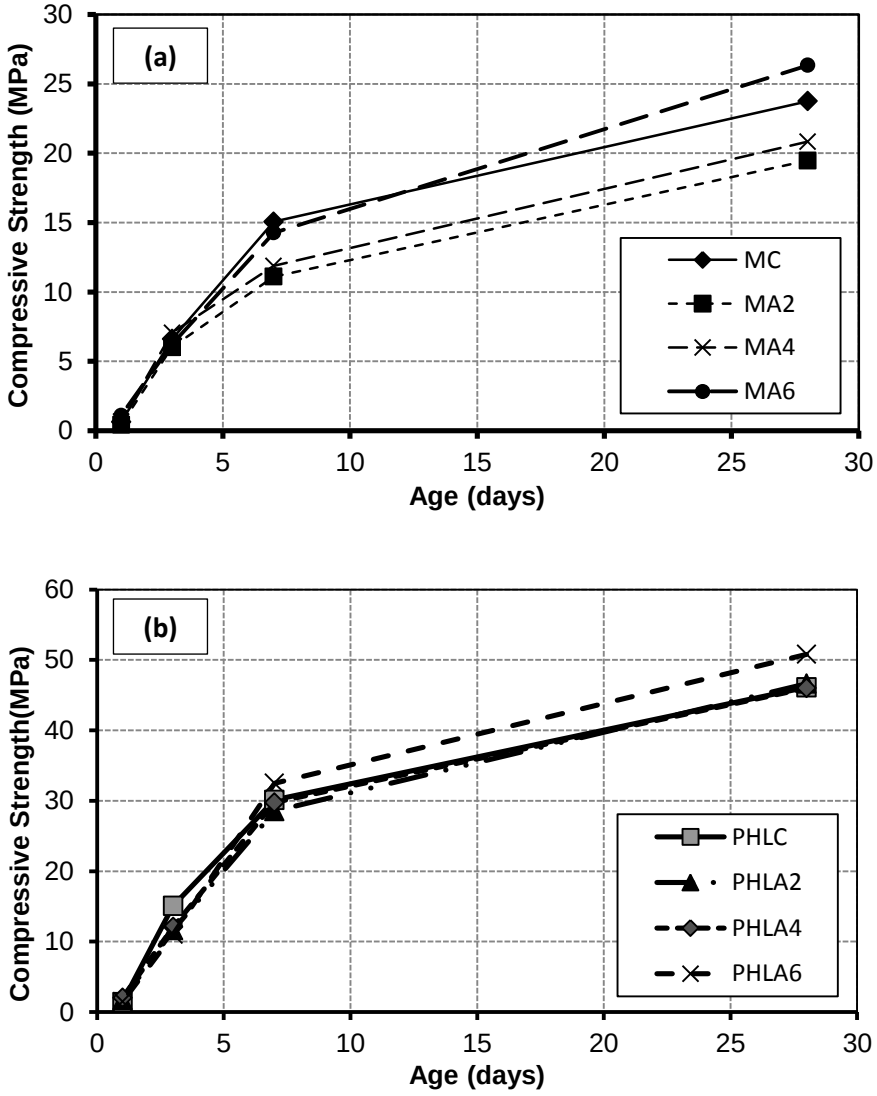

Fig. 4.9. Compressive strength results of mixtures containing NA: (a) group M, and (b) group P.

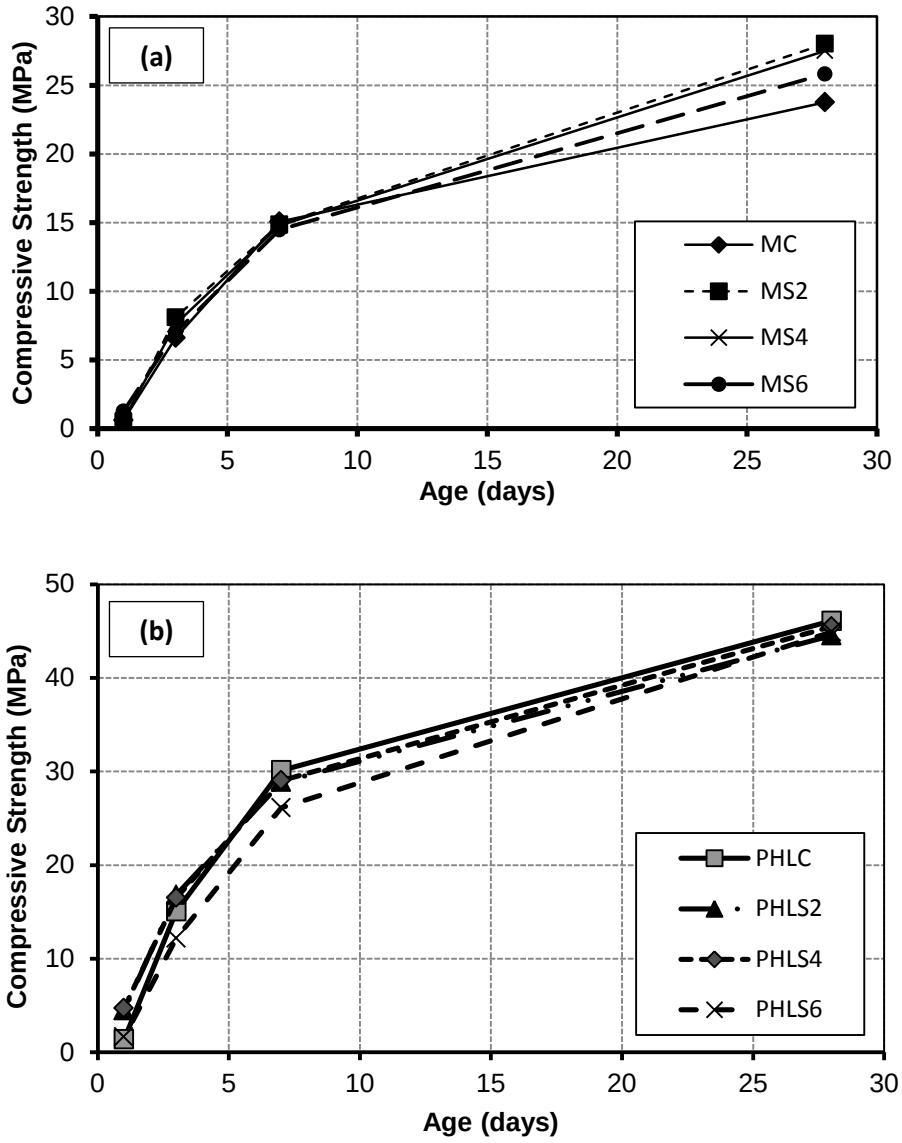

Fig. 4.10. Compressive strength results of mixtures containing NS: (a) group M, and (b) group P.

Early-age compressive strength results were analyzed by ANOVA at a significance level of α=0.05 as shown in Table 4.4. For example, ANOVA confirmed the significant effect of the change in the dosage of NA from 0 to 6% on the compressive strength of group M mixtures at 1 and 3 days with *F* values of 349.67 and 17.54, respectively which are greater than the F_{cr} value (4.06). The compressive strength values at early ages are in general agreement with the trends

obtained from the heat of hydration and the setting time test in the sense that increasing the dosage of NA led to shortening of the dormant period and initial and final setting times. However, the improvement effect of NA diminished after 1 day. The results at 3 days indicated a lower compressive strength for the mixtures comprising NA compared to the control mixtures in groups M and P. For example, as listed in Table 4.3, mixtures incorporating 2, 4 and 6% NA showed a reduction of 23, 20 and 26% in compressive strength, respectively as compared to PLHC. This suggested that the results were offset by the higher air contents of the mixtures containing NA (Table 4.1).

Table 4-3- Early-age compressive strength of mixtures incorporating NA

Group	Mixture	Compressive strength (MPa)	
		1 day	3 days
M	MC	0.6	6.6
	MA2	0.4	6.0
	MA4	0.6	6.4
	MA6	1.0	6.2
P	PHLC	1.3	15.0
	PHLA2	1.6	11.6
	PHLA4	2.0	12.0
	PHLA6	1.4	11.0

Similarly lower compressive strengths were obtained for the specimens incorporating 2% and 4% NA in groups M and P at later ages (7 and 28 days), compared to the control specimens

(Figs. 4.9a and 4.9b). For group M specimens, the reduction in strength relative to the control specimen (MC) varied from 18 to 26% and from 12 to 21% at 7 and 28 days, respectively. For group P mixtures the reduction of the compressive strength of the mixtures incorporating 2 and 4% NA was about 10% at 7 days. The significant effect of the NA dosage on the compressive strength results at 7 days was also shown by ANOVA. Furthermore, with addition of 6% NA the compressive strength of the mortar mixtures was marginally improved after 7 days. For example, the compressive strength of PHLA6 and MA6 was improved by about 10% at 28 days compared to that of PHLC and MC. This behavior may be attributed to the fact that the retardation effect of HRWRA on the larger dosage of NA (6%) was diminished after 7 days, which complies with the setting time trends. However, this effect was only statistically significant for group M mixtures at 28 days (Table 4.4).

After one day, the slower rate of strength development for the mixtures containing NA was due to insufficient degree of hydration, particularly for the lower dosages in group M. These samples had a coarse and porous microstructure, which affected their compressive strength, as will be shown later by the microstructural studies. It has been reported in the literature that addition of NA improves the mechanical properties of cement-based materials at normal mixing and curing temperatures (22 ± 2°C) [e.g.(Campillo *et al.* 2007; Oltulu and Şahin 2013)]. In the present study, however, it seems that the contribution of lower dosages of ultrafine NA in improving the kinetics of hydration at early age was generally offset by the dominant effect of a higher dosage of HRWRA, higher air content and cold temperature, which adversely affected the strength at different (3, 7, 28 days) ages. It is worth emphasizing that there exists some discrepancy between the compressive strength results and heat of hydration in the light that the dormant period of the mixtures incorporating NA was generally shorter than the control

specimens, suggesting the accelerating effect of NA up to 7 days. However, it should be reminded that the retardation effect of HRWRA did not adversely affect the heat of hydration results due to sedimentation of the cement pastes and the heat flow measurement method by the isothermal calorimeter, as explained earlier in the text.

The compressive strength results showed that higher compressive strength values were achieved for many mixtures incorporating NS at certain ages (1, 3, 28 days) as shown in Fig.4.10 and Table 4.5. In agreement with the heat of hydration and setting time trends, the increase in the NS dosage generally led to a notable increase in the compressive strength results at 1 day, as presented in Table 4.5. The highest compressive strength at 1 day was achieved when 6% NS and 4% were added to group M and P mixtures, which led to an improvement of 204 and 345%, respectively, compared to the control mixtures (Table 4.5). Addition of NS to mortar mixtures also increased their compressive strength at 3 days. For example, when 2 and 4% NS was added to group M mixtures a compressive strength of 8.1 and 7.6 MPa was obtained at 3 days, respectively. This indicated about 23 and 15% improvement in compressive strength, compared to the control mixture (MC). Likewise, the compressive strength of PHLS2 and PHLS4 was increased by 11 and 10% at 3 days, respectively, compared to PHLC. The effect of NS on the compressive strength at early-age was also statistically supported by ANOVA for both groups, as listed in Table 4.6. For example, statistical tests confirmed the significant effect of the increase of the dosage of NS on the compressive strength of group P mixtures at 1 day with F and F_{cr} values of 1403 and 4.06, respectively. However, it is worth noting that mortar mixtures with higher compressive strength values at 1 day had lower compressive strength at later ages. For example, introduction of 6% NS to the mixtures in group M (MS6), led to the highest (1.2 MPa) and the lowest (7.0 MPa) compressive strength at 1 and 3 days, respectively (Table 4.5),

compared to the other MS mixtures. Similarly, the incorporation of 4% NS in group P led to a higher (4.7 MPa) and a lower (16.5 MPa) compressive strength at 1 and 3 days, respectively, compared to PHLS2 mixture. The lower compressive strength of the mixtures containing higher dosages of NS after 1 day generally signified the dominant effect of their higher air content on the compressive strength results as discussed earlier in the text (Table 4.1).

Table 4-4–ANOVA results for compressive strength of mixtures containing NA

Group	Age (Days)	F	F_{cr}	Effect
M	1	349.67	4.06	Significant
	3	17.54	4.06	Significant
	7	42.39	4.06	Significant
	28	23.82	4.06	Significant
P	1	72.84	4.06	Significant
	3	38.04	4.06	Significant
	7	6.50	4.06	Significant
	28	1.48	4.06	Insignificant

The results of group M suggested that NS affected the hardened properties of the mortars in two stages. In the first stage, NS particles led to higher compressive strength compared to the control mixtures at early-ages by acting as nucleation sites for the hydration reactions up to 3 days. This is in agreement with the heat of hydration results in the light that the hydration peak of the mixtures incorporating NS occurred earlier than that of the control mixture. In the second stage (7-28 days), the compressive strength values of the mixtures containing NS diverged after

Table 4-5- Early-age compressive strength of mortar incorporating NS

Group	Mixture	Compressive strength (MPa)	
		1 day	3 days
M	MC	0.6	6.6
	MS2	0.5	8.1
	MS4	0.6	7.6
	MS6	1.2	7.0
P	PHLC	1.3	15.0
	PHLS2	4.4	16.8
	PHLS4	4.7	16.5
	PHLS6	1.6	12.1

Table 4-6– ANOVA results for compressive strength of mixtures containing NS

Group	Age (Days)	F	F_{cr}	Effect
M	1	229.63	4.06	Significant
	3	9.86	4.06	Significant
	7	0.40	4.06	Insignificant
	28	1.23	4.06	Insignificant
P	1	1403.25	4.06	Significant
	3	20.36	4.06	Significant
	7	2.03	4.06	Insignificant
	28	0.18	4.06	Insignificant

7 days and increased up to 28 days. This increase was in a range of 8 to 16% compared to the control mixture at 28 days (Fig. 4.10a). On the contrary, the compressive strength of the group P mixtures started to converge after 7 days until a comparable strength was observed at 28 days. This may be related to the fact that group P mixtures had higher early hydration activity compared to group M mixtures as observed in the heat of hydration and the setting time results. The earlier initiation of the hydration reaction in this group led to formation of thicker hydration shells around C_3S. The thick layers of C-S-H prevented the diffusion of water for further hydration which decelerated the hydration activity after 7 days and led to a comparable compressive strength values at the age of 28 days.

Similar to the NA mixtures, the compressive strength development at early ages can be ascribed to the fact that the well-dispersed NS provided nucleation sites which led to acceleration of cement hydration, which conforms to the heat of hydration curves in the sense that addition of nanoparticles shortened the dormant period. In addition, the physical filler effect of NS refined the pore structure and densified the interfacial transitional zone (ITZ) which strengthened the cementitious matrix as will be discussed in the SEM observations later in the text. The compressive strength of the mixtures was also affected by the air content (Table 4.1) as the mixtures with high air content yielded lower strength, particularly at later ages. It is worth noting that the pozzolanic activity of NS for formation of secondary C-S-H was not initiated up to 28 days at cold temperature (5 ± 1°C) and did not affect the compressive strength results as will be discussed in the thermogravimetric analysis section. Generally, the effect of NS on the compressive strength was superior to NA at the early ages in the light that the mixtures incorporating NS had higher strength values (except PHLS6) compared to the control mixtures at 1 and 3 days. Additionally, the effect of NS at 28 days seemed to be superior to NA, specifically

in group M mixtures. The mixtures containing NA lad lower compressive strength (except 6%), while the mixtures containing NS had higher or comparable compressive strength at 28 days.

4.3 Microstructural and Thermogravimetric Analyses

Microstructural analysis for the mixtures incorporating nanoparticles was conducted using BSEM on thin sections from selected specimens at 7 to 12 days. Generally, the trends of microstructure complied with that of the setting time and compressive strength tests. A porous matrix was observed, particularly within the interfacial transition zone (ITZ) between the paste and aggregate phases when NA was added to the mixture. For example, Figs. 4.11a and 4.11b show a coarse ITZ structure in the vicinity of an aggregate particle. EDX analysis showed that this porous zone typically contained intermixed CH and C-S-H with an average calcium-to-silicate ratio (C/S) of about 2.0 to 3.0 (e.g. Fig. 4.11c). Large and discrete CH crystals were also noted (e.g. Fig. 4.12) in the coarse matrix comprising NA. The porosity of the matrix and the ITZ, the high C/S of C-S-H and the occurrence of large and discrete CH crystals indicate an insufficient degree of hydration for the mixtures incorporating 2 and 4% NA, which led to lower compressive strength at certain ages. Direct evidence from microstructural studies supports the argument that the action of lower dosages (2 and 4%) of NA was delayed by the prominent effects of HRWRA and cold temperature.

On the contrary, BSEM analysis showed a dense matrix with a refined ITZ for mixtures containing NS. For example, Figs. 4.13a and 4.13b show a dense microstructure with a high degree of hydration for MS4 and PHLS2 mixture in the vicinity of a sand particle at the age of 7 and 10 days. EDX analysis showed an average calcium-to-silicate ratio (C/S) of 1.07 in the ITZ (Fig. 4.13c), indicating an incipient stage of pozzolanic activity. It was reported that the C/S of

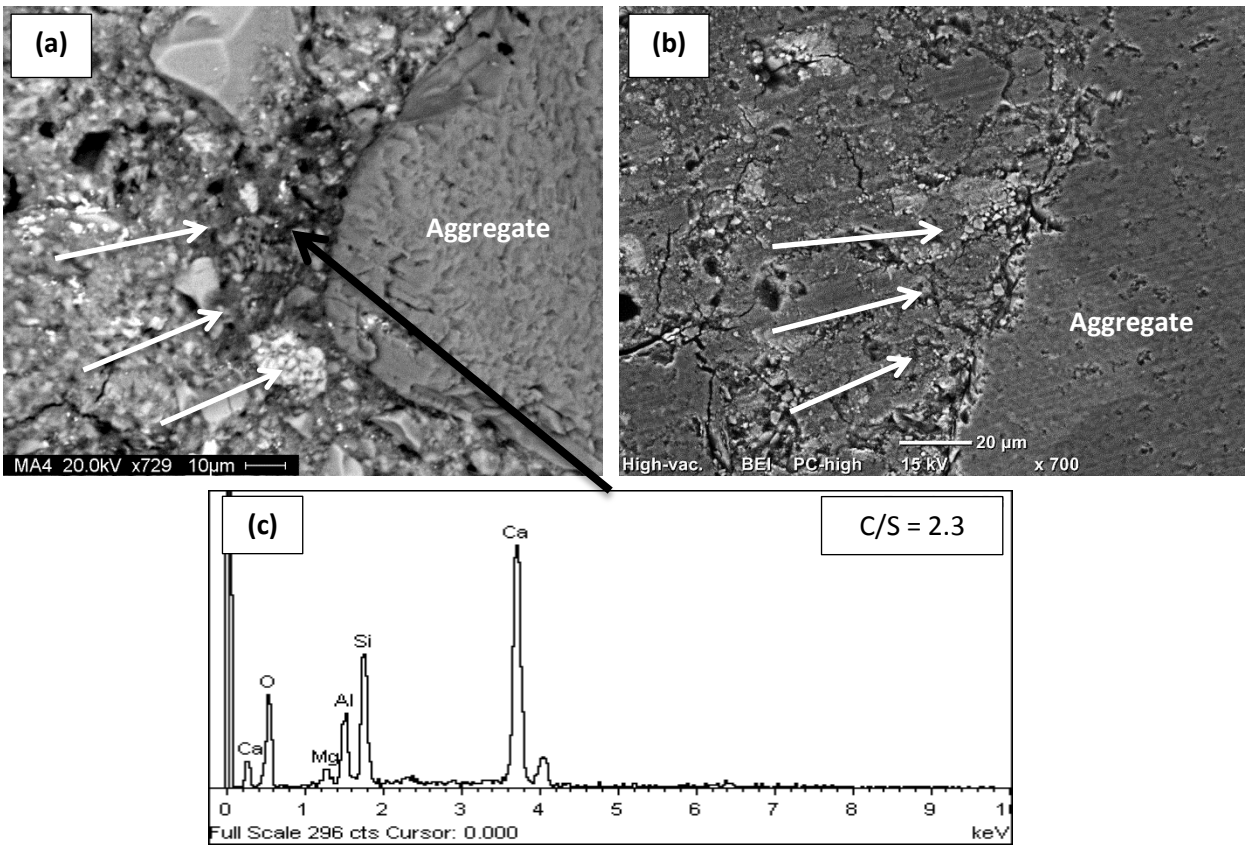

Fig. 4.11. An exemplar BSEM analysis for a thin section showing porous ITZ from: (a) MA4, (b) PHLA2, and (c) associated EDX spectrum for MA4.

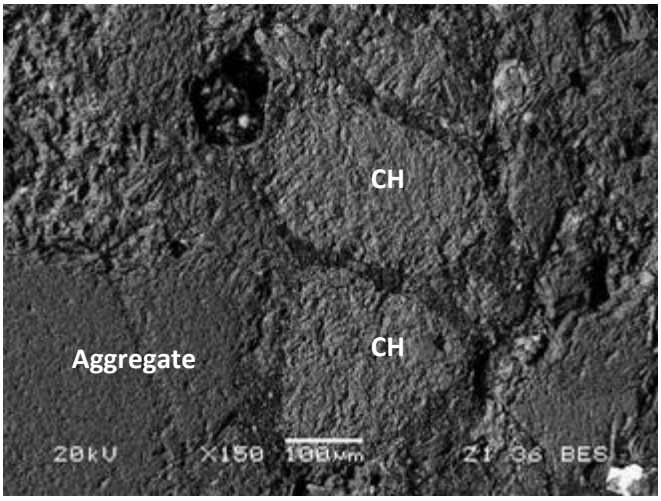

Fig. 4.12. BSEM micrograph for a thin section from MA2.

secondary C-S-H from pozzolanic reactions is lower than that of conventional C-S-H produced from hydration reactions, the former has a ratio of about 1.1, while the latter has a ratio of about 1.7 (Detwiler *et al.* 1996). DSC/TGA analysis, however, showed that the contribution of the pozzolanic effect of NS was significant after 28 days, as will be discussed in the succeeding paragraphs. Observations from the microstructural studies verifies that contribution of NS was not hindered at cold temperature, which explains the higher compressive strength values of many NS mixtures at early or later ages (excluding the effect of air-entrainment).

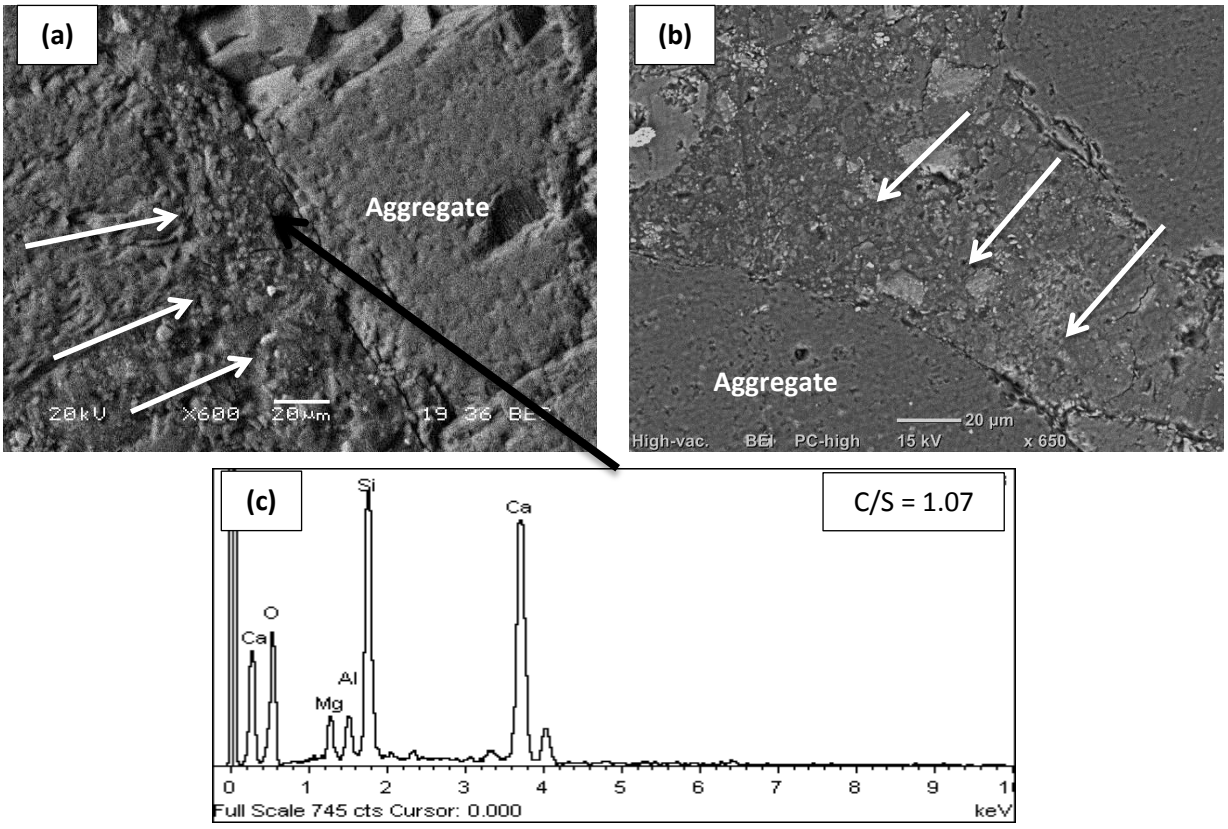

Fig. 4.13. An exemplar BSEM analysis for a thin section showing a dense matrix from: (a) MS4, (b) PHLS2, and (b) associated EDX spectrum for MS4.

DSC/TGA was used to characterize the hydration products and assess the consumption of calcium hydroxide (CH) in the cementitious matrix containing NS. Portlandite (CH) is converted to calcium silicate hydrate (C-S-H) via pozzolanic reaction in the mixtures containing pozzolanic materials. Secondary C-S-H formed by the pozzolanic reaction has shown to improve the properties of hardened mortar and concrete (Senff *et al*. 2010). An exemplar DSC/TGA data for mixture PHLS4 at 28 days is shown in Fig. 4.14. According to many studies [e.g. (Loukili *et al.* 1999; Pane and Hansen 2005; Sha *et al.* 1999)], the first major endothermic peak of an ordinary cement-based mixture is mainly related to the evaporation of free water and de-hydroxylation of different hydrates (calcium silicate hydrate, ettringite, carboaluminates) which may occur up to 100°C. The second major peak, which occurs in a range of 420°C to 500°C, is mainly related to dehydration of CH of the pulverized sample (Alarcon-Ruiz *et al*. 2005; Esteves 2011; Senff *et al.* 2010*)*. It is worth mentioning that the criteria for the selection of range of the vertical axis were based on the mass loss and heat flow of the specimen during the experiment.

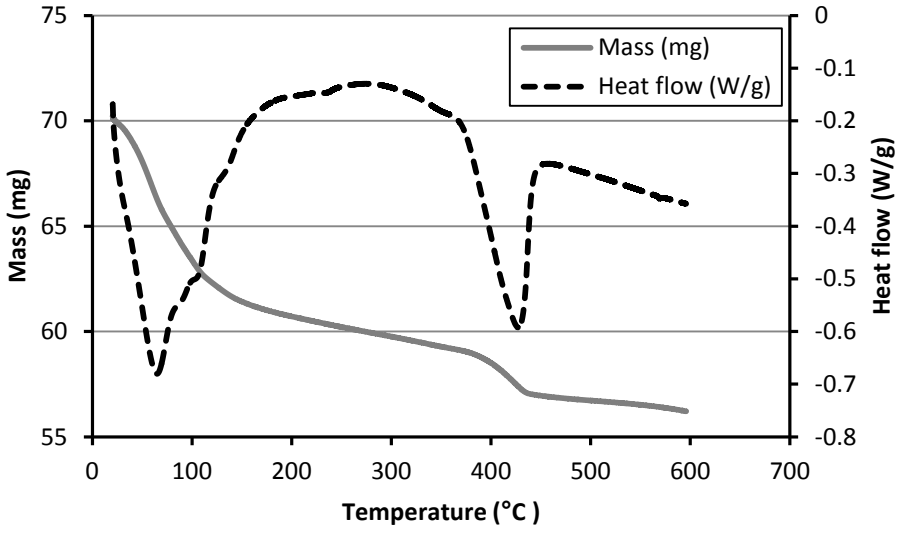

Fig. 4.14. Exemplar thermograms of PHLS4 at 28 days

The CH content at 3 and 28 days for the NS mixtures, which were mixed and cured at 5±1˚C are listed in Table 4.7. The results showed a consistent increase of CH content in the ranges of 0.9 to 1.3% and 1.2 to 1.8% for the NS mixtures in groups M and P, respectively. This indicated that the pozzolanic reaction of NS was not significant within 28 days. In order to investigate the pozzolanic behaviour of NS at cold temperature, control mixtures and samples containing 4% NS were tested at later ages (up to 75 days). The pozzolanic behaviour of these samples was compared to the mixtures mixed and cured at normal conditions, as shown in Fig. 4.15. At normal mixing and curing temperature, while the CH content of the control samples (MCN and PHLCN) increased with time as the hydration process continued, mixtures incorporating 4% NS (MS4N and PHLS4N) showed a notable reduction in CH content after 3 days (Fig. 4.15). This reduction in the amount of CH for the samples comprising NS can be attributed to the consumption of CH in the pozzolanic reaction to produce secondary C-S-H. Comparatively, for the NS mixtures that were mixed and cured at a cold temperature, the results showed that the reduction of CH occurred after 28 days, suggesting a latent pozzolanic activity. This indicated that the pozzolanic reaction in MS4 and PHLS4 was slowed down, but not inhibited, by the cold temperature, and thus it was delayed by 25 days. The amount of portlandite needed to mobilize the pozzolanic activity was in a range of 5.1 and 13.5% for MS4 and PHLS4, respectively. The DSC/TGA analysis indicated that the delayed pozzolanic reaction of NS which started at 28 days did not affect the hardened properties of the mixtures mixed and cured at a low temperature (5 ± 1°C) in this study. Furthermore, results indicated that higher amount of CH was generated in the samples containing 4% NS, particularly for the samples cured at low temperature, compared to the control samples (MC and PHLS4) at 3 and 28 days. This can be an indication that 4% NS accelerated the hydration activity at low temperature in the light that

higher rate of hydration activity in the cementitious binder led to higher amount of CH, compared to MC and PHLS4. This is in agreement with the heat of hydration, setting time and compressive strength results in the sense that incorporation of 4% in the mixtures shortened the dormant period and the setting time and improved the compressive strength at 1 and 3 days.

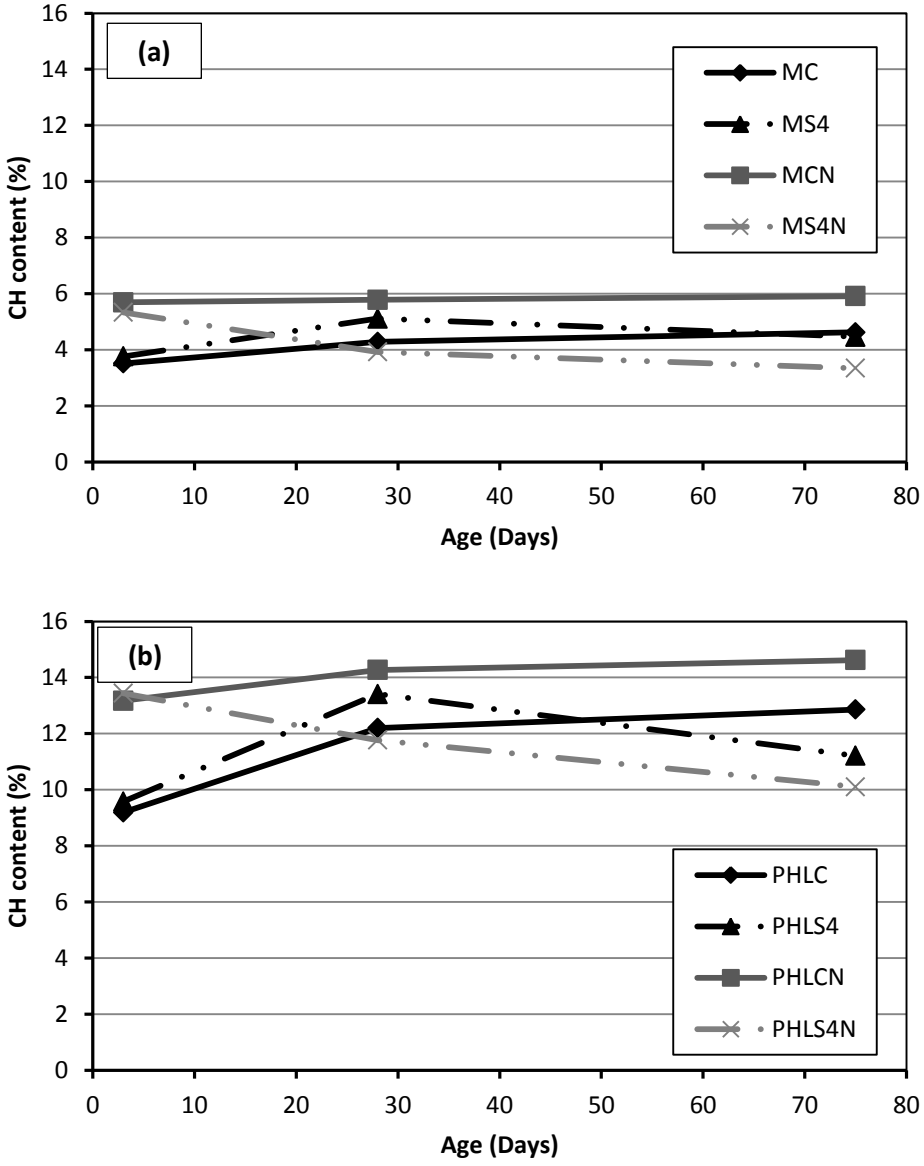

Fig. 4.15. CH contents of some mixtures from; (a) group M, and (b) group P.

Table 4-7- CH content of the mixtures comprising NS at cold temperature

Group	Mixture	% CH content at	
		3 days	28 days
M	MC	3.5	4.3
	MS2	3.6	4.9
	MS4	3.8	5.1
	MS6	4.3	5.2
P	PHL	9.2	12.2
	PHLS2	12.1	13.9
	PHLS4	12.1	13.4
	PHLS6	10.5	11.7

4.4 Mechanical Properties of Masonry Assemblages

4.4.1 **Compressive Strength of Masonry Prisms**

One of the key properties required for designing masonry structures is the specified compressive strength of masonry prisms, f'_m. According to clause 5.1.1 in CSA S304.1-04(CSA 2004c), the compressive strength of the masonry prism at 28 days, f'_m, shall be determined by the compression test on the prism or selected from Table 4 of the standard. As shown in Table 4.8, selection of the masonry prism compressive strength according to the Table 4 in CSA S304.1-04 (CSA 2004c) is based on the type of the masonry mortar (Type S or N), type of the block (hollow or solid) and the compressive strength of the block.

Table 4-8– Specified compressive strength, f'_m, at 28 days normal to the bed joint (reproduced from CSA S304.1-04 (CSA 2004c))

Compressive strength of CMU, MPa	Type S mortar		Type N mortar	
	Hollow	Solid	Hollow	Solid
30	17.5	13.5	12	9
20	13	10	10	7.5
15	9.8	7.5	8	6

In this study, the effect of the nano-modified mortar joints on the compressive strength of stack bonded masonry block prisms were assessed at early and later ages (3 and 28 days), according to Annex D of CSA S304.1-04 (CSA 2004c) and ASTM C1314-12 (ASTM 2012a). Two types of mortar mixtures incorporating nanoparticles along with their corresponding control mixtures were selected for the compressive strength test based on the results obtained from various tests on the mortar mixtures, as discussed in previous sections. The selection criteria of the mixtures were their flowability, air content, hydration performance, setting time, compressive strength and microstructural development at cold temperature. It is worth mentioning that the due to retardation and sedimentation effect of HRWRA on the mixtures incorporating NA, these mixtures were not considered in this phase. The mortar mixtures used to fabricate masonry prisms were MS4 (masonry cement with 4% NS) and PHLS4 (GU blended with hydrated lime and 4% NS). Mortar mixtures were used as 10 mm mortar joints for masonry prisms and a total of 24, three course high masonry block prisms were constructed and cured at 5 ± 1°C by a certified mason. The average compressive strength values at different ages of the group M prisms are shown in Fig. 4.16. At 3 days, the control prism (PMC) and the prism constructed with the mortars mixtures containing 4% NS (PMS4) had comparable average compressive

strength values (about 28 MPa), respectively. At 28 days, only slight enhancement of about 3% was observed in the compressive strength of PMS4, compared to PMC. The results showed that the compressive strength of the prisms was not noticeably affected by the type of the mortar. This trend was supported by ANOVA at 3 and 28 days (Table 4.9). For example, ANOVA for 3 days compressive strength results had F value of 0.50 and F_{cr} of 7.7, indicating an insignificant effect of addition of 4% NS on the compressive strength of masonry prisms. It should be noted that the results are in conformance with the compressive strength of mortar cubes where ANOVA between the control mixtures and the mixtures incorporating 4% NS supported the insignificant effect of the addition of 4% NS at 3 and 28 days on their compressive strength with F values of 6.48, 1.1 and F_{cr} of 7.7, respectively.

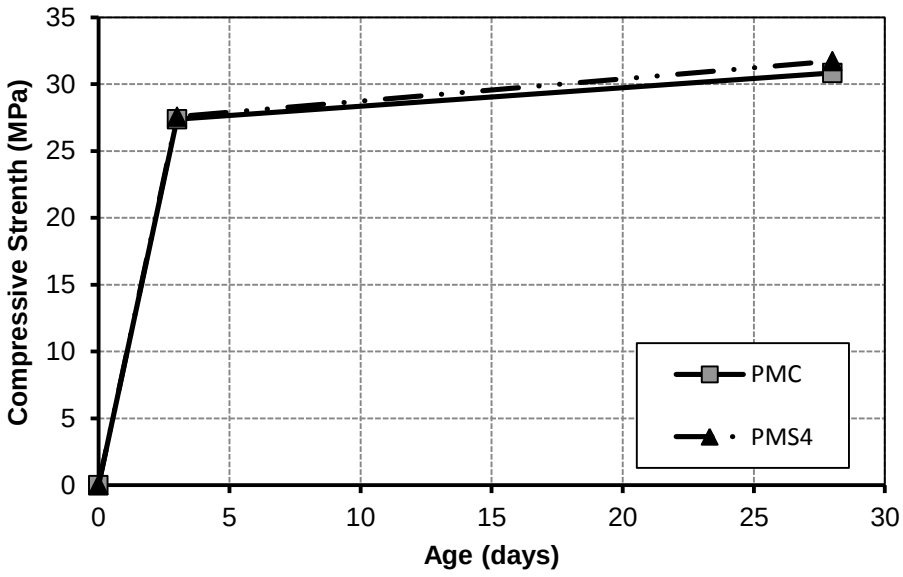

Fig. 4.16. Compressive strength of group M masonry prisms.

In a similar trend, contribution of 4% NS in group P prisms was also insignificant at early and later ages (Fig. 4.17). The increase in the compressive strength in this group was about 4 and

2% at 3 and 28 days, respectively, compared to the control prism (PPHLC). Statistical analysis (Table 4.9) showed that addition of 4% NS to the mixtures did not significantly affect the compressive strength of the masonry block prisms constructed by nano-modified mortars at a cold temperature. The results are generally in conformance with the literature in the sense that in a masonry prism, mortar joint is mostly responsible for transferring stresses to the block (load bearing effect) and its effect on the total compressive strength of the prism is minimal (Chidiac and Mihaljevic 2011; Drysdale and Hamid 1979; Khalaf *et al.* 1995). In a study by Khalaf (1996) an increase of 188% in compressive strength of mortar led to only 20% improvement in the compressive strength of the prism. Similarly, Drysdale and Hamid (2005) suggested that an adequate compressive strength is required for masonry prisms and increasing the compressive strength of mortar joints to high values does not noticeably increase the compressive strength of the prism.

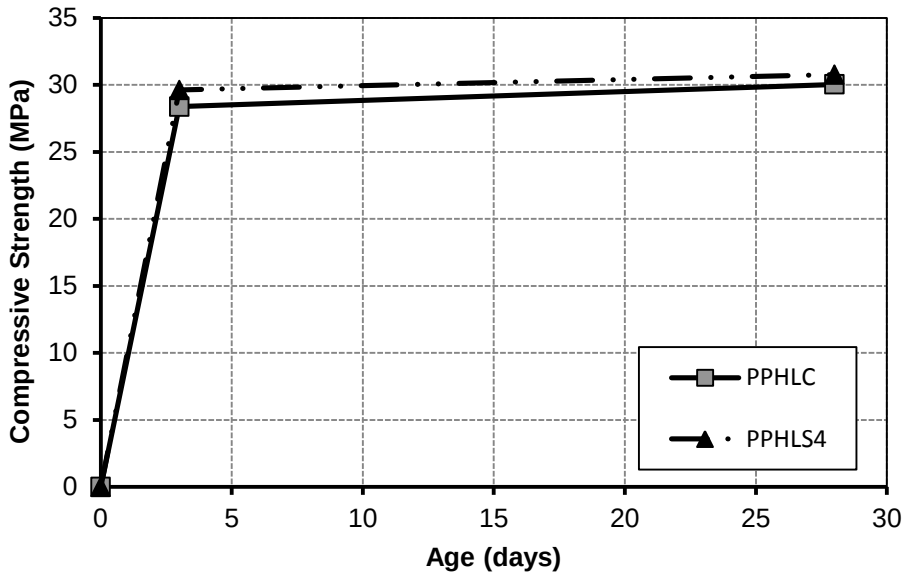

Fig. 4.17. Compressive strength of group P masonry prisms.

Table 4-9– ANOVA results of the prisms constructed using nano-modified mortar

Group	Age (Days)	F	F_{cr}	Effect
M	3	0.50	7.70	Insignificant
	28	0.09	7.70	Insignificant
P	3	3.38	7.70	Insignificant
	28	0.53	7.70	Insignificant

The mode of failure of the prisms bonded by nano-modified mortars were also in agreement with the other studies (Chidiac and Mihaljevic 2011; Drysdale and Hamid 2005). Under axial compression, the mortar joint is under triaxial compression and the bond between mortar and the block creates biaxial tension force in the block (Drysdale and Hamid 2005). As shown in Fig. 4.18, for all prisms, vertical cracks were initiated along the webs of the CMUs and the face shells. In a similar study by Mohamad et *al.* (2007) strong mortar was used in the masonry prisms and a similar mode of failure (vertical cracks) was observed. This is an indication that under axial compression the failure of the block occurs due to the fact that it no longer can stand the tensile stresses applied by the mortar joints.

In addition to the compressive strength of the prisms, the modulus of elasticity, *E*, was determined by means of four pi gauges along the two sides of the masonry prisms as shown in Fig. 4.19. The modulus of elasticity of the prisms was calculated by finding the slope of the chord modulus in the range of 0.05 and 0.33 of the ultimate compressive strength of the prisms according to CSA S304.1-04 (CSA 2004c) and ASTM C1314-12 (ASTM 2012a), as shown in Figs. 20, 21, 22, 23. Calculations of the modulus of elasticity are given in Appendix B. Although results (Table 4.10) indicate a variation in the modulus of elasticity at early and later ages, statistical analyses (ANOVA) showed that the addition of 4% NS to the mortar joints did not significantly affect the modulus of elasticity of the

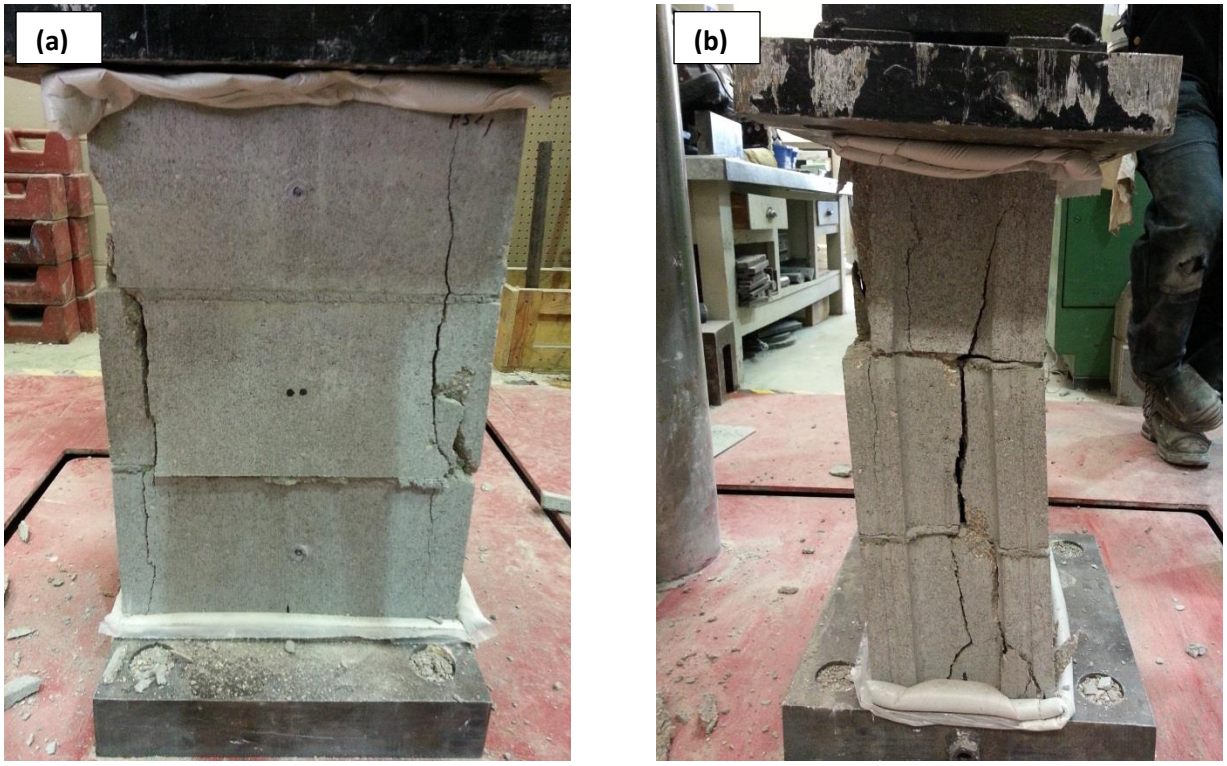

Fig. 4.18. Mode of failure of PMS4 masonry prisms: (a) front view, and (b) side view.

prisms (Table 4.11), except for group M at 3 days. In this group, the prisms constructed by nano-modified mortar mixtures significantly improved the modulus of elasticity at 3 days with *F* and critical *F* values of 19.75 and 7.70, respectively. This variation in results might be due to a large scatter of the strain readings by the pi gauges. Inconsistency of the joint thickness might have led to this scatter (Mohamad *et al.* 2007). However, the higher modulus of elasticity of PMS4 at 3 days signifies that the mortar had higher compressive strength compared to PMC, albeit the compressive strength of the prism was not affected. This is in agreement with the mortar cube compressive strength at 3 days where an improvement of about 15% was observed for MS4 compared to the control mixture (MC), as discussed earlier.

Fig. 4.19. Strain measurement of masonry prism by pi gauges.

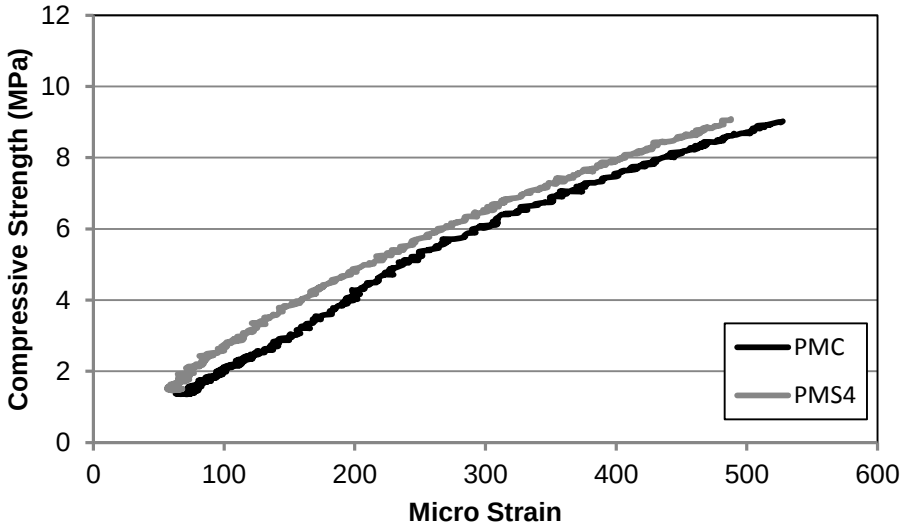

Fig. 4.20. Chord modulus of group M prisms at 3 days.

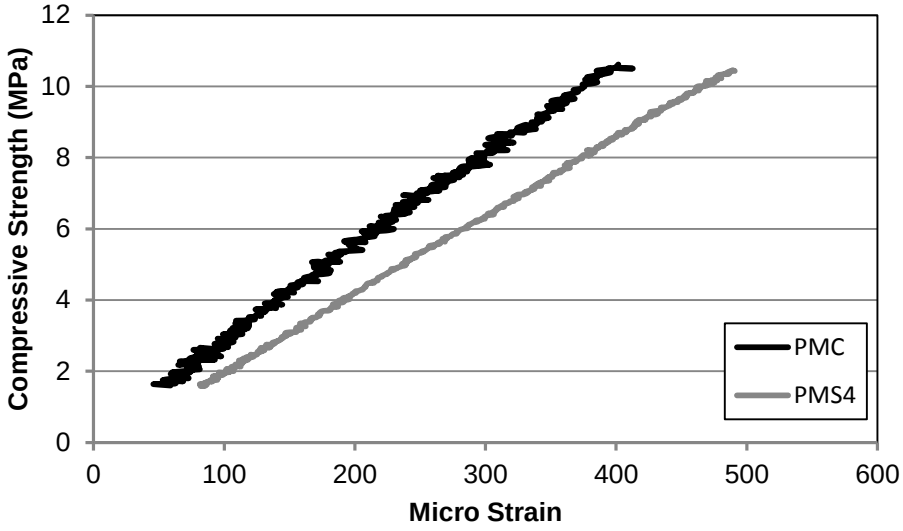

Fig. 4.21. Chord modulus of group M prisms at 28 days.

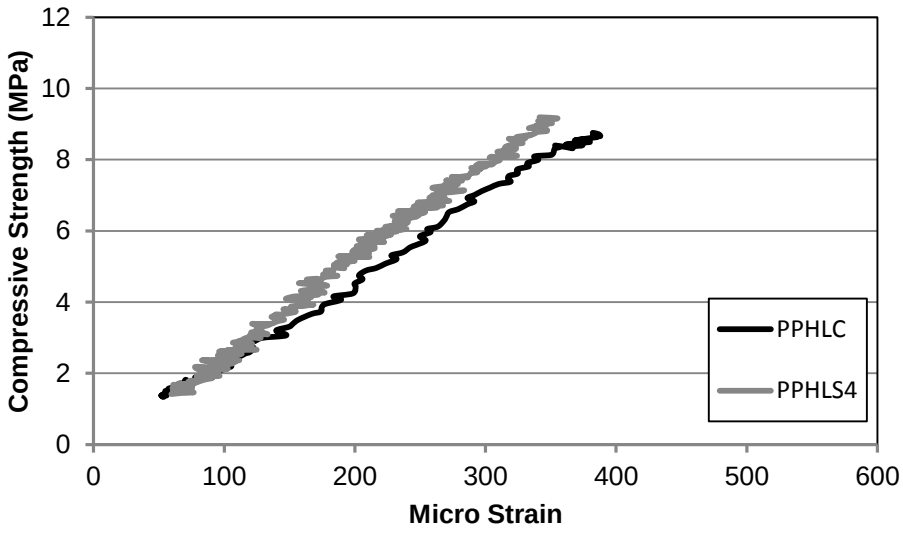

Fig. 4.22 Chord modulus of group P prisms at 3 days.

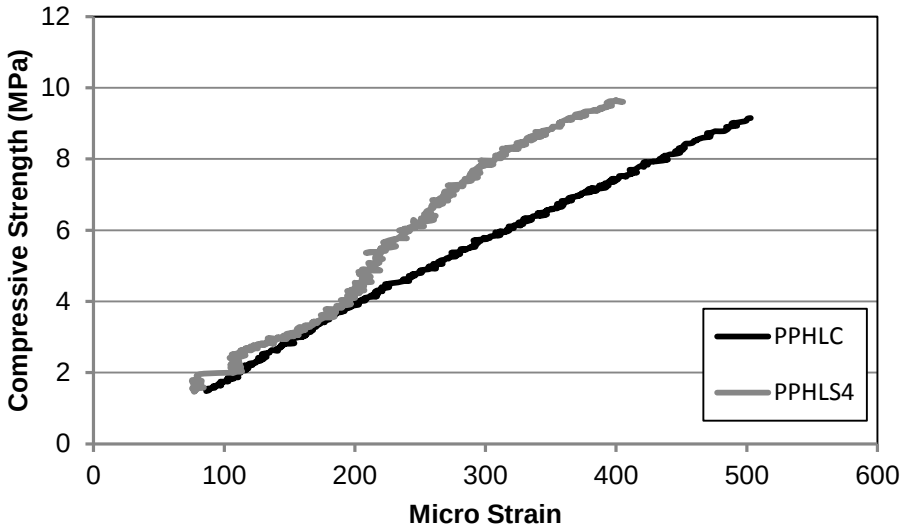

Fig. 4.23. Chord modulus of group P prisms at 28 days.

Table 4-10– Modulus of elasticity of the masonry prisms

Group	Specimen	Modulus of elasticity, *E*, (GPa)	
		3 days	28 days
M	PMC	17	26
	PMS4	18	22
P	PPHLC	21	18
	PPHLS4	26	21

Table 4-11– ANOVA results the for modulus of elasticity

Group	Age (Days)	F	F_{cr}	Effect
M	3	19.75	7.70	Significant
	28	7.60	7.70	Insignificant
P	3	4.82	7.70	Insignificant
	28	7.34	7.70	Insignificant

4.4.2 **Bond Strength Tests**

4.4.2.1 Pull-off Test Results

The pull-off method was implemented in this study to determine the mode of failure and the bond strength of the mortar to CMU under direct tension. This test was performed on the mortar joints that were used to fabricate the masonry prisms for the compressive strength test. As illustrated in Fig. 4.24a, the attached discs were pulled off at early and later ages (3 and 28 days) by the testing equipment. Subsequently, the mode of failure was observed and recorded. For all the four mixtures (MC, MS4, PHLC, PHLS4), the failure took place in the interface between the block and mortar layer at both 3 and 28 days, as shown in Fig. 4.24. This indicated that the bond

interface had the lowest tensile strength (weakest link) as compared to the concrete masonry block and mortar layers.

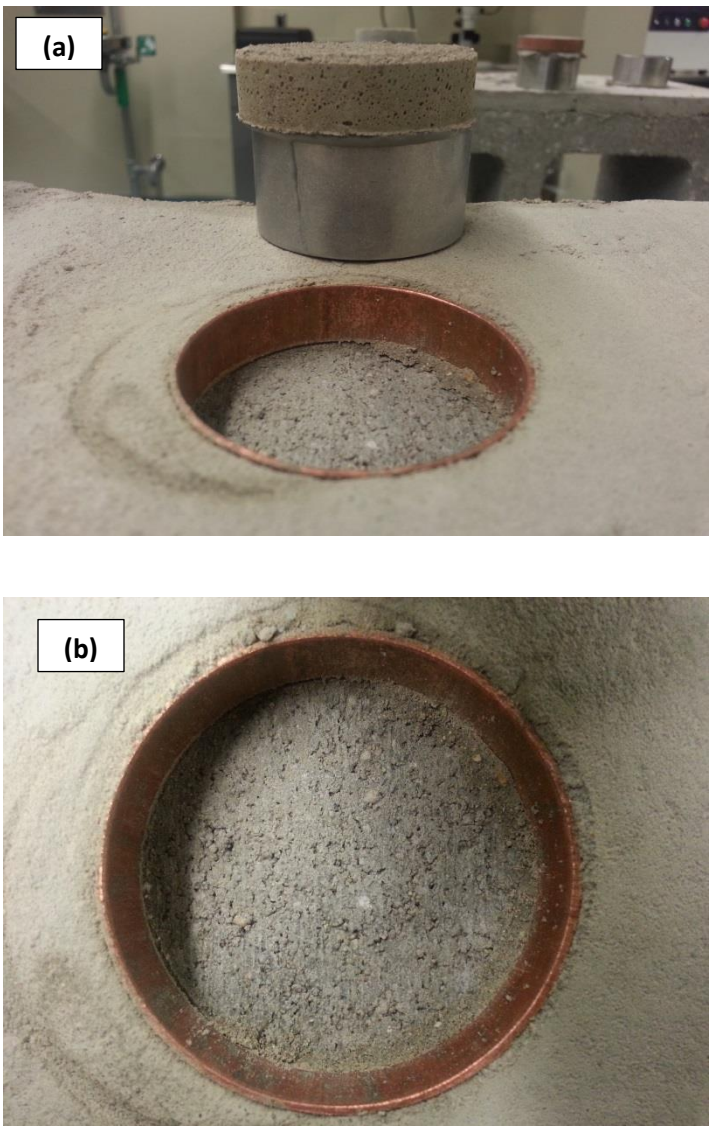

Fig. 4.24. Pull-off test failure mode: (a) full depth of mortar joint, and (b) the interface between the mortar and block.

The results of the ultimate (bond) strength from the pull-off test (Figs. 4.25 and 4.26) indicated that the incorporation of 4% NS in the mortar mixtures did not considerably affect the bond strength, f_b, between the masonry unit and the mortar at these ages. For example, at the age

of 3 days the bond strength for MC and MS4 were 1.68 and 1.38 MPa, which shows slightly lower bond strength for MS4. Similarly, the bond strength of PHLS4 was 2.71, which is about 0.7 MPa lower than the control sample (PHLC). In addition, the error bars of the tests were overlapping at both ages, indicating no statistically significant effect between the nano-modified mortar and the control mortar on the pull-off test results. However, the results generally indicate that the trend of increase in the average bond strength of the samples with time was more pronounced for group M mixtures compared to group P mixtures, which correlates to the different kinetics of hydration and properties of masonry cement and blended GU cement with hydrated lime as explained earlier in the text. The bond strength values measured by this method generally provide lower strengths as compared to the flexural bond strength. This is due to the fact that under the flexural bond test half of the section is under tension and the other half is under compression, while in the pull-off method the entire section is under direct tension. Although lower bond strength is expected by the pull-off test method, the bond strength values from this method exceeded the suggested strength in Table 5 of CSA S301.1-04 (CSA 2004c) by 50 to 400% at 3 days. According to this table, bond strength of 0.4 MPa is recommended for the masonry prisms at 28 days when Type S mortar and hollow concrete masonry unit is used.

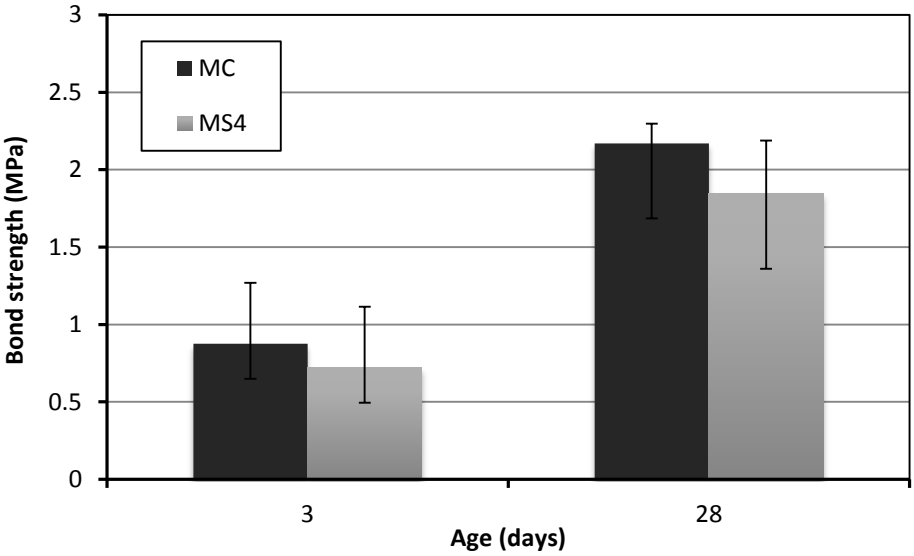

Fig. 4.25. Pull-off test results for group M.

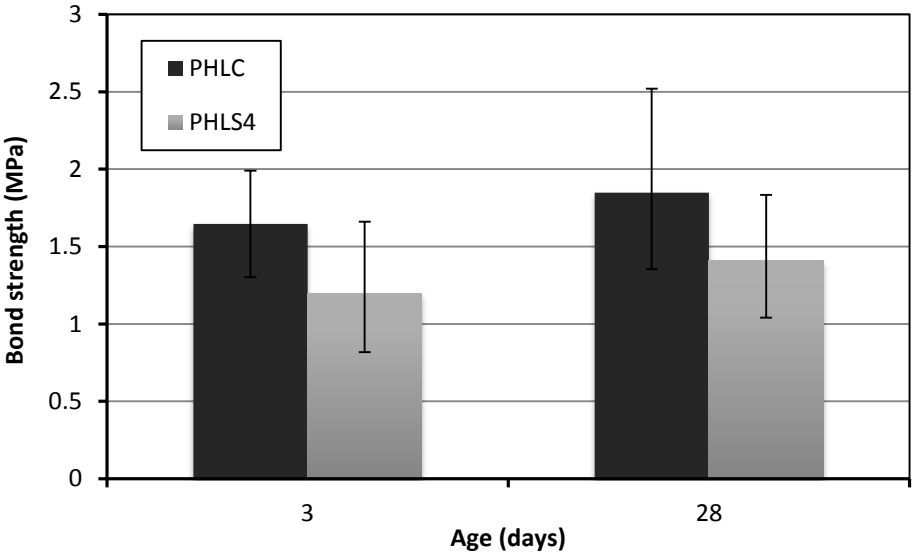

Fig. 4.26. Pull-off test results for group P.

4.4.2.2 Flexural Bond Test Results

To verify the pull-off trends, the flexural bond test according to ASTM E518-10 (ASTM 2010b) and ASTM E72-13 (ASTM 2013b) was performed on four course high stack bonded masonry prisms which were fabricated and cured at 5 ± 1˚C. As shown in Fig. 4.23, upon reaching the ultimate load, the bond between the masonry unit and mortar joint failed at the mid-span of the

masonry prisms, as the highest bending moment applies to this location. The bond strength of the prisms by this method, f_r, was calculated using the four point bending equation as below:

$$f_r = \frac{PL}{S} \qquad \text{(Eq. 4.1)}$$

Where:

f_r = bond strength, MPa

P = maximum applied load recorded by the testing equipment, N

L = span of the test set-up, mm

S = section modulus, mm^3

In this study, span (L) and the section modulus (S) were equal to 600 mm and 5.242×10^6 mm^3, respectively. At 3 days, the average results (Table 4.12) indicate that the bond failed in a narrow range of about 2.65 ± 0.1 MPa for all the prisms, which shows higher bond strength as compared to the pull-off test results for the reasons discussed earlier. As listed in Table 4.12, the bond strength between concrete masonry block and the mortar joint of PMS4 was 2.78 MPa which signifies a slight improvement of about 5% compared to the control specimen (PMC). On the contrary, results from group P indicated a decrease of about 0.16 MPa (6%) as compared to the control specimen (PPHLC). Statistical analysis showed that the addition of 4% NS to the mortar joints did not significantly affect the flexural bond strength of the concrete masonry prisms fabricated and cured at cold temperature (5 ± 1˚C), at 3 days. As listed in Table 4.13, ANOVA with a significance level of α=0.05, for the effect of the addition 4% NS to the mortar joints of group M and P, indicated F values of 1.23, 4.04 and F_{cr} of 7.70. The findings are generally in agreement with the pull-off test results at 3 days in the sense that the bond strength

of the prisms was not significantly affected when nano-modified mortars were used as mortar joints and the failure was due to debonding between the mortar and masonry block.

Table 4-12- Flexural bond test results

Group	Specimen	Bond strength (MPa), f_r, at 3 days
M	PMC	2.65
	PMS4	2.78
P	PPHLC	2.68
	PPHLS4	2.52

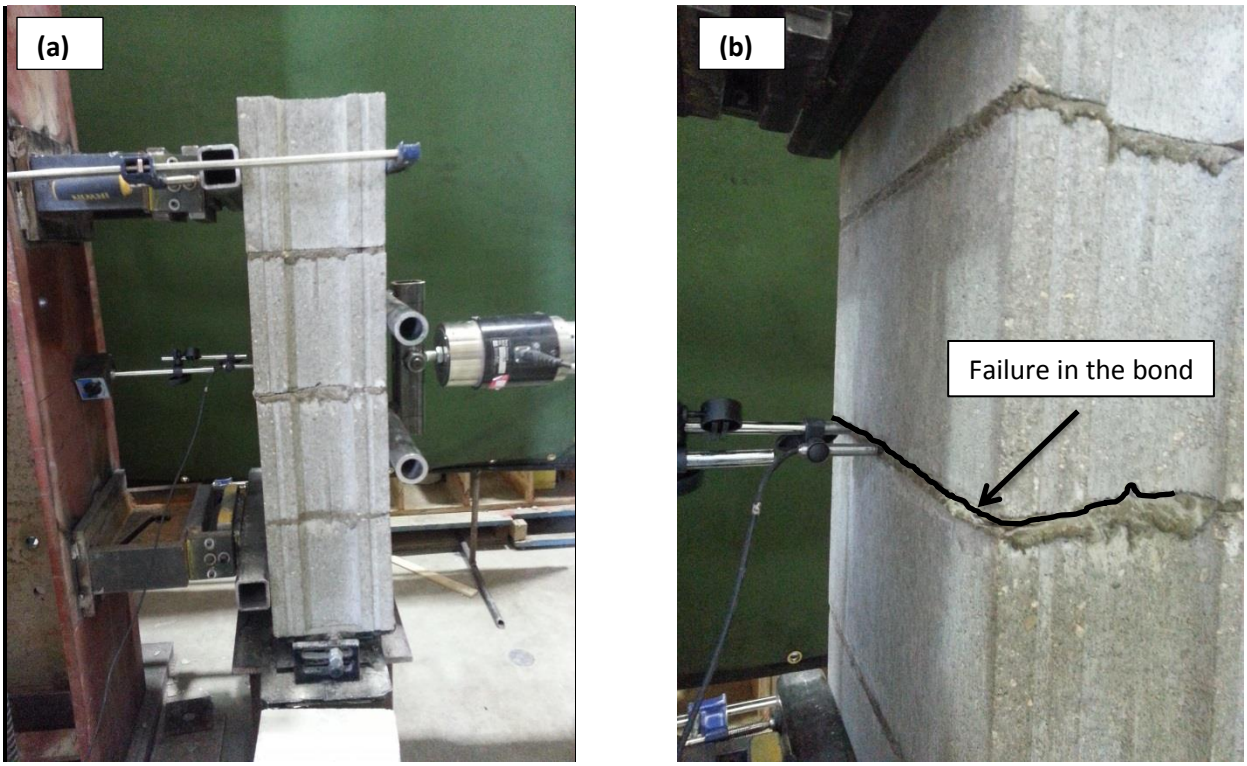

Fig. 4.27. (a) Flexural bond strength test setup, and (b) failure of the bond at the mid-joint.

Table 4-13– ANOVA results for flexural bond strength of masonry prisms

Group	Age (Days)	F	F_{cr}	Effect
M	3	1.23	7.70	Insignificant
P	3	4.04	7.70	Insignificant

5 SUMMARY, CONCLUSIONS AND RECOMMENDATIONS

5.1 Summary and Conclusions

This study explored the potential use of nanoparticles to improve the fresh and hardened properties of masonry mortar mixtures mixed and cured at a low temperature of 5 ± 1°C. The nanoparticles (NA and NS) were added to the cementitious binder at dosages of 2, 4 and 6% by mass of cement. The w/b was fixed at 0.4 and HRWRA was added to the mortar mixtures to obtain the desired flowability of 110 ± 5%. In order to meet the research objectives, this work was divided into two phases. In the primary phase the fresh, hardened and microstructural properties of the nano-modified masonry mortar mixtures mixed and cured at 5 ± 1°C were evaluated. The fresh and hardened properties of the mortar mixtures determined in this phase were: flowability, air content, heat of hydration, setting time and the compressive strength. Microstructural and thermal studies of the mortar mixtures included SEM and DSC analyses.

Based on the trends obtained from the primary phase, the ancillary phase of this work focused on the effect of selected nano-modified mortar joints on the mechanical properties of masonry assemblages fabricated and cured at a cold temperature of 5 ± 1°C. The mechanical properties determined in this phase were the compressive and bond (direct and flexural) strengths. Based on the mixture design and test procedures and mixing and curing conditions implemented in this study, the following conclusions can be drawn:

- The fresh and hardened properties of masonry mortar mixed and cured at a low temperature were altered according to the type and the dosage of nanoparticles added to

each group of mixtures. Generally, mixtures incorporating NS performed better than the mixtures with or without NA.

- The addition of the two types of the nanoparticles (NA and NS) to masonry mortar mixtures affected their flowability at cold temperature (5 ± 1°C). Generally, higher dosages of nanoparticles resulted in lower flow values at a constant w/b and HRWRA dosage. However, results indicated that mixtures incorporating NA needed higher amount of HRWRA for maintaining the desired flow range (110 ± 5%). This behavior of NA is ascribed to its higher SSA of 170 m^2/g compared to 80 m^2/g of NS.
- The addition of the nanoparticles decreased the density of fresh mortar mixtures and increased the fresh air content. The air content, generally, was increased as the dosage of the nanoparticles increased. This disclosed that the dispersing agent in the colloidal nanoparticles provided air entrainment in the cementitious system.
- The heat of hydration curves of the mixtures at 5°C revealed that the hydration of cement pastes at cold temperature was delayed compared to a reference mixture at normal temperature (22 ± 2°C). However, incorporation of the nanoparticles in the cement pastes accelerated the hydration reactions and shortened the dormant period at 5°C. The hydration peak for the mixtures containing nanoparticles was reached up to 35 h earlier than the control mixture without nanoparticles. This trend was more pronounced for group M mixtures. In addition, results indicated that the dormant period of group P mixtures was generally shorter than group M.
- In agreement with the heat of hydration, the setting time results indicated that the setting time of group P mixtures was about 4 h shorter than group M. The higher hydration

activity of group P mixtures related to their higher clinker content, led to shorter dormant period and setting times.

- The addition of nanoparticles influenced the setting time of the mortar mixtures at a cold temperature (5 ± 1°C). Generally, increasing the dosage of nanoparticles led to shorter setting time of the mortar mixtures. The high dosage of HRWRA of the mixtures containing NA created a soft penetration zone for the penetration of testing equipment needles. This led to longer setting time readings for these mixtures, compared to the control samples. However, this effect of HRWRA was not observed in the heat of hydration curves due to the heat flow measurement technique by the isothermal calorimeter. Addition of NS generally resulted in shortened setting times of the mortar mixtures at all dosages by its nucleation effect on the hydration of cement. However, the shortening trend was more noticeable in group M mixtures as masonry cement had better interaction with nanoparticles, compared to group P mixtures.
- The type of binder and dosage of nanoparticles affected the compressive strength of the mixtures depending on the age of testing. Generally, group P mixtures had higher compressive strength compared to group M mixtures. This was ascribed to their lower air content and higher clinker content which led to their superior hydration activity as observed by the heat of hydration and setting time tests.
- The incorporation of NA generally led to a slight improvement of the compressive strength at 1 day; however this trend was diminished at 3 days which led to lower or comparable strength values at later ages. The addition of NS significantly improved the compressive strength at 1 and 3 days and led to higher or comparable compressive strength values at later ages, compared to the control mixtures.

- The SEM observations from masonry mortar mixtures, showed a refined and densified microstructure for the mixtures containing NS with an average C/S of less than 1.4. The low C/S of C-S-H and refinement of the ITZ confirmed the performance of NS at cold temperature which improved the properties of the mixtures up to 28 days. However, for the mixtures incorporating NA a coarse and porous ITZ with C/S of 2 to 3 and discrete CH crystal was observed at 10 days. This signified insufficient degree of hydration of the cementitious matrix in these mixtures which led to lower compressive strength values after 3 days.
- Thermogravimetric analyses on the mixtures incorporating NS revealed that the pozzolanic reaction of these mixtures at cold temperature (5 ± 1°C) started after 28 days. This indicated a delay of about 25 days, compared to the mixtures mixed and cured at normal (22 ± 2°C) temperature. This disclosed that the hardened properties of the masonry mortar mixtures were not affected by the pozzolanic effect of NS. On the other hand, the mixtures incorporating NS had higher CH content at 3 days. In agreement with the compressive strength, setting time and heat of hydration results, the higher CH content of these mixtures at 3 days signified their superior hydration reactions at cold temperature, compared to the control mixtures.
- The compressive strength results of the masonry prisms at 3 and 28 days showed that the compressive strength of the mortar had an insignificant effect on the total compressive strength, which was generally controlled by the strength of the CMUs. All prisms failed after vertical cracks were initiated along the webs and the face shells of the concrete masonry units. The behavior the masonry prisms were generally in agreement with the literature. In addition, the modulus of elasticity of the prisms bonded with nano-modified

mortar joints was generally higher at 3 days, compared to the control prisms. In agreement with the compressive strength results of the mortar cubes, the higher modulus of elasticity signified that the nano-modified mortar joint had higher compressive strength at 3 days.

- Bond strength test (direct and flexural) results of the masonry prisms indicated that the addition of NS to the mortar joints did not significantly affect the bond strength at 3 and 28 days. However, all the bond strength values obtained from the tests were higher than the recommended value stipulated by CSA S301.1-04. In addition, direct bond strength results indicated that trend of increase in the bond strength of samples with time was more pronounced for group M samples. This is correlated to different hydration kinetics of masonry cement and blended GU cement with hydrated lime. Furthermore, the lower bond strength of group M mixtures compared to group P mixture at 3 days agreed to the heat of hydration, setting time and the compressive strength results of the mortar mixtures.
- Results from the present study pinpoint the promising use of NS in cold weather masonry construction to speed up the kinetics of hydration, shorten the setting time and increase the compressive strength development of masonry mortar mixtures within 72 h after mixing. Thus, incorporation of NS in masonry mortar mixtures can speed up the masonry construction in early fall periods, without the need for heating practices. In addition, the delayed (after 28 days) pozzolanic effect of NS improves the long-term hardened and durability properties of mortar joints at 5 ± 1°C.

5.2 Recommendations for Future Work

According to the objectives, scope and test results of this research study, the following future work recommendations can be made:

- Investigating the effect of higher w/b, without the use of HRWRA, on the fresh, hardened and microstructural properties of masonry mortar mixtures incorporating nanoparticles at a cold temperature of 5°C. Upon achievement of satisfactory results, testing the mechanical properties of the masonry prisms at 1 and 3 days is suggested.
- Performing a pilot experimental program in the field during early fall periods to assess and compare the behavior of the nano-modified mortars with the laboratory results.
- Investigating the durability performance (freeze and thaw, porosity, etc.) and the effect of relative humidity on the nano-modified masonry mortars mixed and cured at a cold temperature of 5°C.
- Studying the effect of NS on the properties of masonry mortars at a temperature lower than 5°C with temperature decrements of about 2°C.

REFERENCES

ACI. (2010). *Guide to Cold Weather Concreting*. ACI Committee 306R-10, American Concrete Institute, Farmington Hills, MI, USA, 24.

ACI/ASCE/TMS, J. (2013). *ACI 530.1/ASCE 6/TMS 603 : Specification for Masonry Structures*. Masonry Standards Joint Committee (MSJC), New York, NY, USA, 319.

Alarcon-Ruiz, L., Platret, G., Massieu, E., and Ehrlacher, A. (2005). "The use of thermal analysis in assessing the effect of temperature on a cement paste." *Cement and Concrete Research*, 35(3), 609–613.

Arefi, M. R., and Sarajan, Z. (2012). "Aluminum oxdie nanoparticles in cement mortar." *NACE International*, 51(9), 66–69.

Arslan, M., Çullu, M., and Durmus, G. (2011). "The effect of antifreeze admixtures on compressive strength of concretes subjected to frost action." *Journal of Science*, 24(2), 299–307.

ASTM. (2008). *ASTM C403: Standard Test Method for Time of Setting of Concrete Mixtures by Penetration Resistance*. *Annual Book of ASTM Standards*, ASTM International, West Conshohocken, PA, USA, 7.

ASTM. (2010a). *ASTM C1622/C1622M :Standard Specification for Cold-Weather Admixture Systems*. *Annual Book of ASTM Standards*, ASTM International, West Conshohocken, PA, USA, 8.

ASTM. (2010b). *ASTM E518/518M : Standard Test Methods for Flexural Bond Strength of Masonry*. *Annual Book of ASTM Standards*, ASTM International, West Conshohocken, PA, USA, 5.

ASTM. (2012a). *ASTM C1314 : Standard Test Method for Compressive Strength of Masonry Prisms*. *Annual Book of ASTM Standards*, West Conshohocken, PA, USA, 10.

ASTM. (2012b). *ASTM C1202: Standard Test Method for Electrical Indication of Concrete's Ability to Resist Chloride Ion Penetration*. *Annual Book of ASTM Standards*, ASTM International, West Conshohocken, PA, USA, 7.

ASTM. (2013a). *ASTM C494 : Standard Specification for Chemical Admixtures for Concrete*. *Annual Book of ASTM Standards*, ASTM International, West Conshohocken, PA, USA, 10.

ASTM. (2013b). *ASTM E72 : Standard Test Methods of Conducting Strength Tests of Panels for Building Construction*. *Annual Book of ASTM Standards*, ASTM International, West Conshohocken, PA, USA, 12.

ASTM. (2014). *ASTM C1679 : Standard Practice for Measuring Hydration Kinetics of Hydraulic Cementitious Mixtures Using Isothermal Calorimetry*. *Annual Book of ASTM Standards*, ASTM International, West Conshohocken, PA, USA, 15.

Barna, L., and Korhonen, C. (2012). "Guidance for optimizing admixture dosage rates for cold weather admixture systems." *Cold Regions Engineering 2012 : Sustainable Infrastructure Development in a Changing Cold Environment*, American Society of Civil Engineers, Reston, VA, USA, 175–185.

Bassuoni, M. T., Nehdi, M. L., and Greenough, T. R. (2006). "Enhancing the reliability of evaluating chloride ingress in concrete using the ASTM C 1202 rapid chloride penetrability test." *Journal of ASTM International*, 3(3), 1–13.

Bigelow, O. (2005). "Ensuring quality in cold-weather masonry construction." *The Construction Specifier*, 58(11), 58–63.

Bjornstrom, J., Martinelli, A., Matic, A., Borjesson, L., and Panas, I. (2004). "Accelerating effects of colloidal nano-silica for beneficial calcium-silicate-hydrate formation in cement." *Chemical Physics Letters*, 392(1), 242–248.

Brick Industry Association. (2006). *Technical Notes on Brick Construction : Cold and Hot Weather Construction*. Reston, VA, USA, 1–9.

Camiletti, J., Soliman, A. M., and Nehdi, M. L. (2012). "Effects of nano- and micro-limestone addition on early-age properties of ultra-high-performance concrete." *Materials and Structures*, 46(6), 881–898.

Campillo, I., Guerrero, A., Dolado, J. S., Porro, A., Ibáñez, J. A., and Goñi, S. (2007). "Improvement of initial mechanical strength by nanoalumina in belite cements." *Materials Letters*, 61(8), 1889–1892.

Chidiac, S. E., and Mihaljevic, S. N. (2011). "Performance of dry cast concrete blocks containing waste glass powder or polyethylene aggregates." *Cement and Concrete Composites*, 33(8), 855–863.

CSA. (2004a). *CSA A371 : Masonry Construction for Buildings*. Canadian Standards Association, Mississauga, ON, Canada, 30.

CSA. (2004b). *CSA A179 : Mortar and grout for unit masonry*. Canadian Standards Association, Mississauga, ON, Canada, 47.

CSA. (2004c). *CSA S304.1 : Design of masonry structures*. Canadian Standards Association, Mississauga, ON, Canada, 126.

CSA. (2008a). *CSA A3002 : Masonry and mortar cement*. *Cementitious materials compendium*, Canadian Standards Association, Mississauga, ON, Canada, 33–39.

CSA. (2008b). *CSA A3001 : Cementitious materials for use in concrete*. *Cementitious materials compendium*, Canadian Standards Association, Mississauga, ON, Canada, 3–32.

CSA. (2008c). *CSA A3004-C1: Standard Practice for Mechanical Mixing of Hydraulic Cement Mortars and Test Method for Determination of Flow*. *Cementitious materials compendium*, Canadian Standards Association, Mississauga, ON, Canada, 99–100.

CSA. (2008d). *CSA A3004-C4: Test Method for Determination of Air Content*. *Cementitious materials compendium*, Canadian Standards Association, Mississauga, ON, Canada, 113–116.

CSA. (2008e). *CSA A3004-C2: Test Method for Determination of Compressive Strengths*. *Cementitious materials compendium*, Canadian Standards Association, Mississauga, ON, Canada, 101–109.

CSA. (2014). *CSA A23.2: Determination of Bond Strength of Bonded Toppings and Overlays and of Direct Tensile Strength of Concrete, Mortar, and Grout*. *Test methods and standard practices for concrete*, Canadian Standards Association, Mississauga, ON, Canada, 415–420.

Cultrone, G., Sebastián, E., and Huertas, M. O. (2007). "Durability of masonry systems: A laboratory study." *Construction and Building Materials*, 21(1), 40–51.

Damasceni, A., Dei, L., Fratini, E., Ridi, F., Chen, S.-H., and Baglioni, P. (2002). "A novel approach based on differential scanning calorimetry applied to the study of tricalcium silicate hydration kinetics." *The Journal of Physical Chemistry B*, 106(44), 11572–11578.

Detwiler, R., Bhatty, J., and Bhattacharja, S. (1996). *Supplementary cementing materials for use in blended cements*. *Portland Cement Association*, Skokie, IL, USA, 103.

Dolgikh, R. A., and Rapoport, O. L. (2005). "Induction Heating of concrete floor at Monolith building." *Xl Modern Technique and Technologies*, IEEE, Tomsk, Russia, 96–97.

Essroc. (2012a). *Essroc Technical Notes : Cold Weather Masonry*. Nazareth, PA, USA, 1–2.

Essroc. (2012b). *Essroc Technical Notes : Masonry Construction in Cold Weather*. Nazareth, PA, USA, 1–2.

Esteves, L. P. (2011). “On the hydration of water-entrained cement – silica systems : Combined SEM , XRD and thermal analysis in cement pastes.” *Thermochimica Acta*, 518, 27–35.

Drysdale, R. G., and Hamid, A. A. (2005). *Masonry structures behaviour and design*. Canada Masonry Design Centre, Mississauga, 770.

Drysdale, R. G., and Hamid, A. A. (1979). “Behaviour of concrete block masonry under axial compression.” *ACI journral proceedings*, 76(6), 707–721.

Givi, A. N. ., Rashid, S. A., Aziz, F. N. A., and Mohd Salleh, M. A. (2011). “Particle size effect on the permeability properties of nano-SiO2 blended portland cement concrete.” *Journal of Composite Materials*, 45(11), 1173–1180.

Guefrech, A., Mounanga, P., and Khelidj, A. (2011). “Experimental study of the effect of addition of nano-silica on the behaviour of cement mortars Mounir.” *Procedia Engineering*, 10, 900–905.

Hatzinikolas, M., Longworth, J., and Warwaruk, J. (1984). “Effects of cold weather construction on the compressive strength of concrete masonry walls.” *ACI Journal Proceedings*, 81(6), 566–571.

Hewlett, P. C., and Massazza, F. (2003). *Lea’s Chemistry of Cement and Concrete*. Elsevier B.V., Amsterdam, Netherlands, 635.

Imoto, H., Ohta, A., Feng, Q., and Nicoleau, L. (2013). “Effect of a Calcium Silicate Hydrate-Type Accelerator on the Hydration and the Early Strength Development of Concrete Cured at 5 or at 20 Degrees Centigrade.” *Third International Conference on Sustainable Construction Materials and Technologies*, Kyoto, Japan, 1–9.

International Masonry Intitude (2010). *Cold Weather Masonry Construction*. *Technology Breif*, Annapolis, ML, USA, 1-4.

Ji, T. (2005). “Preliminary study on the water permeability and microstructure of concrete incorporating nano-SiO2.” *Cement and Concrete Research*, 35(10), 1943–1947.

Jo, B.-W., Kim, C.-H., and Lim, J.-H. (2007a). “Characteristics of cement mortar with nano-SiO2 Particles.” *ACI Materials Journals*, 104(4), 404–407.

Jo, B.-W., Kim, C.-H., Tae, G., and Park, J.-B. (2007b). “Characteristics of cement mortar with nano-SiO2 particles.” *Construction and Building Materials*, 21(6), 1351–1355.

Karagöl, F., Demirboğa, R., Kaygusuz, M. A., Yadollahi, M. M., and Polat, R. (2013). “The influence of calcium nitrate as antifreeze admixture on the compressive strength of concrete exposed to low temperatures.” *Cold Regions Science and Technology*, 89(5), 30–35.

Kawashima, S., Hou, P., Corr, D. J., and Shah, S. P. (2013). “Modification of cement-based materials with nanoparticles.” *Cement and Concrete Composites*, 36, 8–15.

Khalaf, F. M. (1996). “Factors influencing compressive strength of concrete masonry prisms.” *Magazine of Concrete Research*, 48(175), 95–101.

Khalaf, F. M., Hendry, A. W., and Fairbairn, D. R. (1995). “Study of the compressive strength of blockwork masonry.” *ACI Structural Journal*, 91(4), 367–375.

Korhonen, C. J. (1990). "*Antifreeze admixtures for cold regions concreting : A literature review*., U.S. Army Cold Regions Research and Engineering Laboratory, Hanover, NH, USA, 19.

Korhonen, C. J. (2002). *New developments in cold-weather concreting*., U.S. Army Cold Regions Research and Engineering Laboratory, Hanover, NH, USA, 7.

Korhonen, C. J., and Orchino, S. A. (2001). *Off-the-Shelf antifreeze admixtures for concrete*., U.S. Army Cold Regions Research and Engineering Laboratory, Hanover, NH, USA, 23.

Korhonen, C. J., Thomas, R. D., and Cortez, E. R. (1997). *Increasing cold weather masonry construction productivity*. U.S. Army Corps of Engineers, Springfield, IL, USA, 53.

Li, Z., Wang, H., He, S., Lu, Y., and Wang, M. (2006). “Investigations on the preparation and mechanical properties of the nano-alumina reinforced cement composite.” *Materials Letters*, 60(3), 356–359.

Lin, D. F., Lin, K. L., Chang, W. C., Luo, H. L., and Cai, M. Q. (2008). “Improvements of nano-SiO2 on sludge/fly ash mortar.” *Waste management*, 28(6), 1081–1087.

Loukili, A., Khelidj, A., and Richard, P. (1999). “Hydration kinetics, change of relative humidity, and autogenous shrinkage of ultra-high-strength concrete.” *Cement and Concrete Research*, 29(4), 577–584.

Mindess, S., Young, J. F., and Darwin, D. (2003). *Concrete*. Pearson Education Inc., Upper Saddle River, NJ, USA, 644.

Mohamad, G., Lourenço, P. B., and Roman, H. R. (2007). “Mechanics of hollow concrete block masonry prisms under compression: Review and prospects.” *Cement and Concrete Composites*, 29(3), 181–192.

Montgomery, D. (2001). *Design and analysis of experiments*. John Wiley & Sons, New York, NY, USA, 60.

Nazari, A., Riahi, S., Riahi, S., Shamekhi, S. F., and Khademno, A. (2010a). “Influence of Al2O3 nanoparticles on the compressive strength and workability of blended concrete.” *Journal of American Science*, 6(5), 6–9.

Nazari, A., Riahi, S., Riahi, S., Shamekhi, S. F., and Khademno, A. (2010b). "Mechanical properties of cement mortar with Al2O3 nanoparticles." *Journal of American Science*, 6(4), 94–97.

Neal, R. (2002). *Problems with Concrete in Cold Weather? What's New?* , Hanley-Wood Press, Washington, WA, USA, 1–4.

Neville, A. (2004). "The confused world of sulfate attack on concrete." *Cement and Concrete Research*, 34(8), 1275–1296.

Neville, A. M. (1996). *Properties of Concrete*., John Wiley & Sons, New York, NY, USA, 868.

Oltulu, M., and Şahin, R. (2011). "Single and combined effects of nano-SiO2, nano-Al2O3 and nano-Fe2O3 powders on compressive strength and capillary permeability of cement mortar containing silica fume." *Materials Science and Engineering: A*, 528(23), 7012–7019.

Oltulu, M., and Şahin, R. (2013). "Effect of nano-SiO2, nano-Al2O3 and nano-Fe2O3 powders on compressive strengths and capillary water absorption of cement mortar containing fly ash: A comparative study." *Energy and Buildings*, 58, 292–301.

Pane, I., and Hansen, W. (2005). "Investigation of blended cement hydration by isothermal calorimetry and thermal analysis." *Cement and Concrete Research*, 35(6), 1155–1164.

Said, a. M., Zeidan, M. S., Bassuoni, M. T., and Tian, Y. (2012). "Properties of concrete incorporating nano-silica." *Construction and Building Materials*, 36, 838–844.

Sanchez, F., and Sobolev, K. (2010). "Nanotechnology in concrete – A review." *Construction and Building Materials*, 24(11), 2060–2071.

Senff, L., Hotza, D., Lucas, S., Ferreira, V. M., and Labrincha, J. a. (2012). "Effect of nano-SiO2 and nano-TiO2 addition on the rheological behavior and the hardened properties of cement mortars." *Materials Science and Engineering: A*, 532, 354–361.

Senff, L., Hotza, D., Repette, W. L., Ferreira, V. M., and Labrincha, J. a. (2010a). "Effect of nanosilica and microsilica on microstructure and hardened properties of cement pastes and mortars." *Advances in Applied Ceramics*, 109(2), 104–110.

Senff, L., Hotza, D., Repette, W. L., Ferreira, V. M., and Labrincha, J. a. (2010b). "Mortars with nano-SiO2 and micro-SiO2 investigated by experimental design." *Construction and Building Materials*, 24(8), 1432–1437.

Senff, L., Labrincha, J. a., Ferreira, V. M., Hotza, D., and Repette, W. L. (2009). "Effect of nano-silica on rheology and fresh properties of cement pastes and mortars." *Construction and Building Materials*, 23(7), 2487–2491.

Sha, W., Neill, E. A. O., and Guo, Z. (1999). "Differential scanning calorimetry study of ordinary Portland cement." *Cement and Concrete Research*, 29, 1487–1489.

Shih, J.-Y., Chang, T.-P., and Hsiao, T.-C. (2006). "Effect of nanosilica on characterization of Portland cement composite." *Materials Science and Engineering: A*, 424(1), 266–274.

Skalny, J., Marchand, J., and Odler, I. (2002). *Sulfate attack on concrete*. *Modern concrete technology series*, CRC Press, Boca Raton, FL, USA, 217.

Sonebi, M., Bassouni, M. T., Kwansy, J., and Amanuddin, A. K. (2012). "Effect of nano-silica on fresh and rheological properties of cement-based grouts." *Fourth International Symposium on Nanotechnology in Construction*, Crete, Egypt, 8.

TCC. (2011). TCC materials technical notes: *Use of mortars and grouts in cold weather construction*. Mendota Heights, MN, USA, 1–2.

Throop, D. (2005). "All-Weather Masonry-Part 2." *Structure Magazine*, (11), Reedsburg, WI, USA, 11–14.

Vera-Agullo, J., Cjpzad-Ligero, V., Portillo-Rico, D., Garcia-Casas, M. J., Gutiérrez-Martínez, A., Mieres-Royo, J. M., and Grávalos-Moreno, J. (2009). "Mortar and concrete reinforced with nanomaterials." *Nanotechnology in Construction 3*, Springer Berlin Heidelberg, 383–388.

Vikulin, V. V., Alekseev, M. K., and Shkarupa, I. L. (2011). "Study of the effect of some commercially available nanopowders on the strength of concrete based on alumina cement." *Refractories and Industrial Ceramics*, 52(4), 288–290.

Zhang, M., and Li, H. (2011). "Pore structure and chloride permeability of concrete containing nano-particles for pavement." *Construction and Building Materials*, 25(2), 608–616.

Appendix A: Rapid Chloride Permeability Test (RCPT)

Rapid Chloride Permeability Test (RCPT)

The rapid chloride penetrability test was performed on mortar discs from all mixtures according to ASTM C1202-12 (ASTM 2012b), and the average penetration depth of chloride ions in the specimens was determined according to Bassuoni *et al.* (2012). While this standard is for testing of concrete, it was conducted on mortar mixtures developed in the current study to qualitatively assess the difference in penetrability among the various mixtures, and thus implicate their long-term durability, for example to ingress of moisture and aggressive media. The passing charges and average penetration depth of all the mixtures are given in Table 10. Generally**,** the current in the control specimens and ones containing NA (except MA2 and MA4) reached 500 mA, which led to electrical overflow and stoppage of the test. Absence of coarse aggregate in the mixtures might have led to this overflow as the test is originally developed for concrete. As shown in Table A.1, although MA2 and MA4 could survive the test, their penetrability class was considered high according to ASTM C 1202-12. However, increasing the NA dosage seemed to increase the chloride ion penetrability to its maximum depth (50 mm).

On the contrary, the results indicated a higher resistance to chloride penetrability for the specimens incorporating NS (Fig. A.1). For group M mixtures, increasing the dosage of NS decreased the penetration depth and passing charges. This was associated with changing the penetrability class from high to moderate. This was statistically supported by ANOVA as the increase in the dosage of NS from 0 to 6% in group M had a significant effect on the penetration depth with F and F_{cr} values of 1649.90 and 4.25, respectively. Results from RCPT indicated that albeit their higher compressive strength, group P mixtures have higher pore connectivity compared to group M. In this group, sample with a substantial amount of NS (6%) was the only sample which survived the test. This sample had a penetrability class of high and an average

penetration depth of 32 mm. The beneficial effect of NS in improving the resistance to chloride penetrability has also been shown in other studies (Said *et al.* 2012; Zhang and Li 2011).In the current study, NS reduced the penetrability of the mixtures by refining the pore structure and providing nucleation sites for hydration, thus decreasing the pore connectivity as was also observed by BSEM. As discussed earlier, in this study, the pozzolanic effect of NS was initiated after 28 days which suggests the fact that it did not contribute in discounting the pore connectivity at low temperature. It should be noted that higher air content of the mixtures is not necessarily an indication of higher chloride penetrability, as RCPT mainly relies on the connectivity of the pores (Said *et al.* 2012). However, in this study the open microstructure and high conductivity of several mixtures mixed and cured at a low temperature of (5 ± 1°C) led to current overflow, and thus no actual assessment and conclusion could be made for these mixtures. According to the results of the RCPT, durability tests (e.g. penetrability, frost resistance, chemical attack) were recommended for the future work on the mixtures developed in the present study in chapter 5.

Table A-1- RCPT test results at 28 days

Group	Mixture	Passing charge (Coulombs)	Penetrability class	Penetration depth (mm)
M	MC	-	NA	-
	MA2	7406	High	48.0
	MA4	8315	High	50
	MA6	-	NA	-
	MS2	5601	High	33.1
	MS4	3280	Moderate	20.7
	MS6	2503	Moderate	17.1
P	PHLC	-	NA	-
	PHLA2	-	NA	-
	PHLA4	-	NA	-
	PHLA6	-	NA	-
	PHLS2	-	NA	-
	PHLS4	-	NA	-
	PHLS6	6542	High	31.5

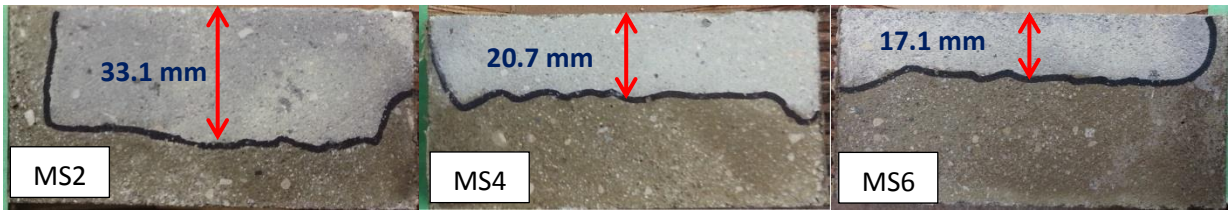

Fig.A.1. Chloride penetration depth of the samples containing NS from group M.

Appendix B: Calculation of Modulus of Elasticity of the Masonry Prisms

Modulus of elasticity of the masonry prisms

The modulus of elasticity was found by finding the slope of the line connecting the point equal to 0.05 and 0.33 of the ultimate compressive strength. For each sample the calculation of the *E* modulus is shown as below according to the age of testing:

Calculation of modulus of elasticity at 3 days:

Specimen PMC:

Compressive strength, MPa	Corresponding strain, micro strain
1.418	66.447
9.121	527.623

$$E = \frac{9.121531 - 1.418845}{527.623 - 66.4471} = = 16.78\ GPa$$

Specimen PMS4:

Compressive strength, MPa	Corresponding strain, micro strain
1.464	72.0723
9.0872	487.962

$$E = \frac{9.087212 - 1.464982}{487.962 - 72.0723} = = 18.32\ GPa$$

Specimen PPHLC:

Compressive strength, MPa	Corresponding strain, micro strain
1.629	53.792
7.363	324.171

$$E = \frac{7.363882 - 1.62993}{324.1719 - 53.79268} = = 21.20\ GPa$$

Specimen PPHLS4:

Compressive strength, MPa	Corresponding strain, micro strain
1.459	60.363
9.337	361.321

$$E = \frac{9.337745 - 1.459949}{401.7037 - 0.603638} = = 26.18\ GPa$$

Calculation of modulus of elasticity at 28 days:

Specimen PMC:

Compressive strength, MPa	Corresponding strain, micro strain
1.598	58.903
10.615	401.703

$$E = \frac{10.61584 - 1.59860}{401.7037 - 58.90366} = = 26.30\ GPa$$

Specimen PMS4:

Compressive strength, MPa	Corresponding strain, micro strain
1.584	81.843
10.451	489.0131

$$E = \frac{10.45191 - 1.584832}{489.013 - 81.8434} = 21.77\ GPa$$

Specimen PPHLC:

Compressive strength, MPa	Corresponding strain, micro strain
1.467	84.319
10.397	590.559

$$E = \frac{10.39789 - 1.467675}{590.5591 - 84.31977} = = 17.64\ GPa$$

Specimen PPHLS4:

Compressive strength, MPa	Corresponding strain, micro strain
1.482	69.574
9.661	443.781

$$E = \frac{9.661511 - 1.482909}{443.7811 - 69.57478} = = 21.35\ GPa$$

Appendix C: Calculation of the Flexural Bond Strength

Calculation of the Flexural Bond Strength

The flexural bond strength was measured according to the four point bending test set-up calculations at discussed in the text. In this chapter the calculation of the flexural bond test is given for each specimen according to Eq. 4.1:

Specimen PMC:

$$f_r = \frac{23.15 \times 10^3 \times 600}{5.242 \times 10^6} = 2.65 \text{ MPa}$$

Specimen PMS4:

$$f_r = \frac{24.36 \times 10^3 \times 600}{5.242 \times 10^6} = 2.78 \text{ MPa}$$

Specimen PPHLC:

$$f_r = \frac{23.45 \times 10^3 \times 600}{5.242 \times 10^6} = 2.68 \text{ MPa}$$

Specimen PPHLS4:

$$f_r = \frac{22.10 \times 10^3 \times 600}{5.242 \times 10^6} = 2.52 \text{ MPa}$$